COMPOSITE BIOSCAFFOLDS FOR ADIPOSE TISSUE ENGINEERING

by

Hoi Ki Cheung

A thesis submitted to the Department of Chemical Engineering

In conformity with the requirements for

the degree of Master of Applied Science

Queen's University

Kingston, Ontario, Canada

(December, 2011)

Abstract

A composite bioscaffold was constructed by encapsulating human decellularized adipose tissue (DAT) within a photopolymerized polysaccharide hydrogel towards the goal of forming an injectable scaffold for adipose tissue engineering. Methacrylated glycol chitosan (MGC) and methacrylated chondroitin sulphate (MCS) were investigated as the hydrogel base materials with varying DAT concentrations. Glycol chitosan and chondroitin sulphate were converted to photopolymerizable prepolymers through graft methacrylation using glycidyl methacrylate and methacrylate anhydride respectively to achieve a degree of substitution (DOS) of 15% and 16%, respectively. MGC and MCS gels containing 0, 3 and 5 w/v% cryo-milled DAT were fabricated and characterized by measuring sol content, equilibrium water content and compressive mechanical properties (n=4, n=3). An increase in stiffness and a decrease in sol and water contents were observed in the gels with higher DAT concentration, suggesting that the DAT was acting as a filler material that contributed to the crosslinking reaction. *In vitro* studies were conducted with primary human adipose-derived stem cells (ASCs) encapsulated in the DAT-polymer constructs to assess cellular viability (n=3, N=3) as well as adipogenic differentiation, quantitatively via glycerol-3-phosphate dehydrogenase (GPDH) enzyme activity (n=3, N=3) and qualitatively through end-point RT-PCR analysis of key adipogenic genes (LPL, PPARγ, and CEPBα) (n=2, N=3) and intracellular lipid staining (n=3, N=3). Incorporating the DAT with MGC or MCS hydrogels enhanced cell viability as compared to the MGC and MCS scaffolds alone, with the MCS + 5 w/v% DAT scaffold having the highest overall cell viability and total cell number. The addition of the DAT in the MGC and MCS scaffold groups enhanced ASC adipogenesis as measured by an increase in GPDH levels, adipogenic gene expression and intracellular lipid accumulation characteristic of adipocytes. The highest GPDH levels were

observed in the induced MCS with 5 w/v% DAT scaffolds, as compared to all other scaffold groups and tissue culture controls. The GPDH activity in this group increased by almost three times between 3 and 14 days, consistent with the progression of differentiation. The results indicated that the MCS-based scaffolds incorporating the DAT promoted cell viability and adipogenesis, demonstrating great promise as composite scaffolds for soft tissue regeneration.

Acknowledgements

First, I would like to thank my supervisors Drs. Lauren Flynn and Brian Amsden, for providing their continuous support, guidance, and direction for this project. I have learnt valuable lessons under their tutelage on how to approach research and on the field of Tissue Engineering as a whole. It has been an honour and pleasure working with them.

I would like to extend my thanks to Drs. Steve Waldman and Ronald Neufeld for generously allowing me to use their laboratory equipment, and Dr. Françoise Sauriol for taking the time to teach me on the procedures for running my NMR samples. I would also like to thank Dale Marecak, Denver Surrao, Jake Kaupp and James Hayami for being constant sources of help on operating various equipments and for being endlessly patient with me. To Drs J. F. Watkins, M. Harrison, K. Meathrel, J. Davidson, C. Watters, and Mrs. K. Martin, thank you for your clinical collaborations in obtaining tissue samples.

Special thanks go to past and present members of the Flynn Lab Group in particular Yimu Zhao, Allison Turner, Sarah Fleming, Justin Lee, Valero Russo, Claire Yu, Juares Bianco, Stuart Young, Adrienne St Hilaire, Lydia Fuetterer, and Adam Bloom for their friendship. Without you all, my experience throughout my Master's study would not be nearly as colourful as it was. My most sincere thanks to my friends Calista Preusser, Derek Park, and Jennifer Li. All of you consistently remind me to look for the silver lining in difficult situations.

Last but not least, I would like to express my deepest gratitude to my family members for believing the best in me. From you, I will always find an unwavering source of support to strive forward.

Table of Contents

List of Figures

List of Tables

List of Major Abbreviations

2-D	Two-dimensional
3-D	Three-dimensional
ABAM	Antibiotic-Antimycotic
ADD-1	Adipocyte determination and Differentiation dependent factor-1
ASC	Adipose-derived stem cell
ATP	Adenosine triphosphate
BAT	Brown adipose tissue
BMI	Body mass index
BSA	Bovine serum albumin
C/EBP	CCAAT/enhancer binding Protein
CS	Chondroitin sulphate
DAT	Decellularized adipose tissue
DMEM	Dulbecco's Modified Eagle's Medium
DNA	Deoxyribonucleic acid
DOS	Degree of substitution
ECM	Extracellular matrix
EWC	Equilibrium water content
FBS	Fetal bovine serum
GC	Glycol chitosan
GPDH	Glycerol-3-phosphate dehydrogenase
IBMX	Isobutylmethylxanthine
LN	Laminin
LPL	Lipoprotein lipase
MCS	Methacrylated chondroitin sulphate
MGC	Methacrylated glycol chitosan
MSC	Mesenchymal stem cell
PBS	Phosphate buffered saline
PLA	Poly(lactic acid)
PGA	Poly(glycolic acid)
PLGA	Poly(lactic-co-glycolic acid)
PEG	Poly(ethylene glycol)
PPAR	Peroxisome proliferator-activated receptor
RT-PCR	Reverse transcription polymerase chain reaction
Sol	Sol Content
SVF	Stromal vascular fraction
TAG	Triacylglycerol
TCPS	Tissue culture poly(styrene)
TCPS I	Tissue culture poly(styrene) induced
TCPS NI	Tissue culture poly(styrene) non-induced
TNF-α	Tumor necrosis factor-α
WAT	White adipose tissue
$m_{dry,ini}$	Mass of the dried gel before swelling
$m_{dry,fin}$	Mass of the dried gel after swelling
m_{wet}	Mass of wet gel
p	Indenting force
ω	Indenting depth
a	Radius of a given indenter a
κ	correction factor that accounts for the finite layer effect
E	Young's modulus
h	Height of gel
v	Poisson ratio

Chapter 1

Introduction

1.1 Current Clinical Strategies and Limitations

A soft tissue defect can be defined as a loss of tissue within the subcutaneous fat layer, resulting in a void that can affect tissue contour and function [1]. Common causes of these defects include traumatic injury and burns, acquired or congenital diseases, such as lipodystrophies, and mastectomy or other tumour resections [1 – 4]. Since adipose tissue has a limited capacity for self-repair, an increasing number of cosmetic and reconstructive surgical procedures are performed to improve and restore tissue function as well as aesthetics, to lessen the negative psychological feelings that are associated with disfigurement [1,3,4]. In 2010 alone, The American Society of Plastic Surgeons reported over 13 million cosmetic surgeries and 5 million reconstructive procedures that were performed, of which 4 million were related to tumour removal procedures [5].

Popular clinical treatments that are presently used to repair soft tissue defects rely on the use of filler materials and autologous fat tissue transplants. Synthetic or natural-based fillers, such as poly(lactic acid) and collagen injections, can be associated with immune rejection, allergic reaction and implant resorption [4,6]. Autologous fat transplantation by injection of aspirated fat is used to correct small defects, but repeated treatment is required due to poor volume retention over time [2,6]. The transfer of

vascularised tissue flaps from a healthy site for large defect reconstruction requires invasive surgical procedures and can lead to donor site morbidity and deformity [6, 7].

These limitations in current clinical treatments call for the need to develop new strategies that can restore soft tissues. Adipose tissue engineering offers a promising and sustainable solution through the construction of viable and vascularised tissue implants derived from the host's own cells, allowing for better implant integration with the surrounding tissues [6, 8].

1.2 Thesis Overview

Adipose tissue engineering represents a treatment option to restore subcutaneous fat loss from injury, tumour resections, and congenital defects. A common approach to engineering soft tissues is to seed regenerative cell populations on a scaffold that will mimic the natural environment of the native extracellular matrix (ECM). Adipose-derived stem cells (ASCs) are a cell source used in adipose tissue engineering since they are abundant, easily accessible and they have the capacity to proliferate and differentiate into mature adipocytes [9]. In order to sustain ASC viability and growth, different synthetic and naturally-based scaffolding materials have been explored [3, 6, 10, 11]. Recent studies have investigated the use of decellularized adipose tissue (DAT), which is comprised of the ECM of adipose tissue with the cellular components extracted. The natural protein composition in DAT was found to promote ASC adhesion and adipogenesis without the addition of exogenous factors [8]. However, like most solid

scaffolds, pre-cut DAT scaffolds are limited by their ability to effectively fill irregularly-shaped defect sites and be delivered via minimally-invasive techniques. A potential solution is to incorporate ground DAT within a pre-hydrogel, polymer mixture. This composite scaffold could then be delivered by injection and crosslinked *in situ* to form a 3-dimensional gel that would fully replace the defect volume.

This project focused on the development scaffolds incorporating ASCs encapsulated within photopolymerizable DAT-polymer hydrogels for adipose tissue engineering. More specifically, methacrylated glycol chitosan (MGC) and methacrylated chondroitin sulphate (MCS) were investigated as the polymers of interest. In addition, this study compared ASC viability and adipogenic differentiation in the MGC-based and MCS-based scaffolds. Photopolymerization is an attractive option as it provides a fast and effective polymer crosslinking method that can be used for cell entrapment with minimal cell death during scaffold preparation [14]. The MGC and MCS were chosen for their ability to facilitate the diffusion of aqueous media and nutrients to support long-term cell viability, contribute to the bulk mechanical properties of the soft tissue composites, and ultimately, to enhance cell infiltration and wound healing [15, 16].

1.3 Research Objectives

The overall objective of this study was to construct DAT-polymer composite scaffolds by combining cryomilled DAT with either methacrylated chondroitin sulphate or methacrylated glycol chitosan. A comparison between the scaffolds was made in terms

of both ASC viability and adipogenic differentiation after the cells were encapsulated and cultured within the various types of gels.

The specific goals for this thesis were:

i. To develop and optimize a protocol for fabricating the DAT-polymer scaffolds, which included (a) the development of a protocol for cryomilling DAT and (b) optimizing the reaction to produce methacrylated chondroitin sulphate.

ii. To characterize composite DAT-MGC and DAT-MCS scaffolds, with varying concentrations of DAT (0, 3 and 5 w/v%) incorporated within the constructs, in terms of sol content, equilibrium water content and mechanical properties.

iii. To assess the *in vitro* ASC response in the cell-seeded MGC and MCS constructs with varying DAT concentrations in terms of ASC viability and adipogenesis, as measured by adipogenic gene expression, enzyme activity, and intracellular lipid accumulation.

Chapter 2

Literature Review

2.1 Adipose Tissue

Adipose tissue, or fat, is a loose connective tissue that is found ubiquitously in the human body. It occurs within other tissues (e.g. muscles) and as discrete depots [6, 17-18]. In mature humans, the distribution pattern of fat differs, with this tissue predominantly accumulating in the upper body, particularly around the abdominal area in men, and around the gluteofemoral region in women [19, 20]. While adipose tissue is primarily known for its role in energy storage, mechanical protection and thermal insulation, it also acts as an active endocrine organ by sending and responding to protein signals that modulate appetite, energy expenditure, insulin sensitivity, inflammation, and immunity [6, 17-18, 21-22]. Overall, adipose tissue contains a collection of specialized, lipid-filled cells called adipocytes along with adipose-derived stem cells (ASCs) and more-committed adipogenic progenitors, leukocytes, macrophages, fibroblastic connective tissue cells, as well as neural and vascular cell populations. These cells are held together by the extracellular matrix (ECM), which is a framework of different fibrous and network-type proteins, glycoproteins and glycosaminoglycans, to form a highly plastic tissue [6, 17, 21-22].

Fat is a dynamic organ that can be divided into 2 major types: brown adipose tissue (BAT) and white adipose tissue (WAT), described in more detail in sections 2.1.2 and 2.1.3 [23]. While both tissues provide insulation and mechanical protection to the body, they differ in their specialized functions. BAT is important for regulating temperature via non-shivering thermogenesis while WAT, being the most abundant type of adipose tissue in mature humans, maintains energy levels through energy storage and release [23-25].

2.1.1 Types of adipose depots

Adipose tissue is distributed throughout the body into major depots. In the subcutaneous regions, large fat reserves can be found in the abdomen, thighs, and buttocks, whereas in the intra-abdominal region, major sources of adipose tissue are the omental, retroperitoneal, and visceral areas [26, 27]. Additional fat can be found in other locations, including the periarticular, intramuscular and pericardial regions, as well as on the face and extremities, and within bone marrow [24]. Fat distribution within the body is heavily affected by genetics, as seen in previous studies where the body mass index (BMI) and waist to hip ratio (WHR) were demonstrated to be heritable traits [19, 20, 27].

Depending on the location of the depot, adipose tissue responds differently to hormonal stimuli. Adipose tissue in the breast and thighs, for example, is more responsive to sex hormones, while the fat on the neck and the back are more responsive to glucocorticoids **[**27, 28**].** Excessive growth of fat on the back of the neck is a common

symptom of Cushing's Syndrome, which is a disorder caused by excess glucocorticoids in the blood [26-28]. Additionally, visceral and intra-abdominal fat are more sensitive to lipid metabolism-related hormones as compared to subcutaneous adipose tissue [29].

2.1.2 Brown Adipose Tissue

The primary function of BAT is the conversion of energy obtained from food into heat [24, 25]. In humans, BAT is most commonly found in newborns where it is distributed throughout the body to protect against the stresses associated with the temperature changes that occur at birth [26]. As the body matures, BAT content decreases while WAT content increases to the point of representing a gross majority of adipose tissue [26, 30].

BAT obtained its name from its colouring, which is attributed to both its vascularized nature and the high number of mitochondria found within brown adipocytes [23-25]. Additionally, these cells possess a unique morphology; they are polygonal with diameters in the 15 – 50 μm range, and they store energy in the form of triacylglycerols (TAG) in multilocular lipid depots [30, 31]. These high-energy molecules are used for non-shivering thermogenesis via metabolism that occurs within the mitochondria. The mitochondria from BAT uniquely express the protein UCP-1 (uncoupling protein-1) that allows for the uncoupling of oxidative phosphorylation, which results in heat generation without ATP production [25-27, 29-30].

2.1.3 White Adipose Tissue

In mature humans, WAT represents the majority of adipose tissue and normally comprises 10% to 20% of the total body mass, depending on the health of the individual [32]. WAT is notably different from BAT as it is less vascularized and it is predominantly composed of mature white adipocytes. Morphologically, these mature cells possess several different attributes as compared to brown adipocytes: they are more spherical, they are larger in size and they possess a unilocular lipid droplet that occupies, on average, 90% of the cell volume within the cytoplasm [31-33]. The sizeable lipid depot within each individual cell allows WAT to act as the largest energy storage site in the body and to play a significant role in the regulation of lipids and glucose metabolism [30, 33].

WAT is adapted to handle increased amounts of energy delivered to it through mature adipocyte expansion (hypertrophy) or adipogenic progenitor recruitment, proliferation, and differentiation (hyperplasia) [6, 34, 35]. A balance between hypertrophy and hyperplasia is necessary to achieve an efficient expansion of the adipose tissue; close contact between the terminally-differentiated adipocytes and undifferentiated preadipocytes exists in order to communicate when the maximum threshold of adipocytic growth has been reached and differentiation of new lipid storage units are required [35].

2.1.4 Lipogenesis and Lipolysis

WAT has the capacity to store and release energy in the form of TAGs through synthesis (lipogenesis) or hydrolysis (lipolysis) of this high-energy molecule [6, 22, 33, 37]. Both processes can occur simultaneously and they are tightly regulated by metabolic (e.g. glucose, non-esterified fatty acids), hormonal (e.g. insulin and catecholamines such as epinephrine), and nutritional (e.g. carbohydrates and lipids) factors [33, 36, 38]. The ability to regulate adipose tissue metabolism is essential for body weight homeostasis, and dysregulation of these processes can contribute to obesity-related illnesses such as insulin resistance and type 2 diabetes [36, 39].

Lipogenesis

Fatty acid uptake in adipocytes is required for the production and storage of energy, which takes the form of TAG. TAG is an ester derived from fatty acids and glycerol-3-phosphate that is mostly obtained through dietary intake, and secreted from the intestine and the liver as lipoprotein-bound molecules [6, 22, 36-38]. Prior to cellular intake, this high-energy molecule is hydrolyzed by lipoprotein lipase (LPL) located on the luminal surface of endothelial cells in the capillaries, resulting in the release of fatty acids into the blood as albumin-bound, non-esterified molecules [33, 36]. The newly-freed fatty acids are transported across the plasma membrane via a series of specific transporters (Fatty Acid Transport Protein (FATP) and the protein CD36), facilitated by lipid binding proteins (aP2) expressed in the mature adipocytes [36]. Once in the

cytoplasm, fatty acids are esterified into acyl-coenzyme A and they are used in conjunction with glycerol-3-phosphate for TAG reassembly [33, 36].

Alternatively, fatty acids can be acquired to a lesser degree through fatty acid synthesis from non-lipid sources, such as carbohydrates [22, 33, 37]. This process, called *de novo* lipogenesis, involves the production of fatty acids from acetyl-CoA and malonyl-CoA by fatty acid synthase enzymes in the liver and adipose tissue [22, 33, 36].

Lipogenesis is induced by insulin through the regulation of glucose transporters and by extension, cellular glucose uptake [22, 36, 37]. Glucose, which is used for the production of glycerol-3-phosphate through glycolysis, is transported across the plasma membrane in a process that involves the translocation of insulin-sensitive glucose transporters (i.e. Glut-4) from intracellular vesicles to the plasma membrane. [36, 39]

Lipolysis

In situations of caloric restriction, stored TAG is released from WAT through the process of lipolysis, which involves the hydrolysis of intracellular TAG to ultimately yield glycerol and free fatty acids. More specifically, TAG is hydrolyzed through a multistep process that allows one fatty acid chain to be released at each step, resulting in the production of diacyglycerol, then monoacylglycerol, and finally glycerol [22, 36, 39, 40].

Lipolysis is primarily induced by glucagon, epinephrine and norepinephrine via a cyclic adenosine monophosphate (cAMP)-dependent pathway [36, 40]. These

extracellular stimuli trigger the activation of G protein-coupled receptors, which leads to an increase in intracellular cAMP that activates cAMP-dependent protein kinase A, and subsequently, lipases in adipose tissue [22, 33, 40]. The complete hydrolysis of TAG into glycerol and fatty acids involve three major lipases, which are adipose triglyceride lipase (ATGL), hormone-sensitive lipase (HSL), and monoglyceride lipase. ATGL and HSL are responsible for hydrolyzing TAG into diacylglycerol, and diacylglycerol into monoacylglycerol, respectively. Monoglyceride lipases, which are unregulated by hormones and are naturally found in abundance within adipocytes, further hydrolyze monoacylglycerol into glycerol and free fatty acids [36, 40-42].

After lipolysis, the newly-released fatty acids are transported to areas in need of energy or they are re-esterified for TAG reassembly within adipocytes [22, 41]. Glycerol, on the other hand, can be allocated to others tissues to be metabolized [42].

2.2 Cellular Composition in Adipose Tissue

Adipose tissue mainly consists of a collection of cells including: adipocytes, fibroblasts, vascular smooth muscle cells, endothelial cells, monocytes, macrophages, and lymphocytes [43-46]. Since adipose tissues have different metabolic and mechanical functions depending on their location within the human body, cell population composition between adipose depots tends to differ, with the exception of terminally-differentiated adipocytes being the most abundant cell type within the tissues [30, 46]. More importantly, studies have shown that adipose tissue provides a rich source of

mesenchymal stem cells (MSCs), which are multipotent adult stem cells with the ability to differentiate along the chondrogenic, myogenic, osteogenic, neurogenic and adipogenic lineages [6, 30, 44, 47]. MSCs are naturally found throughout the body, in locations such as the bone marrow, adipose tissue, skeletal muscle, and human umbilical cord, where they contribute to tissue regeneration and homeostasis [46, 51].

2.2.1 Adipose-Derived Stem Cells

A variety of names have been used in previous studies to describe the plastic-adherent regenerative cell population that can be isolated from adipose tissue through collagenase digestion, including: adipose-derived stem cells (ASCs), adipose-derived adult stem/stromal cells (ADAS), adipose-derived stromal cells (ADSCs or ASCs), adipose mesenchymal stem cells (AdMSCs), lipoblasts, preadipocytes, and processed lipoaspirate (PLA) cells [48 - 50]. In order to minimize confusion, the International Federation of Adipose Therapeutics and Sciences (iFATS) has settled on the term "adipose-derived stem cells (ASCs)" to describe the population of MSCs and more-committed adipogenic progenitors that are located in the stromal vascular fraction (SVF) of adipose tissue [6, 50].

As discussed, ASCs have the potential for multilineage differentiation [6, 16-18, 26, 30, 31, 33]. In the SVF, ASCs comprise roughly 2% of the total cell population, as compared to MSCs in the bone marrow, which represent only 0.002% [2], making adipose tissue one of the most abundant sources of stem cells in adults. Additionally,

ASCs can be obtained in large quantities through minimally-invasive fat procurement procedures such as liposuction [26, 51]. Once harvested, ASCs can be isolated from adipose tissue through a series of separation techniques involving filtration and centrifugation after collagenase digestion [48]. Depending on the donor source, between $1 \times 10^7 - 6 \times 10^8$ ASCs can be obtained by processing 300 mL of tissue, with a high viability (>90%) among the freshly-isolated cells [52]. Due to the ease of harvest, accessibility, and abundance of adipose tissue, ASCs have become an attractive multipotent stem cell source for regenerative medicine [26, 31, 33, 36].

2.2.2 Adipose-Derived Stem Cell Immunophenotype

ASCs can be identified within a mixed cell population by determining cell surface marker expression patterns (Table 2.1). Overall, a similar immunophenotype can be seen in human bone marrow-derived MSCs and human ASCs. Both cell types express: ECM proteins (collagens, osteopontin and osteonectin, CD90 (Thy-1), and the glycoprotein CD146), adhesion molecules (CD9 (Tetraspanin), CD29 (β-1 integrin), CD105 (endoglin), CD166 (activated lymphocyte cell adhesion molecule)), receptor molecules (CD44 (hyaluronan) and transferrin receptor), enzymes (aldehyde dehydrogenase (ALDH), CD73 (nucleotidase), CD10 and CD13 peptidases), cytoskeleton proteins (α-smooth muscle actin and vimentin), complementary regulatory proteins (CD59 and CD55 (decay accelerating factor)), as well as other markers such as ATP-binding cassette superfamily G member 2 (ABCG2) and major histocompatibility complex (MHC) class I

antigen (HLA-ABC). The cell markers that are expressed in ASC populations and not MSCs derived from bone marrow include CD49d (α-4 integrin), CD34, which can be found in early vascular-associated tissue, and Sca-1 (stem cell antigen-1) [1, 50-52]. The Sca-1 protein, along with ALDH and ABCG2, are strongly expressed in hematopoietic stem cells [1, 53]. Previous studies have recorded contrasting results regarding the expression of CD106, resulting from using different cell sources and culturing parameters, both of which can have a profound effect on ASC proliferation and differentiation [52].

A comparison between ASCs from the subcutaneous and visceral depots yielded similar expression profiles at early passages. Both cell populations expressed similar proteins as adult MSCs (CD29, CD44, CD73, CD90, CD105) while having low expression of hematopoietic (CD14, CD34, CD45) and endothelial (CD31) markers [54, 55]. With increasing passages, stromal-associated markers (CD13, CD29, CD44, CD63, CD73, CD90, CD166) were expressed more prominently while the stem cell marker CD34 experienced a decrease in expression [50, 55, 56]. A summary of the cell markers expressed by ASCs is given in Table 2.1 [50-53].

Table 2.1: Summary of cell markers expressed in ASCs [50 - 53]

Category	Surface Marker
Extracellular matrix molecules	CD90 (Thy 1) CD146 (Muc18) Collagen type I Collagen type III Osteopontin Osteonectin
Adhesion molecules	CD9 (Tetraspan) CD29 (β-1 integrin) CD49d (α-4 integrin) CD54 (ICAM-1; Intracellular adhesion molecule) CD105 (Endoglin) CD166 (ALCAM; Activated leukocyte cell adhesion molecule)
Receptor molecules	CD44 (Hyaluronate) CD71 (Transferrin)
Enzymes	CD10 (Neutral endopeptidase) CD13 (Aminopeptidase) CD73 (5'ecto-nucleotidase) Aldehyde dehydrogenase
Category	**Surface Marker**
Cytoskeleton proteins	α-smooth muscle actin Vimentin
Complementary regulatory proteins	CD59 (complement protein) CD55 (DAF; Decay accelerating factor)
Stem cell and others	CD34 (Sialomucin protein) ABCG2 (ATP-binding cassette superfamily G member 2) Sca-1 (Stem cell antigen-1) HLA-ABC (Major histocompatibility complex class I antigen)

2.3 Proliferation and Differentiation of ASCs

ASCs have the ability to self-renew and proliferate by undergoing mitotic division to generate new daughter cells with an identical genetic profile [57]. Furthermore, ASCs

have the potential to commit to a more specific differentiation pathway (ie. chondrogenic, myogenic, adipogenic, osteogenic) when introduced to environmental cues [58, 59].

Adipogenesis is a continuous event that occurs throughout the human life in both prenatal and postnatal states [60]. Adipogenic differentiation can result from cell turnover in a normal tissue renewal procedure or from the generation of more fat mass to accommodate lipid storage increase [57]. Prior to adipogenic differentiation, ASCs must undergo growth arrest, which can be induced by cell-cell contact or from the addition of adipogenic factors [57, 58]. The cells may undergo up to two additional rounds of mitotic clonal expansion after becoming more committed to the adipogenic lineage, followed by a secondary and permanent growth arrest, which then triggers the expression of adipogenic transcriptional factors [57].

2.3.1 ASC *In Vitro* Proliferation

A general approach to *in vitro* cell culturing involves the promotion of cell viability and population growth before the induction of differentiation. Freshly isolated cells from the adipose SVF are plated on tissue culture polystyrene in the presence of culture medium containing 10% fetal bovine serum (FBS), at 37^{o}C and 5% CO_2 [48, 59]. While the exact chemical composition of FBS is poorly characterized and highly variable, FBS is added as a supplement for ASC expansion, cell adhesion, cell growth, and as a source of vital nutrients [60, 61]. Within 1 to 2 days after initial seeding, non-

adherent cells, such as hematopoietic cells, are removed by aspiration, leaving behind the adherent ASC population to undergo expansion [38, 60].

The effects of cell passaging on ASC doubling time have been investigated in previous studies [62, 63]. In earlier passages, the doubling time for ASCs remained under 70 hours up until the 9^{th} passage, when cell proliferation was severely hampered due to senescence [62]. In addition, a correlation exists between the proliferation rate and the donor age and health for ASCs extracted from primary sources. Generally, cells obtained from older donors with higher BMI values possess a longer doubling time [62, 63].

2.3.2 Adipogenic Differentiation

Adipogenesis is a complex process regulated by several transcriptional factors that leads to the formation of mature adipose tissue. Similar to ASC proliferation, adipogenic differentiation is affected by donor BMI, gender, age, and culture conditions [62]. For ASC *in vitro* cultures, adipogenic differentiation is induced using supplemented medium containing compounds that are associated with the cAMP signalling pathways in lipogenesis and lipolysis [38, 58]. These supplements include insulin, insulin like growth factor-1 (IGF-1), glucocorticoids (e.g. dexamethasone and hydrocortisone), isobutylmethylxanthine (IBMX), triiodothyronine (T3), biotin and pantothenate [48, 58].

2.3.3 Transcriptional Control for Adipogenesis

Overall, adipogenesis is associated with changes in cell phenotype and the expression of over 2000 adipogenic genes [58]. The key transcriptional regulators for adipogenic differentiation include peroxisome proliferator-activated receptor-γ (PPARγ) and the CCAAT/enhancer binding protein family (C/EBP) [49, 57, 64]. Upon stimulation from the pro-adipogenic supplements, the transcriptional factors C/EBPβ and C/EPBδ are expressed in the cell population. These in turn serve to activate PPARγ through the C/EBP binding site on the PPARγ promoter, causing an elevation in PPARγ expression [65]. C/EBPα gene expression is triggered, which leads to cellular growth arrest and an enhanced expression in genes responsible for the adipogenic phenotype [57, 64]. Additionally, the raised level of C/EBPα expression further induces PPARγ expression, creating a feedback loop that amplifies both transcriptional components [57, 58, 64]. At this point, the cells undergo massive triglyceride accumulation and they actively produce adipogenic gene products, including glycerol-3-phosphate dehydrogenase (GPDH), fatty acid synthase (FAS), acetyl CoA carboxylase, glucose transporter type -4 (Glut-4), insulin receptor, and the adipocyte-specific fatty acid binding protein (aP2) [57, 64]. Another key transcriptional factor that is involved in adipogenesis is adipocyte determination- and differentiation-dependent factor-1/sterol regulatory element-binding protein-1 (ADD-1/SREBP-1). Expression of this gene primarily serves to modulate PPARγ expression and to stimulate the expression of LPL and other genes associated

with mature adipocytes [58, 64]. Figure 2.1illustrates the series of gene upregulation involved in adipogenesis.

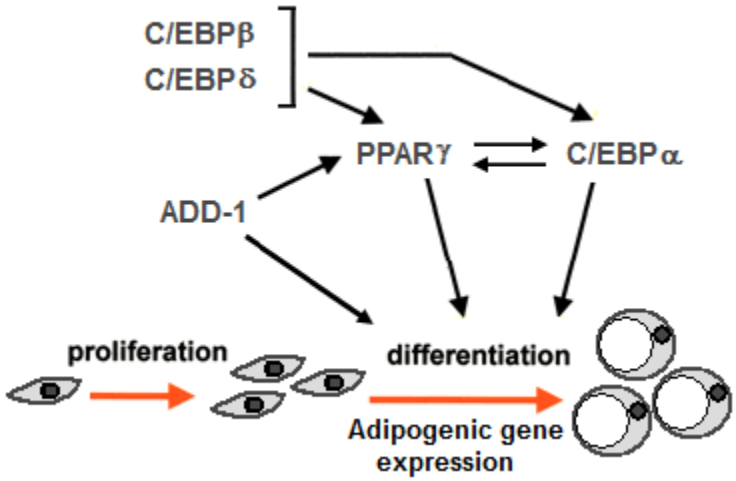

Figure 2.1 Transcriptional regulation for adipogenesis

2.3.4 Adipogenic Differentiation Modulating Factors

Hormones and growth factors can act to promote or inhibit adipogenesis through signal transmission via specific receptor interactions [66]. As previously mentioned, common factors used for adipogenic differentiation induction include insulin, insulin-like growth factor 1 (IGF-1), glucocorticoids (e.g. hydrocortisone), isobutylmethylxanthine (IBMX), triiodothyronine (T3), biotin and pantothenate [48, 58].

Insulin induces differentiation via binding to insulin receptor substrate-1 and -2 (IRS-1, IRS-2), thereby initiating a series of tyrosine phosphorylation events which ultimately lead to the activation of PPARγ and C/EBPα [67, 68]. Differentiation

induction occurs similarly with IGF-1, as the substrates can bind to both insulin receptors as well as IGF-1 receptors, which are both tyrosine kinases [66, 67]. Additionally, IGF-1 has positive effects on differentiation and proliferation, although the degree of adipogenic differentiation is depot-specific, where visceral ASCs are more susceptible to the effects of IGF-1 than subcutaneous ASCs [67].

Glucocorticoids and T3, both of which belong to the nuclear hormone family, influence adipogenesis through gene transcription regulation after binding to their respective receptors [66, 69]. Glucocorticoids were reported to induce the expression of C/EBPδ resulting in the expression of the key transcriptional factors PPARγ and C/EBPα [66]. T3 regulates many important genes involved in adipogenic differentiation including genes for fatty acid synthase, Glut-4, and LPL [70]. IBMX, biotin, and pantothenate promote lipogenesis by functioning to increase cAMP accumulation, acting as a cofactor for fatty acid synthesis, and a substrate for acetyl-coA synthesis, respectively [58, 66].

In contrast, most cytokines, such as tumor necrosis factor-α (TNF-α) and interleukin-1 (IL-1), tend to suppress adipogenic differentiation by inhibiting PPARγ [57]. Other adipogenic inhibiting factors include growth factors belonging to the transforming growth factor- β (TGF-β) family, which support cellular proliferation and the expression of the transmembrane molecule preadipocyte factor-1 (Pref-1), which is involved in the inhibition of C/EBPβ and C/EBPδ and consequently, the suppression of C/EBPα and PPARγ [57, 71].

2.3.5 Adipokines

Mature adipocytes secrete a series of factors, termed adipokines, which contribute to appetite regulation, immunological responses, and vascular function [58, 66]. Common examples of these factors include: leptin, adiponectin (Acrp30), TNF-α, macrophage migration inhibitory factor (MIF), angiotensinogen, and plasminogen activator inhibitor-1 (PAI-1) [66].

Leptin is a hormone encoded by the obese (ob) gene, and its primary role involves the regulation of energy balance [58, 66]. Specifically, leptin binds to its receptors located in the hypothalamus, which causes appetite suppression and the promotion of energy expenditure [66, 72]. As a result, an increase in leptin expression leads to a negative energy balance, where energy expenditure is greater than energy intake through dietary means [72]. Similarly, adiponectin functions as a factor in energy balance regulation; it is secreted at high levels by mature adipocytes, with higher levels found in visceral fat than subcutaneous fat [73]. Adiponectin primarily targets the muscles and liver, where it enhances insulin sensitivity, increases fatty acid oxidation, and decreases hepatic glucose output [73, 74].

TNF-α and macrophage migration inhibitory factor (MIF) are immune-related proteins [66]. Traditionally, TNF-α is associated as a macrophage product that induces fever, inflammation, and apoptotic cell death, although TNF-α has also been reported to

influence metabolic activities by inducing insulin resistance and suppressing both glucose uptake and fatty acid metabolism [73]. MIF functions as an immunoregulatory cytokine by suppressing the anti-inflammatory effects of glucorticoids [74].

Proteins of the renin-angiotension system, such as angiotensinogen and angiotensin II, are also produced in adipose tissue [74, 75]. Generally, these components regulate blood pressure by mediating sodium and water reabsorption in the kidneys, aldosterone secretion from the adrenal gland, and vascular tone [75, 76]. In addition, these factors influence adipogenic development by promoting lipogenesis, which in turn promotes both adipocyte hypertrophy and adipogenic differentiation. Angiotensin II also inhibits lipolysis and preadipocyte recruitment in mature adipose tissue [74, 76].

PAI-1, a member of the serine protease inhibitor family, is one of the proteins involved in hemostasis that is secreted by adipocytes [77]. More specifically, this compound promotes thrombosis and fibrosis [78]. In blood, PAI-1 enhances clot formation by acting as the primary inhibitor to fibrinolysis through the inhibition of urokinase-type and tissue-type plasminogen activator [74]. In tissues, PAI regulates vascular remodeling and promotes ECM accumulation [78]. PAI-1 is also linked to obesity and insulin resistance, with elevated levels of circulating PAI-1 found in the early stages of insulin resistance as well as in diabetes [78, 79]. In contrast, weight loss and improved insulin sensitivity result in lowered levels of PAI-1 [79].

2.4 Adipose Tissue Extracellular Matrix

The ECM is a meshwork of interlocking proteins, glycoproteins and proteoglycans, uniquely arranged in a three-dimensional structure [80, 81]. The ECM is an integral part of all tissues and organs, and it serves many important functions such as providing structural support, mechanical strength, and adhesion sites for cell surface receptors, as well as acting as a reservoir of signalling molecules that can control cell behaviour [80 - 82]. Cellular interactions with the ECM can trigger intracellular signalling pathways mediated through integrins, which are embedded in the cell membranes, and interconnect with the cytoskeleton. This signalling can trigger a cascade of events that can modulate cell migration, proliferation, differentiation, and apoptosis [81]. The protein composition in the ECM varies, and is dependent on a myriad of factors including tissue type, location, and the age of the host [80]. Furthermore, ECM protein components are constantly remodelled by cell-secreted factors to accommodate new tissue growth or to repair damage as a response to wound healing [81].

In adipose tissue, the ECM is well-vascularised and rich in collagen [80, 81]. Each adipocyte is surrounded by a layer of ECM comprised mainly of collagen IV, referred to as the basal lamina [82]. The purpose of this layer is to act as an external, protective casing, minimizing the transfer of external mechanical stresses to the fragile, lipid-filled adipocytes [82].

2.4.1 Extracellular Matrix Components

The main classes of ECM molecules include glycosaminoglycans (GAGs) and fibrous proteins [81-83]. GAGs are often found covalently bonded to a core protein, forming proteoglycans, while fibrous proteins serve both structural and adhesive functions; the most common fibrous protein in the ECM is collagen (e.g. types I and IV). In addition, glycoproteins such as laminin mediate cell adhesion [81, 83].

Collagen Type I

Collagen type I is the most abundant extracellular protein in many human tissues [81]. Like all molecules belonging to the collagen class, collagen I possesses a right-handed triple helix structure, composed of three α-chains [84, 85]. Each α-chain possesses a left-handed helix conformation, and the three chains twist together to give rise to the quarternary, right-handed super helix structure that is stabilized by hydrogen bonds [85]. A glycine residue is located at every third position of the polypeptide chain, forming the characteristic $(\text{Glycine-X-Y})_n$ amino acid sequence repeat of collagen [84]. Proline and hydroxyproline are commonly found in the amino acid sequence, in the order of (Glycine-Proline-Y) or (Glycine-X-Hydroxyproline), where X and Y are arbitrary amino acids [84-86]. In the collagen structure, glycine, being the smallest amino acid, is generally located at the interior of the helix near the central axis, thereby leaving proline and hydroxyproline to the outer positions [84, 86]. This arrangement helps to stabilize collagen, rendering it a tightly-packed molecule [84]. Type I collagen is a heterotrimer in

which two of its α-chains are identical (α_1), while the third differs slightly in its chemical composition (α_2) [84, 86].

Collagen Type IV

Collagen type IV is the most common structural protein in the basal lamina [81]. Similar to collagen type I, collagen type IV is a heterotrimer molecule composed of three α-chains coiled together [84-86]. The triple helical regions of collagen type IV are interrupted by non-collagenous regions that lack glycine, which is necessary for the formation of a tight helix, as seen in collagen type I, and as such, collagen IV contains more kinks [84, 85]. Additionally, the C-terminus contains regions for dimers to form through disulfide linkages, causing collagen IV fibres to link head-to-head at the C-terminus [84]. These two features allow collagen type IV to form a 3-D mesh, characteristic of a network-type collagen [84, 86].

Laminin

Laminin is a glycoprotein that is found in abundance in the basal lamina [82, 87]. Visually, these trimeric proteins have a cross-shaped structure with three distinct regions that form three short arms (referred to as α-chain, β-chain, and a γ-chain), and one long arm [87]. Due to the size and shape of laminin, this glycoprotein can span across the basal lamina and bind to the cell surface, as well as collagen IV, heparan sulfate, nidogen,

and to itself, thereby forming an integrated structure within the basement membrane [82, 87, 88]. Laminin can bind to cells through integrin receptors, allowing these proteins to contribute to cell adhesion, differentiation, and migration [88].

A summary of the proteins that make up the adipose ECM is provided in Table 2.2.

Table 2.2: Summary of proteins found in adipose-derived extracellular matrix. [82]

• Calreticulin • Chitinase-3-like protein 1 • Collagen I, III, IV, V, VI, XII, XIV, XV, XVIII • Decorin • Dermatopontin • Elastin • Fibronectin • Fibulin-1, -3, -5 • Galectin-1, -3 • Glypican 1 • Heparan sulfate proteoglycan • Laminin α-4, β-1, β-2, γ-1 • Lumican	• Matrilin-2 • Microfibril-associated glycoprotein 4 • Mimecan • Nidogen 1, 2 • Periostin • Proteoglycan 4 • SPARC • Spondin-1, -2 • Tenascin-C, -X • Thrombospondin-1, -2 • Transforming growth factor-β-induced protein • Versican core protein (fibroblast proteoglycan)

2.5 Clinical Strategies for Soft Tissue Augmentation and Reconstruction

The loss of soft tissue can be caused by trauma, post-surgical defects, tumours, congenital deformities, and from aging [6]. In order to restore soft tissue volume, current clinical techniques involve the use of autologous, synthetic, and allogenic implants [7]. For large-volume defects, autologous tissue transfer using vascularized flaps of fat and muscle represents the gold standard for soft tissue augmentation. Unfortunately, these procedures require invasive surgery that can lead to deformity and morbidity at the donor

site [4, 89]. Free fat grafts lack the required vasculature to support tissue viability, which ultimately results in graft resorption and replacement by fibrous tissue and oil cysts. Similarly, autologous lipoaspirate transfer to correct small-volume defects leads to graft volume reduction over time, due to reabsorption [4, 6, 7]. While the reconstruction of large-volume defects is presently limited to surgery, small soft tissue defects can be temporarily corrected through minimally invasive means via commercially available, injectable dermal fillers [7].

2.5.1 Collagen

Collagen, being a naturally occurring compound in the human body, should exhibit biocompatibility and as a result, this protein from xenogenic and allogenic sources was the first to be investigated as a dermal filler [7, 85]. The bovine collagen-based fillers Zyderm® and Zyplast® were the first to achieve approval from the US Food and Drug Administration (FDA). However, xenogenic proteins can initiate allergic hypersensitivity reactions and as such, allergy tests are required prior to treatment [7]. Collagen derived from engineered human dermal fibroblasts (Cosmoderm® and Cosmoplast®) was developed as an alternative collagen-based dermal filler to lessen the chance of causing an allergic response [7, 90]. However, these dermal fillers do not have a long lasting effect, and they undergo complete implant resorption within 3 to 6 months [90].

2.5.2 Hyaluronic Acid

Hyaluronic acid (HA) is one of the most prevalent GAGs in the human body [6]. In the skin, HA has several functions including hydration, lubrication, and stabilization of connective tissues [91]. Since this compound is structurally identical within all species, the risk of sensitivity to xenogenic-derived HA is remote [90, 91].

Currently, the bacterial-cultured HA dermal filler Restylane® is the most commonly used facial rejuvenation product in the world [91, 92]. This dermal filler primarily consists of highly cross-linked HA particles that result in a longer and more stabilizing volume augmentation effect once implanted [90, 92]. Other similar bacterial-cultured HA products include Perlane®, which has a larger particle size, and Juvederm®, which uses an HA gel rather than particles [90-92]. While HA fillers show superior cosmetic results compared to collagen-based products, these fillers offer only a temporary solution and will undergo resorption 6 – 12 months after implantation [92].

2.5.3 Synthetic Injection

A series of synthetically-derived soft tissue augmentation fillers have been fabricated with the goal of producing a longer-lasting, if not permanent, filling effect [92]. Injectable poly(L-lactic acid) (PLA) microspheres, marketed in the US as Sculptra®, is a non-immunogenic, biocompatible, α-hydroxy acid polymer [92, 93]. Once implanted, PLA will induce an increase in fibroblast and collagen production as part of an inflammation response [94]. The cosmetic effects for Sculptra® have been reported to

last between 18 – 30 months [93, 94]. Sculptra® is primarily dependent on the host's ability for new collagen production to sustain its volumizing effect, which diminishes over time and as a result, repeated injections are required to sustain the desired volume [94].

Artefill® is another commercially available product designed to be a permanent dermal filler. It is composed of poly(methyl methacrylate) (PMMA) microspheres (30-50 μm in diameter) that are suspended in a water and collagen-based carrier gel [92]. PMMA, commonly known as Plexiglas, has an established history of being biocompatible as it is chemically inert, and it has been used in other clinical applications such as joint replacement, cataract surgery, and dental procedures [95]. Since PMMA microspheres are not resorbed, they can provide a longer-lasting correction of approximately five years [92, 96]. However, implantation is challenging since PMMA must be positioned superficially enough for the effects to be visible, while deep enough not to be palpable [92]. Additionally, the long-lasting results seen with PMMA when used in normal skin may not be possible with damaged tissues [96].

Injectable calcium hydroxyapatite (CaHA) microspheres have been developed as an alternative synthetic-based dermal fillant. Known commercially as Radiesse®, CaHA is biodegradable and biocompatible since the microspheres that are present have the same chemical composition as the inorganic constituent of teeth and bone [92, 97]. When injected, Radiesse® triggers new collagen formation, which is a similar tissue response as seen in the PLA-based fillers [97]. The cosmetic effects for injected CaHA, while not

permanent, are longer lasting than those seen with collagen and HA injections, and can generally persist for up to 2 years [92].

2.6 Adipose Tissue Engineering

Clinical strategies used for correcting soft tissue defects tend to have short-term effects and can lead to complications such as pathogen transmission and immune rejection issues [4, 6]. Engineered adipose tissue has the potential to avoid these disadvantages while providing permanent soft tissue augmentation [1-4]. To date, the most common tissue engineering strategy involves *in vitro* cell seeding of scaffolds, which mimic the ECM, followed by a culture period to allow for cell growth and tissue maturation [3, 4, 6].

2.6.1 Challenges in Adipose Tissue Engineering

In order to successfully engineer adipose tissue, the construct must be host compatible, sustainable, and bioactive to trigger tissue growth by lipogenesis (Table 2.3) [1, 26]. Ideally, the construct should be matched to the host so as to avoid triggering an immunological response upon implantation and from toxic implant degradation products [26]. Furthermore, the construct should be able to interact with surrounding tissues at the implantation site by recruiting neighbouring host cells to induce tissue growth and sustain long-term viability and function [2, 3, 26]. The scaffold should ideally be degradable,

lasting long enough to allow for the seeded cells to secrete their own extracellular matrix components [6].

A rational scaffold design is imperative in order to meet these key requirements. Since the scaffold is meant to mimic the natural ECM environment, the scaffold should be biocompatible and promote cell viability, proliferation, and differentiation [1 - 3]. A porous scaffold is important for adipose tissue engineering to facilitate nutrient transport to the cells and pore sizes should accommodate adipocyte expansion as the differentiating cells accumulate lipid [2, 26]. Scaffold mechanical stiffness should closely resemble that of fat to avoid frictional irritation with the surrounding host tissues and as such, the scaffold should remain soft and flexible [2]. Currently, there is evidence to support that scaffold mechanical properties can impact MSC lineage commitment by influencing the different tensile stresses that cells experience in their cytoskeletons when adhered to the scaffold surface [98]. However, the specific mechanisms involved in how these stresses can control lineage commitment have yet to be fully elucidated. Generally, soft surfaces tend to promote stem cell differentiation into adipocytes or myocytes, while harder surfaces will promote osteogenic differentiation [98].

Table 2.3 Requirements for adipose tissue engineering [1, 26]

Host compatibility
- Minimal immune response from implantation
- Degradation products of constructs compatible with host
Bioactivity
- Regeneration of functional tissue
- Incorporation of functional vascular supply
Construct sustainability
- Viability and function of constructs are long-term

2.6.2 Cell Sources

The cells selected for tissue engineering strategies should be easily accessible, exist in abundance, and they should have the capability of contributing to tissue regenerative responses [6, 9]. In most cases, primary ASCs are favoured as they can be autologously sourced, are able to undergo mitotic division in ischemic conditions and can be stimulated to differentiate along the adipogenic lineage [1, 4, 9, 26]. In contrast, terminally-differentiated mature adipocytes are fragile and have limited cellular proliferation capability, thereby limiting their application for tissue regeneration [1, 6].

Cell lines

The most extensively characterized cell lines for adipose tissue engineering applications are the 3T3-L1 and 3T3-F442a murine cloned lines [37]. These lines are

widely used as simple models for preadipocyte differentiation, as they exhibit the morphological and biochemical characteristics of fat cells [37, 99]. In addition, these immortalised cell lines are well studied, commercially available, can be grown indefinitely in culture and are capable of differentiating *in vitro* when they enter a resting state. In general, cell lines were used to pioneer adipose tissue engineering and they have helped contribute to a better understanding of cellular effects from different culture conditions [2, 99]. However, primary cells may give a more accurate model to the complex *in vivo* state since cell lines have undergone significant mutations to become immortal [37]. Other less frequently used preadipocyte cell lines include Ob17, which is derived from the epididymal fat pads of mice, TA1 and 30A5 murine cells [37].

Primary stem cells

Stem cell sources used in adipose tissue engineering applications include embryonic stem cells (ESCs), bone marrow-derived MSCs, and ASCs [1, 6, 26]. ESCs are pluripotent and as such, are capable of differentiating into any cells derived from the endoderm, mesoderm, or ectoderm [1, 26, 34]. ESCs are harvested from the inner cell mass of the blastocyst, which is an early stage embryo [1, 26]. Due to the source from which they are cultivated, the use of human ESCs in research has been met with strong opposition and ethical concerns. For these reasons, adult stem cells are preferred over ESCs [1]. Bone marrow-derived MSCs (bMSCs) can be obtained from bone marrow aspirates and previous studies have demonstrated the capacity for these MSCs to undergo

adipogenic differentiation, making them a potential cell source for adipose tissue engineering [31, 37, 47]. However, the process of procuring bone marrow is painful and it has a low yield (0.002% of the cell population) of regenerative cells [2, 6]. Alternatively, ASCs have shown great promise for adipose tissue engineering. As previously mentioned, a substantial number ($3 \times 10^5 - 2 \times 10^6$/mL) of ASCs can be obtained through processing lipoaspirated or excised adipose tissue [2, 6, 26, 51, 52]. ASCs have the potential to be used in both autologous and allogenic applications, as they have been shown to have an immuno-privileged status and can mediate inflammation [9].

2.7 Scaffold Material

As previously discussed, a tissue-engineered scaffold provides structure and allows for cell adhesion while supporting cell viability and growth [1 - 3]. The material used for scaffold construction must be able to facilitate the regenerative function of the cells, to ultimately restore a fully viable and functioning tissue [1 – 3, 26]. A variety of synthetic polymers and natural-based biomaterials have been studied with the goal of building a scaffold that could best mimic the ECM in native adipose tissue. Table 2.4 provides a general summary of the most commonly investigated scaffolding materials [6, 11, 26]. Furthermore, the scaffolds used for adipose tissue engineering can either exist in a predefined shape, such as disks or sponges, or as injectable compounds, such as pre-hydrogels solutions, prior to *in vivo* delivery [1]. Synthetic and naturally-based materials have been used for the construction of both types of these scaffolds [1, 6, 26].

Table 2.4 Summary of scaffolding materials used in adipose tissue engineering [6, 11, 26]

Synthetic polymers	*Naturally-derived*
Polylactic acid (PLA)	Collagen
Polyglycolic acid (PGA)	Hyaluranon
Polylactic-co-glycolic acid (PLGA)	Gelatin
Polyethylene glycol (PEG)	Alginate
	Chitosan
	Decellularized tissue

2.8 Hydrogels

Hydrogels are water insoluble networks formed by the crosslinking of water soluble polymer chains [100]. In addition, these scaffolds can absorb water and swell while maintaining a specific geometry [100-101]. Injectable hydrogels make promising scaffolds for tissue engineering applications as they can retain a high, tissue-like water content and they can be chemically manipulated to achieve the desired physical properties [10, 101, 102]. Furthermore, they can be formed *in situ* following minimally-invasive injection to the site of interest. The injection of the liquid pre-polymer solution fills the injection site, and upon *in situ* gelation, results in an even distribution in the defect to restore the lost tissue volume [10, 101, 102-104]. The high water content in hydrogels provides a soft and elastic material that mimics native soft tissues to minimize frictional irritation [10, 101, 104].

Hydrogels possess a similar microstructure to the ECM, and can provide a microenvironment that is favourable for cell proliferation and differentiation [12, 101,

105, 106]. The highly-hydrated and porous environment also allows for nutrient, oxygen and waste transfer by diffusion, thereby promoting cell viability [102, 105]. Further, cells seeded within hydrogels are able to secrete ECM-components as part of the tissue remodelling response [101, 104].

2.9 Synthetic-Based Materials

Synthetic polymers have been used frequently as the building blocks for scaffold construction since they are a reliable source that can be chemically modified to control the degradability, mechanical properties and chemical properties of the scaffold, to create a well-defined and reproducible biomaterial [26]. Additional advantages to using synthetic scaffolds over natural ones include a significantly reduced risk for disease transmission and potentially, lower immunogenicity when implanted [107]. Poly(lactic acid) (PLA), poly(glycolic acid) (PGA), and poly(lactic-co-glycolic acid) (PLGA) are some of the most extensively studied materials for scaffolds as they are well characterized, easy to manufacture, and have previously been used in Food and Drug Administration approved devices [26, 99, 108]. When subjected to acid hydrolysis, these polymers degrade to form lactic and glycolic acid [26].

Two studies were conducted using PGA with a number average molecular weight (M_n) of 70 kDa as mesh scaffolds for *in vitro* and *in vivo* culturing, after seeding with 3T3-L1 preadipocytes. For the *in vitro* study, the scaffolds yielded an uneven distribution of white, fat like tissues, with the majority located at the rim of the constructs, after

culturing the scaffolds in adipogenic differentiation medium for 2 weeks [109]. For the *in vivo* study, the seeded scaffolds were implanted into the backs of immunodeficient NMRI mice for up to 24 weeks. When harvested, the scaffolds showed signs of viable mature adipocytes and blood vessel formation [108, 109]. In the second study, bone marrow-derived MSCs and ASCs were seeded on separate PLA scaffolds (M_n = 30 kDa), followed by 21 weeks of *in vitro* culturing by Mauney et al. Due to the rapid degradation of PLA, the scaffold was unable to support the production of adipose tissue. No *in vivo* studies have been performed using PLA scaffolds [110].

Macroporous PLGA (M_n = 80 kDa, 75:25 PLA to PGA) microspheres that were seeded with human ASCs showed an increase in proliferation and adipogenic differentiation levels after 7 days of *in vitro* culturing. The cell-seeded microspheres were then implanted in the sternal subcutaneous space of athymic mice for up to 16 weeks. The *in vivo* study showed that PLGA microspheres were able to support cell viability and adipose tissue growth, despite losing 30 – 40% of their initial volume [111]. A longer-term *in vivo* study was conducted where murine ASCs were seeded on PLGA disks and subsequently implanted in the back musculature of Lewis rats for up to 12 months. While adipose tissue formation was reported to peak at 2 months after implantation, this was followed by a sharp decrease due to scaffold degradation. After 5 months, the PLGA disk experienced complete degradation [112].

Poly(ethylene glycol) (PEG) with a molecular weight of 10 kDa was chemically crosslinked with branched, amino acid-modified PEG-amines to form hydrogels for

adipose tissue engineering in a study conducted by Brandl et al [105]. After seeding with 3T3-L1 preadipocytes, the cells on this scaffold showed evidence of adipogenesis 9 days after adipogenic induction. However, neither *in vivo* studies nor long-term studies were performed [105]. Overall, synthetic scaffolds have shown varying degrees of success for the maintenance of cell viability and the promotion of adipogenesis over a short period of time [26].

2.10 Naturally-Based Materials

Naturally-based materials are components that can be extracted from other living organisms and as such, they typically have good biological performance [26, 113]. An advantage to using natural scaffolds is that they possess naturally-derived molecules that can trigger positive cell responses [104]. In adipose tissue engineering, the effects of various naturally-based scaffolds on seeded cells have been studied, including collagen, hyaluranon, gelatin, alginate, chitosan, and decellularized tissue [6, 11, 16].

2.10.1 Chitosan

Chitosan is a linear polysaccharide of N-acetyl-glucosamine and N-glucosamine units linked by a β(1-4)(glycosidic)linkage, and it is obtained from deacetylation of chitin, which is derived from the shells of crustaceans [114]. Recently, this biocompatible compound has attracted attention for tissue engineering applications due its favourable properties; chitosan is not only structurally similar to ECM components, it can also

promote cell attachment and viability [114-116]. Furthermore, chitosan naturally exerts antimicrobial properties [114, 116].

The physicochemical properties of chitosan, such as solubility and degree of ionization, can be modified by chemically reacting with the free amine groups attached to its backbone [116, 117]. Chitosan in its natural form is only soluble at low pH, but this compound can be chemically modified to form glycol chitosan, thereby rendering it water-soluble. A water-soluble glycol chitosan has many potential uses in tissue engineering, particularly for the construction of biocompatible hydrogel scaffolds [105].

In addition, the cationic amine group in chitosan can support cell adhesion [114, 115]. When degraded, saccharides and glucosamines are formed, which are naturally found in mammal metabolism [116]. Furthermore, N-acetyl-glucosamine receptors on macrophages can interact with these compounds, allowing macrophages to become activated and secrete platelet-derived growth factor (PDGF) and Interleukin 1 (IL-1), both of which are necessary for wound healing [114-116].

Chitosan and chitosan derivatives have been used in adipose tissue engineering applications, mostly blended with collagen or gelatin, to improve cell adhesion and viability, as injectable hydrogel scaffolds [101, 117]. *In vitro* studies using chitosan-based hydrogels have shown promise in supporting cell viability, proliferation and adipogenesis after the ASC-seeded scaffolds were cultured for up to 14 days [101, 117, 118]. *In vivo* studies conducted for 14 days showed a peak in lipid content and vascular density at 7 days, followed by a slight decrease at 2 weeks after implantation in Lewis rats [101].

2.10.2 Adipose Extracellular Matrix-derived Scaffolds

The ECM is an attractive source of scaffolding materials since it naturally contains the native proteins and growth factors that can induce cell adhesion, proliferation and differentiation [80]. Decellularized ECM has been successfully extracted from multiple sources, including the dermis of the skin, submucosa of the small intestine and urinary bladder, pericardium, liver, and tendon [80, 119]. Decellularization involves the removal of cellular and nuclear compounds, while preserving the matrix and natural proteins found within ECM [119]. Overall, decellularization involves a combination of chemical, physical, and biological treatments in order to disrupt the cells to facilitate cell content removal [110, 120].

In previous work in the Flynn lab group, the *in vitro* culture of adipose-derived ECM with human ASCs demonstrated that the decellularized adipose tissue (DAT) matrix provided a microenvironment that supported adipogenesis. The cultured ASCs expressed high levels of the adipogenic markers PPARγ and C/EPBα, which as discussed, are master regulators of adipogenesis [120]. In another group, a powderized form of the human adipose-derived ECM was cultured with human ASCs and injected into the backs of nude mice. The seeded ECM showed signs of adipogenesis, with accumulated intracellular lipid droplets. In addition, the adipogenic genes PPARγ, C/EPBα, aP2, adiponectin and leptin, were expressed within the constructs at 20 days post implantation [121].

2.11 Chondroitin Sulphate

Chondroitin sulphate (CS) consists of repeating D-glucuronic acid and N-acetyl galatosamine disaccharide units, sulphated at either the 4- or 6-position [122]. In the human body, CS is an important structural component in the ECM and it is most predominantly found in cartilage [123, 124]. CS has shown a number of useful biological properties, including anti-inflammatory activity, as well as water and nutrient absorption [122, 123]. In tissue engineering applications, CS and CS-derivatives are commonly used to form biocompatible hydrogels through various chemical or photocrosslinking methods [124, 125]. Recently, photopolymerizable CS has been developed by utilizing glycidyl methacrylate to react with CS in a heterogeneous reaction, forming methacrylated chondroitin sulphate (MCS) [100]. Photopolymerization is an attractive option as it is a fast and efficient crosslinking method that provides significant spatial control over the hydrogel shape [100]. When exposed to UV light, photopolymerizable polymers can effectively form a crosslinked, insoluble, three-dimensional network in any shape desired [11]. While no studies to date have been reported on CS-based scaffolds for adipogenic tissue engineering, *in vitro* cultures of MSCs have shown promise that CS can readily support cell viability and growth after cell encapsulation [126].

Chapter 3

Materials and Methods

3.1 Overview

Figure 3.1 summarizes the overall procedures used for scaffold construction, cell culturing and sample analysis in this study:

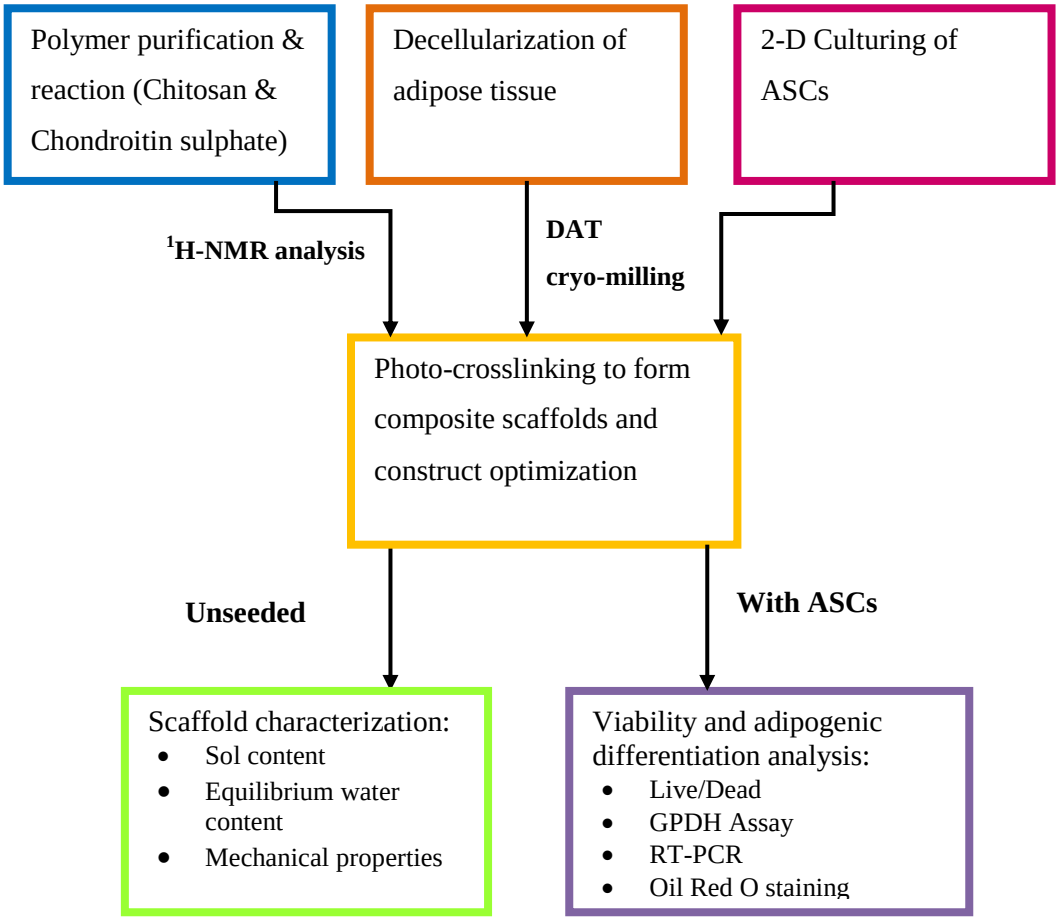

Figure 3.1 Methodologies used for scaffold construction, seeding and sample analysis.

3.2 Materials

Deionized water used was of type I purity, obtained from a Millipore Milli-Q Plus ultrapure water system. Chondroitin sulphate was donated by Stellar Pharmaceuticals Inc. (London, ON, Canada). All other chemicals used in the experiments were purchased from Sigma-Aldrich Canada Ltd. (Oakville, ON, Canada) and were used as received, unless otherwise stated.

3.3 Polymer Purification and Reaction

3.3.1 Purification of Glycol Chitosan

Insoluble impurities were removed following a previously established protocol [115]. First, 1 g of glycol chitosan (Wako Chemical USA, Inc.) was dissolved in 75 mL of deionized water, followed by filtration through a Fisherbrand qualitative filter paper (coarse porosity). The filtrate was then dialyzed against 5 L of deionized water for 8 h using Spectra/Par dialysis tubing with a molecular weight cutoff of 50 kDa (Spectrum Laboratories Inc., Rancho Dominguez, CA, USA) to remove the soluble, low molecular weight impurities. The water was replaced four hours into the dialysis process. The purified glycol chitosan was transferred into 50 mL centrifuge tubes before being frozen at -20°C for 8 h and lyophilized for 48 h.

3.3.2 Methacrylation of Glycol Chitosan via Glycidyl Methacrylate

Glycol chitosan was methacrylated following an established protocol [115]. Purified glycol chitosan (0.4 g) was dissolved in 20 mL of deionized water to obtain a 2.0 % (w/v) solution and the dissolved glycol chitosan was adjusted using 1 M sodium hydroxide to pH 9.0. Glycidyl methacrylate (3 % (v/v)) was added to the solution to achieve an initial molar ratio of glycidyl methacrylate to free amine (per mol glycol chitosan residue) of 0.1. The solution was then allowed to react for 24 h before the reaction was neutralized (pH 7) with 1 M hydrochloric acid. In order to remove any unreacted glycidyl methacrylate, the methacrylated glycol chitosan (MGC) solution was dialyzed against 5 L of deionized water with dialysis tubing (molecular weight cutoff of 12 kDa, obtained from Fisher Scientific, Hanover Park, IL, USA) for 4 h and the deionized water was replaced 2 h into the dialysis process. Finally, the purified MGC solution was transferred into 50 mL centrifuge tubes where it was subsequently frozen to -20°C for 8 h, then lyophilized.

3.3.3 Methacrylation of Chondroitin Sulphate via Methacrylate Anhydride

The procedure used to methacrylate chondroitin sulphate was based on the study by Li et al. but it was optimized to meet the requirements for this study [100]. Chondroitin sulphate (1 g) was dissolved in 5 mL of 1.0 M sodium phosphate. A blend of methacrylic anhydride (0.15 mL) and dimethylsulfoxide (0.15 mL) was prepared and then added to the dissolved chondroitin sulphate. After 2 h incubation at room

temperature, the pH was adjusted with 5 M sodium hydroxide to pH 10 before the solution was allowed to react for an additional 22 h. The reacted chondroitin sulphate solution was dialyzed against 5 L of deionized water for 12 h in dialysis tubing (Fisher Scientific, Hanover Park, IL, USA) with a molecular weight cut-off of 3.5 kDa. The purified methacrylated chondroitin sulphate (MCS) solution was then lyophilized for 48 h and the final product was stored at -80°C.

3.3.4 Nuclear Magnetic Resonance Spectroscopy

^{1}H-NMR spectra of the polymers were obtained with a Bruker Avance-600 Ultrashield spectrometer, equipped with a 5 mm TBI S3 probe, with the data collected with the Bruker's XWINNMR software. Samples were prepared by dissolving the polymer in deuterium oxide to yield a concentration of 20 mg/mL and left to equilibrate for a minimum of 2 h at room temperature. Prior to analysis, the MGC samples were adjusted to pH 10 using 1 M sodium hydroxide and they were allowed to equilibrate within the spectrometer at 90°C for 10 min to ensure homogenous temperature distribution within the samples. MCS samples were also prepared using similar methods and the spectra recorded at room temperature.

3.4 Acquirement of Adipose Tissue Samples

Breast or subcutaneous abdominal adipose tissue samples were collected from female patients undergoing breast reduction or abdominoplasty surgery at the Kingston

General Hospital or Hotel Dieu Hospital in Kingston, Canada. The samples were transported to the lab on ice within 2 hours of harvesting in 100 mL of sterile, cation-free phosphate buffered saline (PBS), supplemented with 20 mg/mL bovine serum albumin (BSA). The age, weight and height of the patient from which the tissue originated were recorded. Research ethics board approval was obtained from Queen's University for this study (REB# CHEM-002-07).

3.5 Decellularization of Adipose Tissue

Cauterized portions were removed and discarded from the tissues upon arrival at the laboratory. The remaining portions were divided into 20 – 25 g sections and placed in a 250 mL plastic tub, where they were decellularized by following a previously optimized, detergent-free protocol summarized in Table 3.1. The 5-day extraction process involves a combination of mechanical disruption, polar solvent extraction, and enzymatic digestion. Overall, the tissue portions were decellularized after being exposed to a series of solutions (100 mL working volume), supplemented with 1 % (v/v) antibiotic/antimycotic (ABAM) solution (Invitrogen, Burlington, ON, Canada) and 0.27 mM phenylmethylsulfonylfluoride (PMSF) solution, a protease inhibitor.

Table 3.1: Detergent-free, 5-day protocol for the decellularization of adipose tissue [6]

Day	Processing Steps
1.	• Freeze-thaw 3 times in Solution A (Freezing Buffer Solution) • Incubate for 16 h (overnight) in Enzymatic Digestion Solution 1
2.	• Polar solvent extraction in 99% isopropanol
3.	• Polar solvent extraction in 99% isopropanol
4.	• Rinse 3 times (30 min each) in Sorenson's Phosphate Buffer (SPB) Rinse (Rinsing Buffer Solution) • Incubate for 6 h in Enzymatic Digestion Solution 1 • Rinse 3 times (30 min each) in SPB Rinse (Rinsing Buffer Solution) • Incubate for 16 h (overnight) in Enzymatic Digestion Solution 2
5.	• Rinse 3 times (30 min each) in SPB Rinse (Rinsing Buffer Solution) • Polar solvent extraction in 99% isopropanol (8 hours) • Rinse 3 times (30 min each) in SPB Rinse (Rinsing Buffer Solution)

Initially, the tissue portions were submerged in a tris-ethylenediaminetetraacetic acid (Tris-EDTA) buffer at pH 8 (Solution A) and frozen at -80°C for 30 min. The samples were subsequently thawed under constant agitation at 37°C on an Excella^{TM} 24 Benchtop Incubator (New Brunswick Scientific, Edison, NJ, USA) at 150 rpm. The tissue portions were then transferred into fresh Solution A and refrozen. This cycle was repeated for a total of three times before the samples were incubated overnight under constant agitation in Enzymatic Digestion Solution 1, consisting of 0.25% (v/v) trypsin and 0.1% (v/v) EDTA (Gibco, Burlington, Canada).

Next, the tissues underwent a 48-h, polar solvent extraction to remove lipid content in 99% isopropanol. The isopropanol was changed every 8 h and the tissue was physically massaged by hand after the fresh solvent was supplied. Afterwards, the tissues

were rinsed three times (30 min) in SPB Rinsing Buffer Solution (8 g/L NaCl, 200 mg/L KCl, 1 g/L Na_2HPO_4, and 200 mg/L KH_2PO_4, at pH 8.0), followed by a second digestion in Enzymatic Digestion Solution #1 under agitation at 37°C, for 6 h. Again, the tissues were rinsed in SPB Rinsing Solution before they were subjected to overnight digestion in Enzymatic Digestion Solution #2 (55 mM Na_2HPO_4,17 mM KH_2PO_4, 4.9 mM $MgSO_4 \bullet 7H_2O$, 15,000 U DNase Type II (from bovine pancreas), 12.5 mg RNase Type III A (from bovine pancreas), and 2000 Units Lipase Type VI-S (from porcine pancreas)). The processed tissues were rinsed three times (30 min per rinse) in Rinsing Buffer Solution then immersed in 99.9% isopropanol for 8 h for a final polar solvent extraction. Finally, the decellularized matrix was rinsed three more times in Rinsing Buffer Solution, three times in 70% ethanol (30 minutes each rinse), and stored in sterile PBS at 4°C, supplemented with 1% (units) ABAM.

3.6 Cryo-milling of Decellularized Adipose Tissue

An optimized protocol to lyophilize and ball-mill grind the decellularized adipose tissue (DAT) was developed in order to homogenously blend the matrix within the composite scaffold constructs. Shortly after the decellularization process, the DAT was divided into 20 g portions, placed within 50 mL sterile centrifuge tubes, and snap frozen in liquid nitrogen. Afterwards, the DAT sections were lyophilized (~48 h) and then finely minced with sharp scissors. Approximately 20 mg of minced and dried DAT was transferred into a 1 mL cryogenic vial (Nalgene Nunc International, Rochester, NY), and

a freshly cleaned stainless steel milling ball (8 mm in diameter; Sartorius, Goettingen, Germany) was added to each vial. Up to 4 vial samples were prepared at one time, and they were frozen in liquid nitrogen before being loaded into the laboratory ball mill grinder (Sartorius, Goettingen, Germany), set to operate at 2500 rpm. The tissues were ground for a total of 2 min, and the samples were kept frozen during processing by reintroducing fresh liquid nitrogen into the vials every 20 s while grinding. The freshly ground DAT was stored at 4°C in 50 mL centrifuge tubes until further use. For use in cell culture studies, the DAT was sterilized by exposure to UV light for 60 min immediately before scaffold fabrication.

3.7 Fabrication of Polymer-DAT Composite Hydrogel Scaffolds

3.7.1 Fabrication of Methacrylated Glycol Chitosan-Based Scaffolds

MGC hydrogels were fabricated via photo-polymerization using a previously-established protocol (Amsden, Sukarto, Knight, & Shapka, 2007). Polymer solutions were formed by dissolving the MGC in proliferation medium (Dulbecco's Modified Eagle's Medium and Ham's F-12 (DMEM:Ham's F-12) nutrient mixture, 10% (v/v) fetal bovine serum (FBS) and 1% (w/v) Pen-Strep (100 U/mL penicillin and 0.1 mg/mL streptomycin)) to achieve a concentration of 1.5 % (w/v). The photoinitiator Irgacure 2959 (2-hydroxy-4′-(2-hydroxyethoxy)-2-methylpropiophenone), which was dissolved (0.05 % (w/v)) in deionized water and sterilized by filtration through a 0.22 μm pore Millex GP Syringe Driven Filter Unit (Millipore Express PES Membrane, Millipore, Carrigtwohill, Ireland),

was used for the polymerization. For the composite scaffold groups, UV-sterilized cryomilled DAT at varying concentrations (3 % (w/v) and 5 % (w/v)) were also added to the solutions and mixed by pipetting. Finally, 0.1 mL of each solution was transferred by pipette into a 16-well chamber glass slide (Nalgene Nunc International, Rochester, New York) and exposed to long wavelength ultraviolet light (320 – 390 nm, EXFO Lite, EFOS Corporation, Mississauga, Canada) at an intensity of 10.2 mW/cm^2 for 3 min, to form a hydrogel with a diameter of 7 mm and a height of 3 mm.

3.7.2 Fabrication of Methacrylated Chondroitin Sulphate-Based Scaffolds

Methacrylated chondroitin sulphate (MCS) was photo-polymerized to yield hydrogels using very similar methods. In brief, sterile MCS was dissolved in proliferation medium (DMEM:Ham's F-12, 10% (v/v) FBS and 1% (w/v) Pen-Strep) at a concentration of 10 % (w/v). Irgacure 2959 photoinitiator was sterilized and added (0.05 %(w/v)) to the dissolved polymer solution. Sterile cryo-milled DAT was added to the polymer solution at varying concentrations (0, 3 and 5 % (w/v)). The solutions were transferred into the 16-well chambers and exposed to UV light at an intensity of 10.2 mW/cm^2 for 3 min to form the hydrogels.

3.8 Scaffold Characterization

3.8.1 Sol Content Measurement

Immediately after photo-polymerization, the unseeded hydrogels were frozen in liquid nitrogen and lyophilized for 24 h. The initial dry mass was then recorded and each gel was incubated three times in 10 mL of deionized water for 3 h, to extract the sol content from the crosslinked gel. After the rinses, the gels were frozen in liquid nitrogen, lyophilized, and re-weighed to obtain their final dry masses. Since sol content should reflect the unreacted monomer in each hydrogel, the amount of DAT loss in the composite scaffolds during the washes was accounted for in the mass differences. To measure the amount of DAT that was lost, the wash water was filtered through a Whatman type I qualitative filter paper, and the remaining residue was lyophilized and weighed. The sol content was calculated using the following equation:

$$Sol = \frac{m_{dry,initial} - m_{dry,final}}{m_{dry,initial}} \quad [3.1]$$

where $m_{dry,initial}$ is the dry mass of the gel before the washes and $m_{dry,final}$ represents the recorded dry mass of the gel after the washes, accounting for the DAT mass loss. Sol content was measured in quadruplet samples (n = 4) with the overall study repeated for three times (N = 3) for MCS and MGC gels containing 0, 3 and 5 % (w/v) DAT.

3.8.2 Equilibrium Water Content Measurement

The sol-extracted, lyophilized gels were equilibrated for 6 h in a series of aqueous media comprised of PBS and deionized water, with an increasing water content over time, as described in detail below. This concentration series ensured that the scaffold hydration resulted in a gradual volume increase in the swollen gels, to minimize the potential for gel breakage. This process was repeated for MCS and MGC gels containing 0, 3 and 5 % (w/v) DAT (n = 4, N = 3).

Immediately after lyophilization, the sol-extracted gels were immersed in PBS at pH 7.4 (5 mL) for 1 h at room temperature. The 5 mL of medium was then replaced with a 75:25 PBS in deionized water mixture, and the gels were incubated at room temperature for 1 h. This process was repeated with 50:50 and 25:75 blends, and finally, pure deionized water. The mass of the fully hydrated gels was recorded after surface water was removed with a kimwipe. The equilibrium water content (EWC) was measured using the formula below:

$$EWC = \frac{m_{wet} - m_{dry,initial}}{m_{wet}} \quad [3.2]$$

where $m_{dry,\ initial}$ is the mass of the lyophilized gels prior to sol content removal and m_{wet} represents the equilibrium mass of the fully hydrated gel.

3.8.3 Mechanical Properties Measurement of Scaffold Construct

The indentation method described in the study by Hayes et al. was used to measure the Young's modulus of the sol-extracted gels that were fully hydrated in the EWC measurement protocol (n=3, N=4) [128]. A TA XT plus texture analyzer (Texture Technologies Corp., New York) equipped with flat-ended cylindrical indenters (3 and 7 mm diameter) was used to create indentations in the gels that were 0.5 mm deep from the gel surface, at a rate of 0.05 mm/s. The indentation forces caused by the different flat-ended indenters were recorded using Texture Exponent Software (Texture Technologies Corp., New York) and the data allowed for the Poisson ratio (υ) of the gels to be calculated through the following formula:

$$\frac{(\rho/\omega)_1}{(\rho/\omega)_2} = \frac{\alpha_1}{\alpha_2} \frac{\kappa_1\ (\alpha_1/\ h_{1,}\upsilon_1)}{\kappa_2\ (\alpha_2/\ h_{2,}\upsilon_2)} \quad [3.3]$$

where α is the radius of the indenter used (the subscripts 1 and 2 refer to the 3 mm- and 7 mm-diameter indenters respectfully), ρ is the indenting force, ω is the indenting depth, h is the height of the gel, and κ is a correction factor, obtained from Hayes et al. [128]. The values for (ρ/ω) were obtained from the linear portion of the slopes of the force-

indentation depth curves using both 3 mm- and 7 mm – diameter indenters. The slopes were calculated using a linear regression. After solving for the Poisson ratio (υ), the Young's modulus (E) for each gel was calculated using the following equation:

$$\frac{\rho}{\omega} = \frac{2\alpha E\kappa}{(1-\upsilon^2)} \quad [3.4]$$

3.9 Isolation of Adipose-Derived Stem Cells

Human adipose-derived stem cells (ASCs) were extracted using previously established protocols from the literature [6]. Freshly excised adipose tissue samples, delivered on ice, were processed within 2 hours of their acquirement. The adipose tissue (~10 g) was minced, with removal of any blood vessels and excess fibrous tissues, and the sample was transferred into a sterile 50 mL centrifuge tube. A 25 mL digest solution was made containing 3 mM glucose, 2 mg/mL collagenase type II, and 5 mM HEPES in Kreb's Ringer Buffer (KRB) solution, and syringe filtered through a 0.22 μm pore filter (Millipore Express PES Membrane, Millipore). The digest solution was supplemented with 1.4 mL of 35 % (v/v) sterile BSA solution and warmed to 37°C before being added to the minced adipose tissue. The tissue was incubated at 37°C for 45 min under constant agitation at 100 rpm. Any undigested tissues were removed by filtering the sample through a 250 μm pore stainless steel filter into another sterile 50 mL centrifuge tube. The filtrate was allowed to gravity separate for 5 min, to yield an upper layer of mature adipocytes, which was discarded by aspiration, and the ASC-rich bottom layer. An equal volume of complete cell culture medium (DMEM:Ham's F-12, 10% FBS and 1% Pen-Strep) was added to the sample in order to inactivate the collagenase. The sample was then centrifuged at 1200 x g for 5 min. The supernatant was discarded and the cell pellet

was then resuspended in 20 mL of erythrocyte lysing buffer (0.154 M ammonium chloride, 10 mM potassium bicarbonate, and 0.1 mM EDTA in sterile deionized water). The sample was gently agitated for 10 min at room temperature, re-centrifuged at 1200 x g for 5 minutes, and the supernatant was discarded. The cell pellet was suspended in 20 mL of complete cell culture medium before it was filtered through a 100 μm pore size nylon mesh. The sample was centrifuged again (1200 x g for 5 min), its supernatant discarded, and resuspended in complete medium. Finally, the cell suspension was seeded on T-75 tissue culture polystyrene (TCPS) flasks (Corning, NY, USA) at an approximate density of 1 x 10^6 cells/flask, and complete medium was added to each flask to achieve 15 mL of liquid volume per flask. The cells were incubated for 24 h (37°C, 5% CO_2), allowing the ASCs to attach to the bottom of the flasks. After 24 h, cellular debris and unattached cells were removed by aspirating the medium and then rinsing the cells with sterile, cation-free PBS.

Every 2 – 3 days, each flask was resupplied with 15 mL of fresh, complete cell culture medium until the proliferating cells reached approximately 80% confluence. In this case, the medium was aspirated and 5 mL of 0.25% trypsin/0.1% EDTA (Gibco®, Invitrogen, Burlington, ON, Canada) mixture was added to each T-75 flask in order to detach the cells from the surface of the plastic. The cells were re-plated at a density of approximately 1 x 10^6 cells in 15 mL of complete medium per T-75 flask. Passage 2 ASCs were used for all encapsulation experiments.

3.10 Photo-encapsulation of ASC in Scaffold

ASCs were incorporated within the hydrogels by adding the cell suspension at a seeding density of $1x10^6$ cells/gel to the pre-polymer solutions before photo-crosslinking. As described, the solutions were made by dissolving MGC or MCS in proliferation medium (DMEM:Ham's F-12, 10% FBS and 1% Pen-Strep), with the addition of 0.05 % (w/v) I2959 photoinitiator and the cryo-milled DAT. The suspension was mixed by gentle pipetting and transferred into a 16-well chamber (Nalgene Nunc International, Rochester, New York) and exposed to UV light (320 – 390 nm) for 3 min, at an intensity of 10.2 mW/cm^2. Immediately after the ASC-seeded hydrogels were photo-polymerized, they were transferred into individual wells in 6-well plates containing 5 mL of proliferation medium (DMEM:Ham's F-12, 10% FBS and 1% Pen-Strep). The cell-encapsulated hydrogels were incubated at 37°C with 5% CO_2. As controls, ASCs were directly seeded on 6 – well TCPS plates at a density of $1x10^6$ cells/well. Each well was supplied 5 mL of proliferation medium.

3.10.1 Induction of Adipogenic Differentiation

The cell-seeded scaffolds and TCPS controls were maintained in proliferation medium (DMEM:Ham's F-12 supplemented with 10% FBS and 1% Pen/Strep) for 24 h (37°C, 5% CO_2) after seeding. Adipogenic differentiation was then induced using serum-free adipogenic differentiation medium [6] (DMEM:Ham's F12 supplemented with 33 μM biotin, 17 μM pantothenate, 66 nM human insulin, 1 nM triiodothyronine, 10 μg/mL transferrin, 100 nM hydrocortisone, 100 U/mL penicillin, and 0.1 mg/mL streptomycin).

For the first 72 hours, the differentiation medium was supplemented with 1 μg/mL of troglitazone and 0.25 mM isobutylmethylxanthine (IBMX). Fresh medium was provided every 2 days to each well (5 mL).

3.11 Live/Dead

The LIVE/DEAD® Viability/Cytotoxicity Assay (Invitrogen) allows for the identification of live and dead cells simultaneously through the use of calcein AM and ethidium homodimer (EthD-1) dyes. Live cells are distinguished by the presence of intracellular esterase activity, which can be detected when calcein AM is enzymatically converted to the fluorescent calcein. Dead cells are detected when EthD-1 enters cells with damaged membranes, fluorescing when it binds to nucleic acids. Calcein and EthD-1 cause live and dead cells to fluoresce green (494 nm/517 nm) and red (528 nm/617 nm), respectively [128]. In this study, the assay was used to measure ASC viability in the scaffolds after photo-encapsulation, at 24 h after seeding (before adipogenic induction), as well as at 7 and 14 days after the induction of differentiation (n=3, N=3).

To facilitate visualization using confocal microscopy, before the polymer-DAT composite scaffolds were fabricated, the DAT was pre-labeled with an amine-reactive Alexa Fluor® 350 carboxylic acid, succinimidyl ester (Molecular Probes, Burlington, Canada). In brief, a stock solution (10 mg/mL) was prepared by dissolving the dye in dimethyl sulfoxide (DMSO). The DAT was transferred into a 24-well plate filled with sterile, 0.15 M $NaHCO_3$ buffer (pH 8.3), where 1 mL of the buffer was used per 200 mg

of DAT. The stock solution was added to the DAT (25 µL/200 mg) and the tissue was agitated for 1 h at room temperature. The labeling reaction was stopped with incubation in 1.5 M hydroxylamine (pH 8.5) for 1 h. Finally, the DAT was rinsed three times in sterile PBS before it was added to the MGC or MCS pre-polymer solutions, for scaffold fabrication, as previously described.

At each time point, the cell-seeded scaffolds were rinsed with PBS. A 4 µM EthD-1 solution was prepared by mixing sterile PBS with the stock 2 mM EthD-1 that was provided with the LIVE/DEAD® kit. The calcein AM stock solution was then added to the EthD-1 solution to achieve a concentration of 2 µM. The hydrogels were incubated in 2 mL of the diluted dye solution for 45 min at room temperature.

Following incubation, the ASCs in the scaffolds were imaged using an Olympus FV 1000 laser scanning confocal microscope. A mosaic stitching technique was used to capture and stitch together 25 – 31 images, forming one image that captured the complete cross-sectional area of the gel at a specific depth. For each scaffold, five layers were scanned, with each layer separated by 100 – 200 µm. The images were then processed using ImageJ analysis software to calculate the number of live and dead cells.

3.12 Glycerol-3-Phosphate Dehydrogenase Activity

Glycerol-3-phosphate dehydrogenase (GPDH) is an enzyme involved in lipid biosynthesis. GPDH activity is measured to assess adipogenic differentiation as maturing adipocytes accumulate intracellular lipid. In this study, the GPDH activity of the ASCs

that were seeded in the MGC- or MCS-based scaffolds was measured at 3, 7 and 14 days after the induction of adipogenic differentiation (n=3, N = 3). Additionally, the ASCs seeded on 6-well plates were used as 2-D controls, where induced (cultured in adipogenic differentiation medium) and non-induced cells (cultured in proliferation medium) served as positive and negative controls respectively.

Prior to assaying, the samples were washed three times in PBS (5 mL/wash) to remove residual culturing medium. The scaffolds were transferred into individual 1.5 mL microcentrifuge tubes and they were minced roughly to help release the encapsulated cells. Enzyme extracting reagent (5 mM tris base, 20 mM tricine, 1 mM EDTA-2Na, pH 7.4) was added to each microcentrifuge tube (1 mL/tube). The samples were then sonicated to lyse the cells using a sonic dismembrator (Model-100, Fisher Scientific, Toronto, Canada) at a setting of 4. Afterwards, the samples were centrifuged (12,800 x g, 5 min, 4°C) to isolate the cystolic fraction, including the intracellular GPDH, in the supernatant.

The 2-D TCPS controls were similarly prepared prior to assaying. The controls were rinsed 3 times in PBS and 1 mL of enzyme extracting reagent was added to each well. Using the sonic dismembrator, the cells in the samples were disrupted and the fluid from the well was transferred to 1.5 mL microcentrifuge tubes. Finally, the samples were centrifuged for 5 min (12,800 x g, 4°C).

After centrifugation, the supernatant from each sample was assayed in triplicate for total protein content, which was used to normalize the GPDH activity levels. The

cytosolic protein content was measured using the Bio-Rad Protein Assay (Bio-Rad Laboratories, Inc., Hercules, CA). A standard curve was constructed using a concentration series of albumin in enzyme extracting reagent to yield concentrations of 0 μg/mL, 10 μg/mL, 20 μg/mL, 40 μg/mL, 60 μg/mL and 80 μg/mL. From the supernatant of each sample, 160 μL was transferred to each well of a 96-well microplate. Bio-Rad Coomassie® Brilliant Blue G-250 dye solution (40 μL) was added to each well and the sample was mixed to ensure homogeneous distribution of the dye. The plate was then incubated at room temperature for 5 min and the absorbance from the standards and samples was measured at 595 nm using a Synergy™ HT multidetection microplate reader and KC4TM (Bio-Tek Instruments, Inc., Winooski, VT, USA) data analysis software. The protein content of the samples was calculated using the albumin standard curve.

The GPDH Activity Measurement Kit from Kamiya Biomedical Corporation (Seattle, WA, USA) was used to measure the activity of GPDH, which can generate glycerol 3-phosphate from dihydroxyacetone phosphate (DHAP) provided as a substrate in the kit using nicotinamide adenine dinucleotide NADH as a coenzyme. The decrease in NADH concentration associated with the GPDH from the samples was measured over time and used to calculate the GPDH activity. After the protein content was determined, 50 μL of the supernatant from each sample was transferred in duplicates to the wells of a 96-well microplate. Immediately before analysis, 100 μL of the GPDH substrate reagent solution provided in the kit was added to each sample using a multi-channel pipettor. The absorbance of each sample was measured using a Synergy™ HT multi-detection

microplate reader (Bio-Tek Instruments, Inc., Winooski, VT, USA) at 340 nm at 25°C. Over the span of 10 min, the absorbance was measured every 15 s, using the KC4TM software.

The change in absorbance (ΔOD/min) was determined by plotting the absorbance data with respect to time and calculating the slope of the linear portion of the curve via linear regression. Using the intracellular protein content that was previously measured, the GPDH activity levels were normalized and obtained from the following equation:

$$GPDH\left(^{mU}/_{mg}\right) = \frac{\Delta OD_{avg} * 0.4823 * 0.5 * 1000}{Pr_{avg}/1000} \quad [3.5]$$

where 1 unit of GPDH was defined as the activity for 1 mL of sample to consume 1 μmol of NADH in 1 minute. ΔOD_{avg} represents the average of the change in absorbance for each sample that was measured in duplicate and Pr_{avg} is the average intracellular protein content. The activity levels were expressed in mU of GPDH activity per mg of total intracellular protein.

3.13 End-Point Reverse Transcriptase Polymerase Chain Reaction (RT-PCR)

Expression of the adipogenic genes PPARγ, C/EPBα, LPL and the housekeeping gene glyceraldehyde-3-phosphate dehydrogenase (GAPDH) were assessed in the cell-seeded MGC- and MCS-based scaffolds (MGC, MGC+5%DAT, MCS, MCS+5%DAT), as well as cell-seeded DAT and TCPS controls at 7 and 14 days after adipogenic

induction (n=3, N=3). Prior to RNA extraction, the MGC- and MCS-based scaffolds were agitated in lysozyme-digest solution (10 mg/mL in PBS) at 37°C for 48 h, followed by mincing with sharp scissors. The total RNA content from the scaffolds and control groups was extracted by homogenizing each sample in 1 mL of TRIzol® Reagent (Invitrogen Canada Ltd., Burlington, ON, Canada). The scaffolds were processed as per the manufacturer's instructions to extract RNA content from tissues. RNA concentration and purity were determined using a NanoDrop spectrophotometer (ND1000; NanoDrop Products, Wilmington, DE, USA).

First-strand cDNA was synthesized from 1 µg of total RNA, using random primers (Invitrogen) and SuperScript™ II Reverse Transcriptase (RT) (Invitrogen). The reverse transcription was carried out in a 20 µL reaction volume, which contained first strand buffer (50 mM Tris-HCl, 75 mM KCl, 3 mM $MgCl_2$), 10 mM dithiothreitol (DTT), 0.09 OD_{260} units of random primers (Invitrogen), and 0.5 mM of each dNTP (Invitrogen). For each sample, minus-RT controls were also prepared. Table 3.1 summarizes the gene specific primers (Invitrogen; 50 nM, desalted), which were previously designed from another study [1]. Additionally, each primer set has a melting temperature of 60°C. Each PCR reaction was conducted in a 50 µL reaction volume containing 2.5 µL of diluted cDNA (50 ng of RNA per 2.5 µL sample of diluted cDNA). 1X Taq buffer (10 mM Tris-HCl, 50 mM KCl, 0.08% Nonidet P40), 250 nM forward primer, 250 nM reverse primer, 250 nM of each dNTP, 2.5 mM $MgCl_2$ and 0.375 units of recombinant Taq DNA Polymerase (Fermentas International Inc., Burlington, ON, Canada) were

added to each reaction. PCR was conducted (including the minus-RT and no template controls) for 40 cycles using a Bio-Rad C1000 thermal cycler. The conditions used were 95°C for 5 minutes, followed by 40 cycles of 30 s at 95°C, 30 s at 58 °C, 1 minute at 72°C, followed by a final extension for 5 min at 72°C.

Gel electrophoresis was used to separate the PCR products on 5% agarose. The gels were stained with ethidium bromide and detected using ultraviolet light (G:box Chemi HR16, Syngene, Cambridge, UK).

Table 3.2 Primer sets used for RT-PCR gene expression studies [6]

Gene	**Primer sequence (5'~3')**	**Fragment length (bp)**
PPARγ	Forward: TTCAGAAATGCCTTGCAGTG Reverse: CCAACAGCTTCTCCTTCTCG	84
C/EBPα	Forward: CAGAGGGACCGGAGTTATGA Reverse: TTCACATTGCACAAGGCACT	107
LPL	Forward: GTCCGTGGCTACCTGTCATT Reverse: TGGCACCCAACTCTCATAGA	94
GAPDH	Forward: ACAGTCAGCCGCATCTTCTT Reverse: ACGACCAAATCCGTTGACTC	94

3.14 Oil Red O Staining

Oil Red O was used to stain intracellular lipid droplets that were accumulated within the differentiating ASCs in the scaffolds at 7 and 14 days after adipogenic differentiation was induced. Oil red O stock solution was prepared in 99.9% isopropanol at a concentration of 3 g/L.

As described in the viability staining methods, prior to scaffold photo-polymerization, the cryo-milled DAT was pre-labeled with Alexa Fluor® 350 carboxylic acid, succinimidyl ester (Molecular Probes, Burlington, Canada). At each time point, the scaffolds were fixed overnight in 10% neutral buffered formalin. Each scaffold was rinsed three times in PBS and incubated at room temperature in 2 mL of working Oil Red O solution (3 parts Oil Red O stock:2 parts deionized water v/v) for 10 minutes. The samples were repeatedly rinsed in water to remove excess dye, and then visualized using the Olympus FV 1000 laser scanning confocal microscope.

3.15 Statistical Analysis

All data are expressed as means ± standard error of the sample mean. Statistical analyses were performed using the software program OriginPro 8.0 (OriginLab Corp., Northampton, MA, USA) to compare gel stiffness, cell viability, cell count, and GPDH activity between different MGC- and MCS – DAT composite scaffolds, as well as cells seeded on both tissue culture polystyrene and DAT as controls. Arcsin values obtained by converting the cell viability percentages were used for statistical analysis. One-way ANOVA with a Tukey's post-hoc comparison of means was used and all differences were considered statistically significant at $p < 0.05$.

Chapter 4

Characterization of Photo-Crosslinkable Decellularized Tissue-Polymer Composite Hydrogels

4.1 Introduction

Decellularized extracellular matrix (ECM) is an attractive scaffolding choice for adipose tissue engineering as it naturally contains proteins, growth factors, and other biopolymers that help promote cell adhesion, proliferation and differentiation through cell-matrix communication [80-82]. Previous *in vitro* studies where decellularized adipose tissue (DAT) was cultured with adipose-derived stem cells (ASCs) have shown promise in supporting cell viability and adipogenic differentiation induction [121, 122]. Clinically, the loss of soft tissue often results in defects with irregular shapes and volumes. Therefore, a scaffold for soft tissue reconstruction should be designed in such a way that it can be easily implanted while effectively and evenly filling the volume within the defect sites [10]. An injectable scaffold would fulfill both of these requirements and as such, the scope of this project was to construct an injectable composite DAT-based scaffold by suspending cryo-milled DAT in a hydrogel pre-polymer solution that could subsequently be photo-crosslinked *in situ*. ASCs were encapsulated within this composite scaffold with the goal of generating viable adipose tissue.

Methacrylated glycol chitosan (MGC) and methacrylated chondroitin sulphate (MCS) hydrogels were chosen due to their favourable properties. Chitosan was reported to have wound healing and antimicrobial properties while chondroitin sulphate is a

component naturally found in the ECM that contributes to its high water retention capabilities [114, 116, 123, 124]. Both polymers were methacrylated to render them susceptible to photo-polymerization. Photo-crosslinking is an effective method that enables the formation of a crosslinked network *in situ* under physiological conditions. Photo-polymerization can also provide for spatial control during the gelation process [11].

This chapter focuses on the optimization of the methodologies used for the construction of DAT-MGC and DAT-MCS composite scaffolds, as well as scaffold characterization. Sol content, equilibrium water content and gel stiffness (measured in terms of Young's modulus) of both groups of hydrogels were measured and compared as part of the process to determine which polymer would be better suited to act as the hydrogel carrier in the composite scaffold.

4.2 Results and Discussion

4.2.1 Glycol Chitosan and Chondroitin Sulphate Methacrylation Reaction

In order for glycol chitosan (GC) and chondroitin sulphate (CS) to be photo-polymerizable, both of these polymers had a methacrylate group grafted to their backbone. The degree of methacrylation was reported as a degree of substitution (DOS) percentage, which refers to the number of methacrylate groups on the GC or CS backbone per 100 residues. Generally, a greater DOS value is indicative of a higher degree of crosslinking that can be formed within these photo-polymerizable

methacrylated polymers. As such, a higher DOS percentage results in greater hydrogel stiffness.

Glycol chitosan contains the reactive hydroxyl and amine groups [Fig 4.1a]. In the presence of glycidyl methacrylate, both of these functional groups can undergo a nucleophilic substitution reaction to form methacrylated glycol chitosan [Fig 4.1b]. However, the primary amine is the most favorable nucleophile since reaction with the hydroxyl group requires strongly basic conditions (i.e. pH 11 – 12) while yielding low degrees of substitution [115].

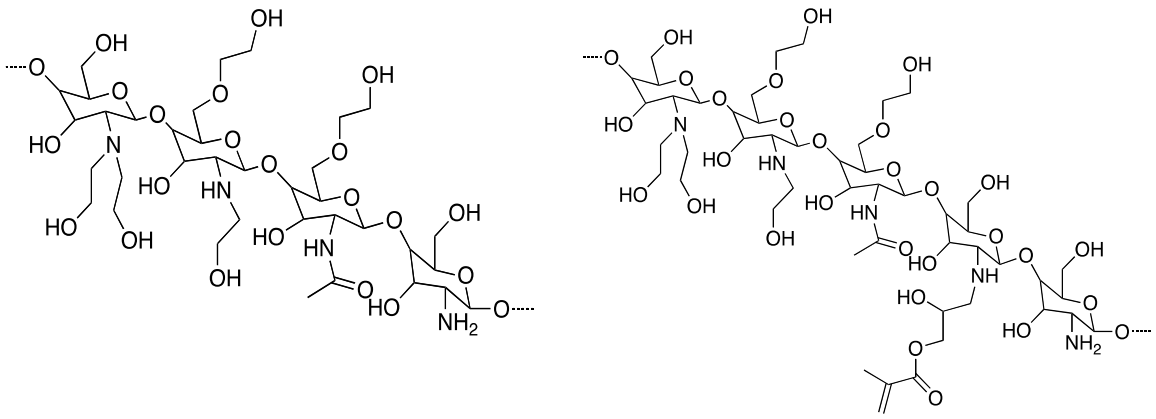

Figure 4.1 Molecular structures of glycol chitosan (left) and *N*-methacrylate glycol chitosan (right)

Following established protocols, purified glycol chitosan was reacted with glycidyl methacrylate to yield N-methacrylate glycol chitosan with 14% DOS [115]. To demonstrate that the methacrylation reaction was successful, 1H NMR spectroscopy was used to analyze both glycol chitosan and methacrylated glycol chitosan [Fig 4.2]. The

peak at 2.3 ppm corresponds to the methyl group on the methacrylate, while the peaks at 5.9 ppm and 6.3 ppm are due to protons on the vinyl carbon. Additionally, the decrease in the peak at 3.2 ppm and the appearance of a new one at 3.3 ppm are associated with the H-2 proton for the deacetylated residues and the H-2 proton for the N-methacrylate residue, respectively. A reduction in peak area at 5.1 ppm and the appearance of one at 5.2 ppm correspond with the H-1 proton in the deacetylated residue and the H-1 proton in the N-methacrylate residue.

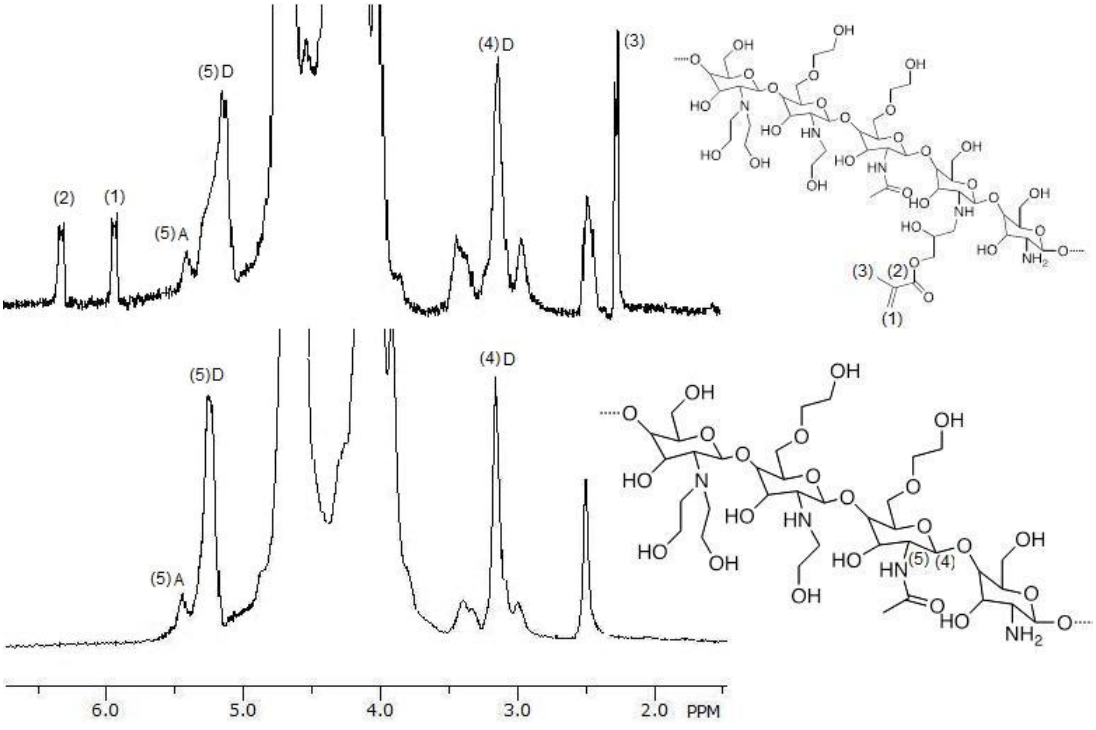

Figure 4.2 ^{1}H NMR spectra of *N*-methacrylate glycol chitosan (top) and glycol chitosan (bottom). The (A) represents acetylated residues and the (D) represents deacetylated residues.

Likewise, chondroitin sulphate (CS) was reacted with methacrylic anhydride to form *O*-methacrylate chondroitin sulphate (DOS 16%). CS contains three hydroxyl groups that could nucleophilicly attack the carbonyl groups on methacrylic anhydride. The reaction forms ester bonds while generating methacrylic acid as a by-product [130]. In order to drive the reaction forward, the reaction was adjusted with 5 M NaOH to pH 10 to neutralize the acid formed. Figure 4.3 illustrates the chemical structures for both unmodified and modified chondroitin sulphate.

Methacrylation of CS was confirmed through ^{1}H NMR spectra (Fig 4.4). The peaks located at 5.65 ppm and 6.2 ppm correspond to the protons from the vinyl group on the grafted methacrylate. The peak at 1.7 ppm is associated with the protons from the methyl group in the methacrylate while the peak at 1.9 ppm is due to the protons from the methyl group of the *N*-acetyl residues in native CS. The peak at 2.6 ppm in the top spectrum corresponds to residual dimethyl siloxide (DMSO) used in the MCS synthesis process.

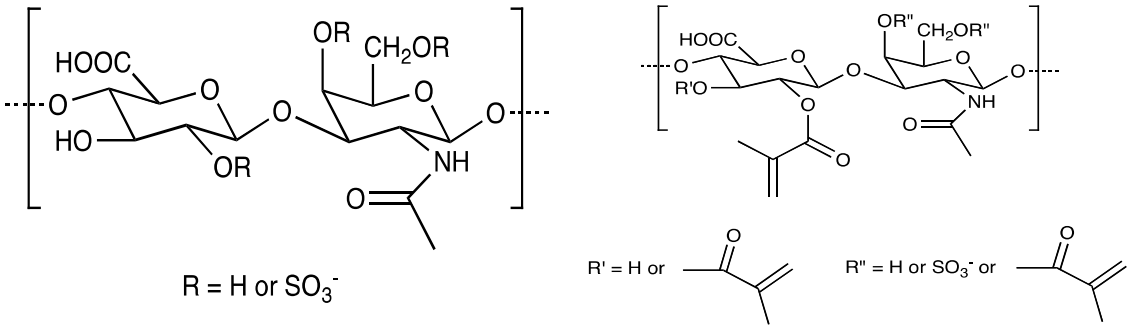

Figure 4.3: Molecular structure of chondroitin sulphate (left) and methacrylated chondroitin sulphate (right).

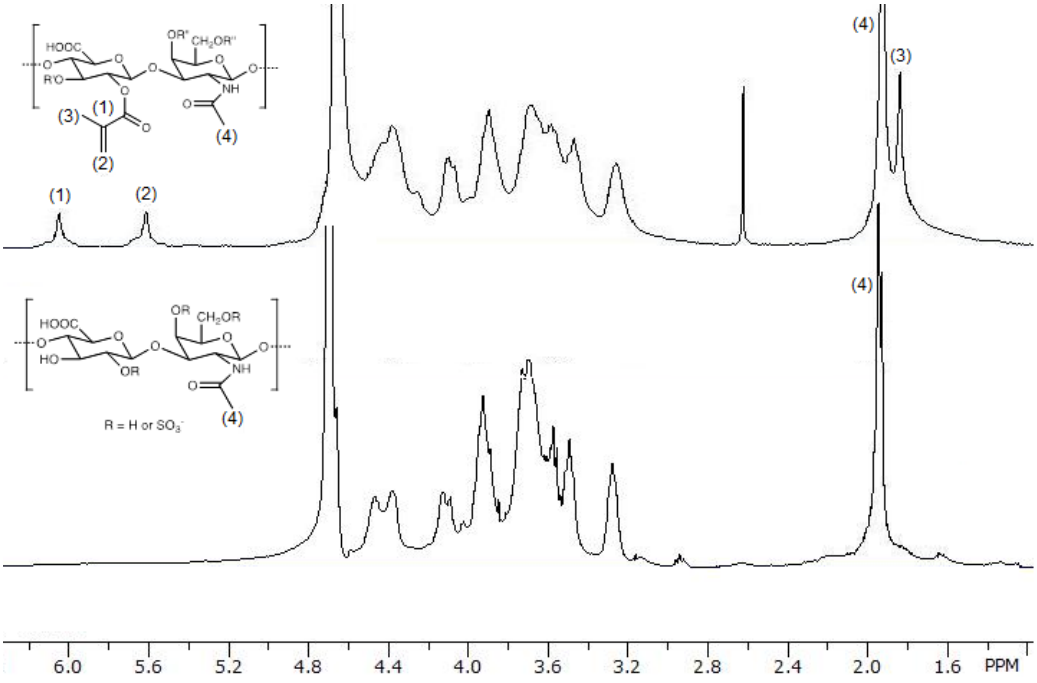

Figure 4.4: ^{1}H NMR spectra of *O*-methacrylate chondroitin sulphate (top) and unreacted chondroitin sulphate (bottom).

4.2.2 Hydrogel Stiffness Comparison

Current studies show that scaffold mechanical properties can impact stem cell lineage commitment by influencing the different tensile stresses that cells experience in their cytoskeletons when adhered to the scaffold surface [98]. Generally, softer scaffolds will promote adipogenic or myogenic differentiation. [98] As such, it is important that the gel stiffnesses were the same between the MGC and MCS scaffolds, to set the basis of comparison between the MGC and MCS hydrogels and attempt to control for the role of this factor in mediating the cell response. In order to achieve this goal, the polymer

concentrations required to produce MCS and MGC hydrogels with comparable Young's moduli were determined. A series of MGC and MCS polymer solutions at varying concentrations were prepared prior to photo-crosslinking. The methacrylate groups photopolymerized through free-radical reaction to form short chain poly(methacylate) between the chondroitin sulphate or glycol chitosan chains [125].

Immediately after the gels were formed, they were subjected to an indentation measurement to determine the mechanical properties of the scaffolds (Fig 4.5a and b). The indentation method works by measuring the reaction force required to indent the hydrogel at a single area to a predefined depth, and is a popular method for characterizing the mechanical properties of hydrogels [132].

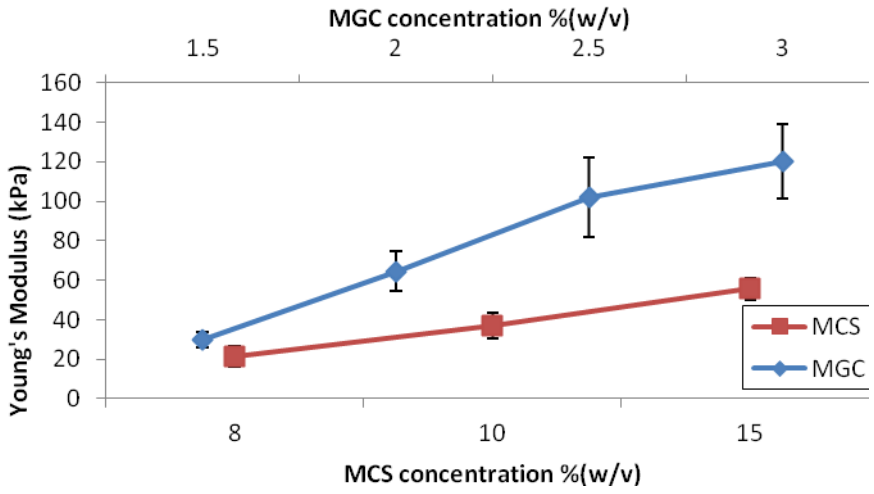

Figure 4.5a: Young's modulus of MGC and MCS hydrogels at varying polymer concentrations (% w/v), n=3, N=3.

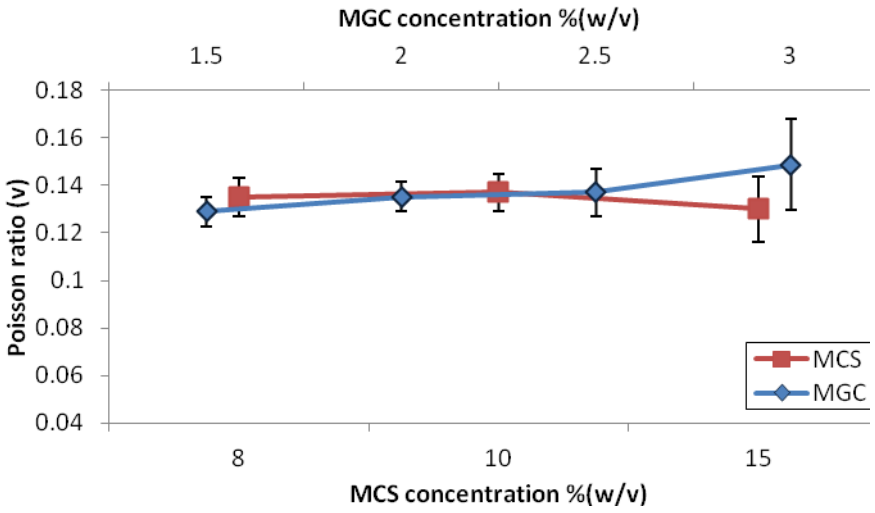

Figure 4.5b: Poisson ratio (bottom) of MGC and MCS hydrogels at varying polymer concentrations (% w/v), n=3, N=3.

MGC hydrogels made from prepolymer solution concentrations of 1.5, 2, 2.5 and 3% (w/v) were compared against MCS hydrogels, prepared from prepolymer solution concentrations of 8, 10 and 15% (w/v) (n=4, N=3). A general upward trend in Young's modulus can be seen as polymer concentration is increased for both gels, with MGC experiencing greater gel stiffness at a lower increment of concentration increase. The Young's modulus for MGC made from 1.5% (w/v) (30.1±4.0 kPa) is comparable to that of MCS made from 10% (w/v) (37.1±5.0 kPa) thereby establishing the two concentrations to be used for MGC and MCS hydrogel construction for the rest of this study. Additionally, these two polymer concentrations were chosen as they yielded hydrogels with the lowest matching Young's moduli, which allowed for the construction of the softest scaffolds possible from the range of polymer concentration that was used. This was done to best mimic the natural mechanical properties of native adipose tissue.

The Poisson ratio remained relatively constant between concentrations and gel type, with the ratio ranging from 0.129 to 0.149 in MGC gels and 0.130 to 0.137 in MCS gels. These values are consistent with those reported in a previous study involving the fabrication of MGC gels [128].

4.2.3 Decellularization and Cryo-Milling of Adipose Tissue

Recently harvested adipose tissue appeared yellow in colour due to the large amount of adipocytes [Fig 4.6a]. The cells and other antigenic contents were subsequently removed during the decellularization process through a combination of physical, chemical and enzymatic reactions over 5 days. The resulting product was a highly hydrated, loose, white matrix [Fig 4.6b].

Towards the goal of developing an injectable scaffold, DAT was rendered into powder form [Fig 4.6c]. This goal was achieved through the development and optimization of a protocol, involving a combination of lyophilization and cryo-milling.

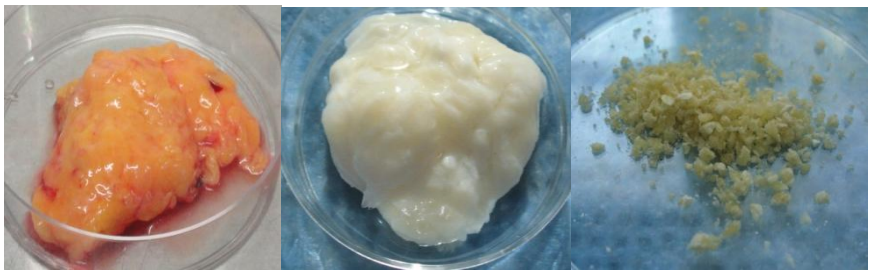

(B) **(C)**

Figure 4.6 Adipose tissue a) prior to decellularization, b) after decellularization, and c) cryo-milled.

4.2.4 DAT-Polymer Composite Scaffold Construction via Photo-Crosslinking

The cryo-milled DAT was incorporated into both MGC and MCS polymer solutions at a concentration of 3 and 5% (w/v), with 5% (w/v) being the uppermost limit that could be added to the gels without interfering with the gelation process. When too much DAT was added, the solid, opaque DAT effectively blocked the UV light from penetrating the clear gel solution thoroughly. Prior to crosslinking, the DAT was mixed into the prepolymer solutions, which also contained the photo-initiator Irgacure 2959 (I-2959), by gentle pipetting. MGC and MCS solutions containing 0, 3, and 5% (w/v) suspended DAT particles were injected into a mold and photo-polymerized to yield cylindrical gels with a diameter of 7 mm and a height of 3 mm (Fig 4.7).

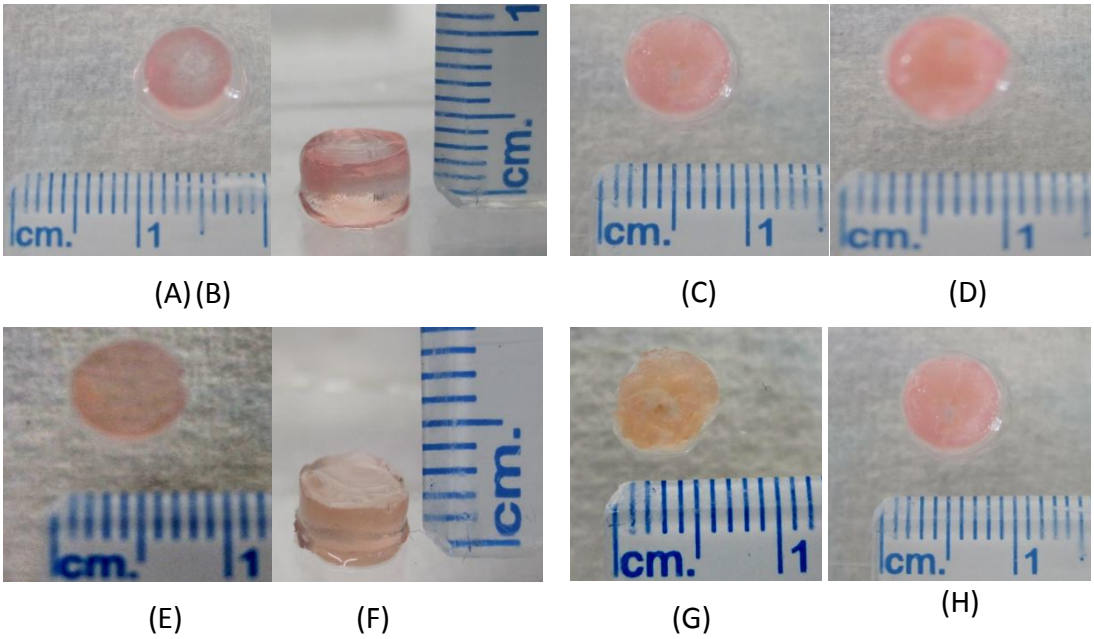

Figure 4.7 MGC (a – d) and MCS (e – h) hydrogels shortly after crosslinking; Specifically, MGC gels with (a) and (b) no DAT, (c) 3% (w/v) DAT (d) 5% (w/v) DAT. MCS with (e) and (f) no DAT, (g) 3% (w/v) DAT, (h) 5% (w/v) DAT

4.2.5 Sol Content and Equilibrium Water Content Measurements

Sol content is a measurement of the unreacted, and hence extractable, polymer in the hydrogel after its formation. Therefore, a higher sol content correlates to a lower crosslink efficiency within the gels. Fig. 4.8a shows that the sol content for both MCS and MGC hydrogels were relatively similar, with both gels experiencing relatively the same amount of sol content decrease as the DAT concentration was increased. MGC and MCS without the addition of DAT possessed a sol content of 27.2 ± 1.1 % and 29.9 ± 1.0%. After the addition of 5% (w/v) DAT, the sol content for MGC and MCS dropped to 17.2 ± 1.0 % and 20.2 ± 1.5%, respectively. A possible explanation for this downward trend in sol content as more DAT was incorporated within the gels could be the protein molecules in the DAT contributing to the free-radical polymerization reaction either by reacting with the methacrylate groups on the polymer backbones or with other proteins. Proteins contain a myriad of functional groups that could participate in the reaction depending on their amino acids; some of these include primary amines, carboxyls, triols, and in particular, phenyl groups [136, 137]. In a study that investigated collagen photo-crosslinking, it was observed that free radicals generated during photo-polymerization reacted with the aromatic groups on amino acids in the collagen, such as tyrosine and phenylalanine [137]. Further chemical analyses would be required to confirm the specific effect of the DAT on the crosslinking density.

All MGC and MCS hydrogel groups contained a significant amount of water as reflected in the equilibrium water content (EWC) measurements, with MGC and MCS having values of 86.5 ± 1.6% and 96.2 ± 2.1% with no DAT addition (Fig 4.8b). MGC and MCS with 5% (w/v) DAT experienced a slight drop in EWC at 82.7 ± 2.7% and 94.0 ± 3.2%, respectively. Overall, the EWC remained relatively constant across both hydrogel groups; the small decrease in EWC value in the DAT-containing gels could be attributed to the proteins essentially acting as a space-filler, thereby decreasing the volume of water that the hydrogels could hold.

The unique water absorption and retention properties of CS are well documented. Structurally, chondroitin sulphate is composed of repeating units of N-acetylgalactosamine and glucuronic acid, along which the negatively charged carboxyl or sulphate functional groups are attached. The negatively charged functional groups are electrostatically attracted to positively charged molecules, such as certain growth factors, nutrients and other cations. The build-up of cations along the chondroitin sulphate backbone in turn draws water to the molecule. As such, high water content in chondroitin sulphate-based hydrogel is characteristically seen among other studies [100, 123, 125, 130]. Similarly, glycol chitosan also contains charged groups, except they are cationic. These cationic groups behave in the same manner as the anionic groups in chondroitin sulphate by attracting anions to the glycol chitosan backbone, which in turn attracts water [101].

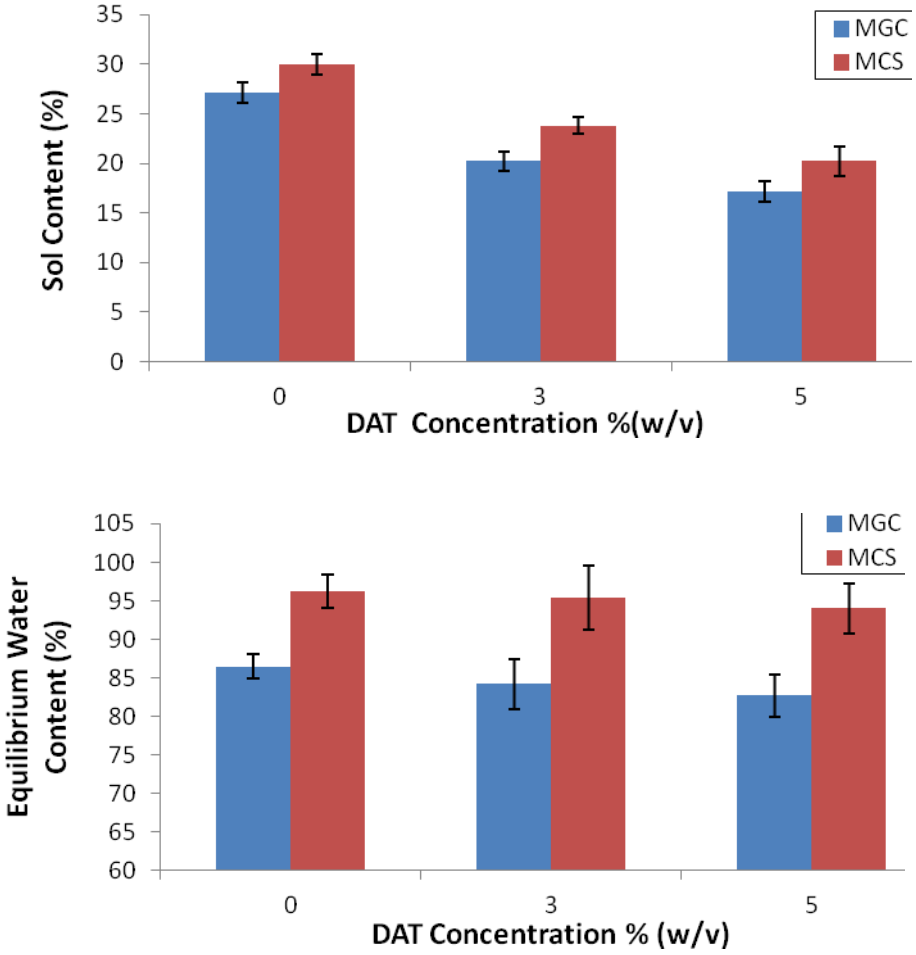

Figure 4.8 a) Sol content and b) equilibrium water content in 14% DOS MGC and 16% DOS MCS gels with added DAT at 0, 3 and 5 % (w/v) (n=4, N=3)

4.2.6 Mechanical Properties

The mechanical properties of the scaffolds were measured through indentation in order to gain a better understanding of both materials and to identify any differences between the MGC-DAT and MCS-DAT interactions. Fig. 4.9a shows a near-linear, upward trend in the Young's modulus as the DAT concentration was increased within

both MGC and MCS hydrogels, suggesting that the gels were becoming stiffer with increased DAT content. Without any DAT, the Young's modulus for MGC and MCS were 30.1 ± 4.0 kPa and 37.1 ± 5.6 kPa while MGC and MCS with 5% (w/v) DAT had a Young's modulus of 75.5 ± 6.3 kPa and 81.1 ± 9.7 kPa, respectively. No statistically significant differences were found between the MGC and MCS scaffolds containing the same DAT concentration, while increasing the DAT content in the hydrogels derived from the same polymer resulted in mean values that were significantly different from each other. This suggests that the DAT was contributing to the gel stiffness irrespective of the polymer type, without any additional interactions that would favour either polymer. Since the composite hydrogels were shown to have improved crosslinking with the inclusion of the DAT based on the measured sol content [Fig. 4.8a], it is likely that this was a contributing factor to gel stiffness.

DAT could also be contributing to the gel stiffness through binding of the protein molecules within the DAT with the polymer chains through electrostatic interactions [136 - 138]. As mentioned in the previous chapter, DAT is comprised of the ECM derived from adipose tissue after the extraction of the cellular and nucleic acid content [80-82]. As such, the structural elements of DAT are primarily comprised of collagens (type I and type IV), and it is mostly through collagen and polymer interaction that gel stiffness would be affected [80-81]. Studies have shown that collagens have a large range in stiffness values depending on the tissue sourcing. For example, collagen derived from cartilage can have a Young's modulus of 2-46 MPa while the collagen derived from skin

can have a modulus as low as 0.002-0.022 MPa [140]. The Young's moduli in MGC and MCS with 5% (w/v) DAT were 75.5 ± 6.3 kPa and 81.1 ± 9.7 kPa respectively, which lie closer to the those found in skin [138-140].

The Poisson ratio for MGC and MCS gels were relatively similar, ranging from 0.13 to 0.15 for the MGC hydrogel group and 0.14 to 0.16 for the MCS hydrogel group. While this range is relatively low in comparison to the standard ratio of 0.5 assumed for most hydrogels, it is expected from the high equilibrium water content in the gels. In addition, this Poisson ratio range is similar to those obtained with MGC hydrogels prepared in another study [123].

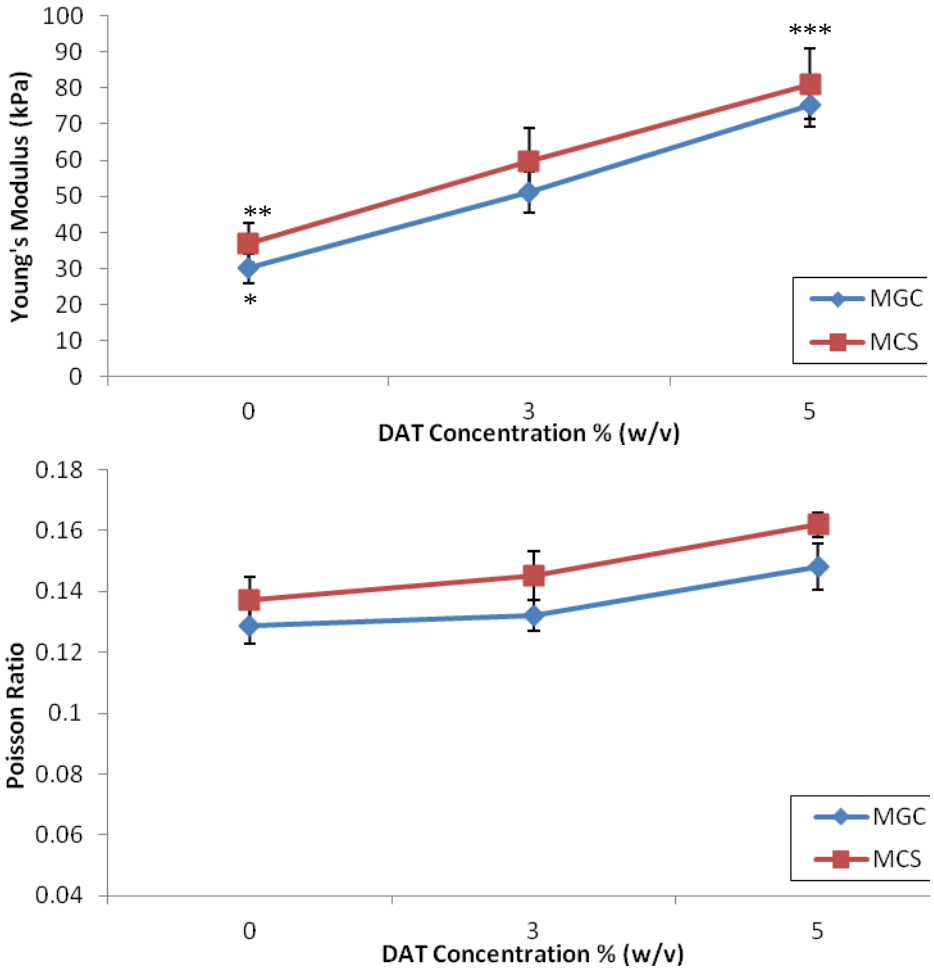

Figure 4.9: Mechanical properties of 14% DOS MGC and 16% DOS MCS hydrogels with 0, 3, and 5% (w/v) DAT; a) Young's modulus, and b) Poisson ratio (n=4, N=3). Statistical significance in Young's modulus was determined by one-way ANOVA with a Tukey's post-hoc comparison of means ($p<0.05$). * MGC hydrogels were statistically different than all other MGC-derived gels, and MCS gels at 3 and 5 % (w/v) DAT; **MCS hydrogels were statistically different than all other MCS-derived gels and MGC at 5% (w/v) DAT; ***MCS at 5% (w/v) DAT were significantly different than all other gels except MGC at 5% (w/v) DAT.

4.3 Conclusions

Glycol chitosan and chondroitin sulphate were reacted with glycidyl methacrylate and methacrylate anhydride to yield *N*-methacrylate glycol chitosan and *O*-methacrylate chondroitin sulphate, respectively. These water soluble polymers were photo-polymerized with the addition of cryo-milled DAT to form an injectable, polymer-DAT construct for adipose tissue engineering applications. A comparison between MGC and MCS scaffold groups (with varying concentrations of DAT) was made based on the sol content, equilibrium water content, and mechanical properties. Overall, the hydrogels with higher amounts of DAT had lower sol and equilibrium water content measurements, which could be attributed to the DAT participating in the crosslinking process while occupying volume within the gels. The presence of DAT also contributed to gel stiffness.

Chapter 5

Proliferation and differentiation of adipose-derived stem cells in injectable photo-polymerizable DAT-polymer composite scaffolds

5.1 Introduction

The reconstruction of adipose tissue proves to be a clinical challenge. Soft tissue augmentation methods currently require the implantation of synthetic or natural-based filler materials at the defect site to correct small volume soft tissue loss [7]. Unfortunately, these treatments have a limited lifespan and in order to sustain filler volume, multiple treatments are often required [4, 6, 7]. For larger defects, the use of vascular flaps is considered to be the gold standard for treatment, although the techniques require highly invasive surgery and may lead to donor site morbidity [4, 89]. As such, there exists a clinical need for an adipose tissue engineering strategy that would provide a permanent solution to soft tissue augmentation through the regeneration of viable, functioning tissue.

One of the most common approaches to adipose tissue engineering is the cell-seeded scaffold method, where a cell source with regenerative function is cultured on the scaffold *in vitro* before implantation [3, 4, 6]. The design of the scaffold is extremely important as it serves to anchor the cells and to mediate cell function, which can influence cell viability and growth [1, 26]. Ideally a scaffold for adipose tissue engineering should closely mimic the natural extracellular matrix (ECM) in native

adipose tissue, and it should support cell adhesion, proliferation, and promote adipogenesis. Since soft tissue defect sites tend to be irregularly shaped, a scaffold that could evenly fill the volume within the site would be desirable.

With these design requirements, in the previous chapter, a composite scaffold was developed by combining an injectable hydrogel with decellularized adipose tissue (DAT). Methacrylated chondroitin sulphate (MCS) and methacrylated glycol chitosan (MGC) hydrogels containing varying weight percentages of DAT were characterized and compared. The results suggested that the DAT contributed to the gel stiffness and, to some extent, the crosslinking density, while decreasing the equilibrium water content by acting as a volume filler in both polymer gel systems.

This chapter focuses on the characterization of the cell response after *in vitro* culturing the MGC- and MCS-DAT composite scaffolds with encapsulated human adipose-derived stem cells (ASCs) for up to 14 days. ASCs are a readily accessible regenerative cell source, and depending on the culture conditions, can undergo mitotic cell division and adipogenesis, and were therefore chosen as the cell source to regenerate viable adipose tissue. Cell viability after adipogenic differentiation induction, as well as the level of adipogenic differentiation of the cells within the composite scaffolds were investigated in detail. More specifically, cell viability was assessed by confocal microscopy through the use of fluorescent calcein-AM and ethidium homodimer-1 dyes, causing live and dead cells to fluoresce green and red respectively. Adipogenic differentiation of encapsulated ASCs was characterized through the quantification of

glycerol-3-phosphate dehydrogenase (GPDH) activity, adipogenic gene expression using end-point reverse transcriptase-polymerase chain reaction (RT-PCR), and intracellular lipid visualization. GPDH was chosen as a marker of adipogenesis as it is an enzyme that is up-regulated during adipogenesis and is involved in the synthesis of triacylglycerides in lipogenesis [121].

5.2 Results and Discussion

5.2.1 Adipose Derived Stem Cell Extraction and 2-D Culture

Primary ASCs were isolated from freshly excised human adipose tissue following the protocols listed in Chapter 3. The cell density acquired varied somewhat between the donor, sample volume, and the depot type from which the tissue was extracted (subcutaneous or breast). In general, the ASCs appeared rounded shortly after cell isolation, eventually adopting a more fibroblast-like morphology after they were seeded on tissue culture polystyrene (TCPS) for 24 h.

5.2.2 Cell Encapsulation in Photo-Polymerizable DAT-Polymer Hydrogel

Passage 2 human ASCs were photo-encapsulated into the MGC and MCS-DAT composite scaffolds at a density of $1x10^6$ cells per scaffold. Overall, MCS and MGC containing 0, 3, and 5% (w/v) DAT were seeded to determine the effects of each type of hydrogel and the varying DAT concentrations on the cell response. Immediately after crosslinking, the hydrogels without DAT appeared cylindrical (diameter = 7 mm, height

= 3 mm) and lightly translucent pink from the culture medium that was used to dissolve the MCS and MGC. As the DAT concentration increased, the hydrogels became more opaque, developing a more off-white appearance from the cryo-milled DAT. The hydrogels were cultured in proliferation medium for 24 h before adipogenic differentiation was induced by culturing the seeded scaffolds in serum-free, adipogenic differentiation medium.

5.2.3 Cell Viability Analysis and Cell Count

To ensure that both the scaffold fabrication method and the scaffolds themselves were cytocompatible, cell viability was assessed 24 h after cell encapsulation, as well as 7 and 14 days after adipogenic differentiation was induced, using the LIVE/DEAD® Viability/Cytotoxicity Assay (Invitrogen). The DAT was also pre-labeled with amine-reactive Alexa Fluor® 350 carboxylic acid, succinimidyl ester (Molecular Probes, Burlington, Canada) to facilitate visualization. Confocal microscopy was used to capture gel images at different xy-planes along different depth levels.

The Live/Dead assay confirmed the presence of live cells throughout the culture period [Fig. 5.1 – 5.2]. The encapsulated ASCs retained a rounded morphology throughout all of the gels, which may be more characteristic of the ASCs within native adipose tissue than cells cultured on TCPS [Fig. 5.1] [18, 31]. In addition, the ASCs generally remained evenly distributed within the xy-planes of the hydrogels, with more dead cells gradually settling near the bottom of the scaffolds as time progressed.

Cell viability within the hydrogels at 24 h after encapsulation ranged between 68-76%, with MGC hydrogels alone possessing the lowest value and MCS with 5 % (w/v) DAT possessing the highest one in the range, although these values were not statistically different [Fig. 5.3]. At 14 days after adipogenic differentiation was induced, cell viability in the MGC gels alone dropped to 53.3 ± 3.3%, while the MCS gels with 5% (w/v) DAT sustained a smaller drop (69.7 ± 6.2%). Similarly, cell viability in the MCS alone gels dropped significantly over 2 weeks (70.2 ± 3.1% to 56.6 ± 5.3%), while the MGC gels with 5% (w/v) DAT experienced a smaller drop from 74.2 ± 5.9% to 65.5 ± 3.5%.

An average cell count per xy-plane was determined before ASC differentiation induction to the end of the culturing period [Fig 5.4]. The cell numbers were relatively constant amongst all of the hydrogels before adipogenic differentiation, but they steadily decreased with time, with the MGC and MCS alone gels experiencing the greatest reduction in cell count. In contrast, the decrease in the cell count in all of the DAT-containing hydrogels was not significant. The overall decrease in cell count indicated that the cells were not undergoing proliferation, a feature characteristic of terminally differentiated adipocytes [18, 31].

From the viability assay results, the DAT-containing gels retained a larger number of viable cells over the duration of the culturing period. In addition, the concentration of DAT added to the gels had a positive effect on cell viability and cell adhesion; the scaffolds with 5% (w/v) DAT achieved an overall better result in comparison to all other scaffold types. These positive effects may be associated with the rich basement

membrane found within the ECM of DAT, which includes collagen IV and laminin, a glycoprotein that can bind to cells through integrin receptors, contributing to cell adhesion and influencing cell survival [82, 87, 88]. Decellularized ECM powder was developed by Choi et al. through manual milling [140]. After seeding with human ASCs, Choi et al. reported that the decellularized ECM powder promoted high levels of cell viability over 20 days of culturing, thereby further supporting the positive properties of decellularized tissue as a scaffolding material [140].

MGC and MCS alone had very similar results, suggesting that there was not much of a distinction between the polymers for supporting ASC viability. Interestingly, MCS gels containing 5% (w/v) DAT appeared to provide the most supportive microenvironment in terms of cell number and viability.

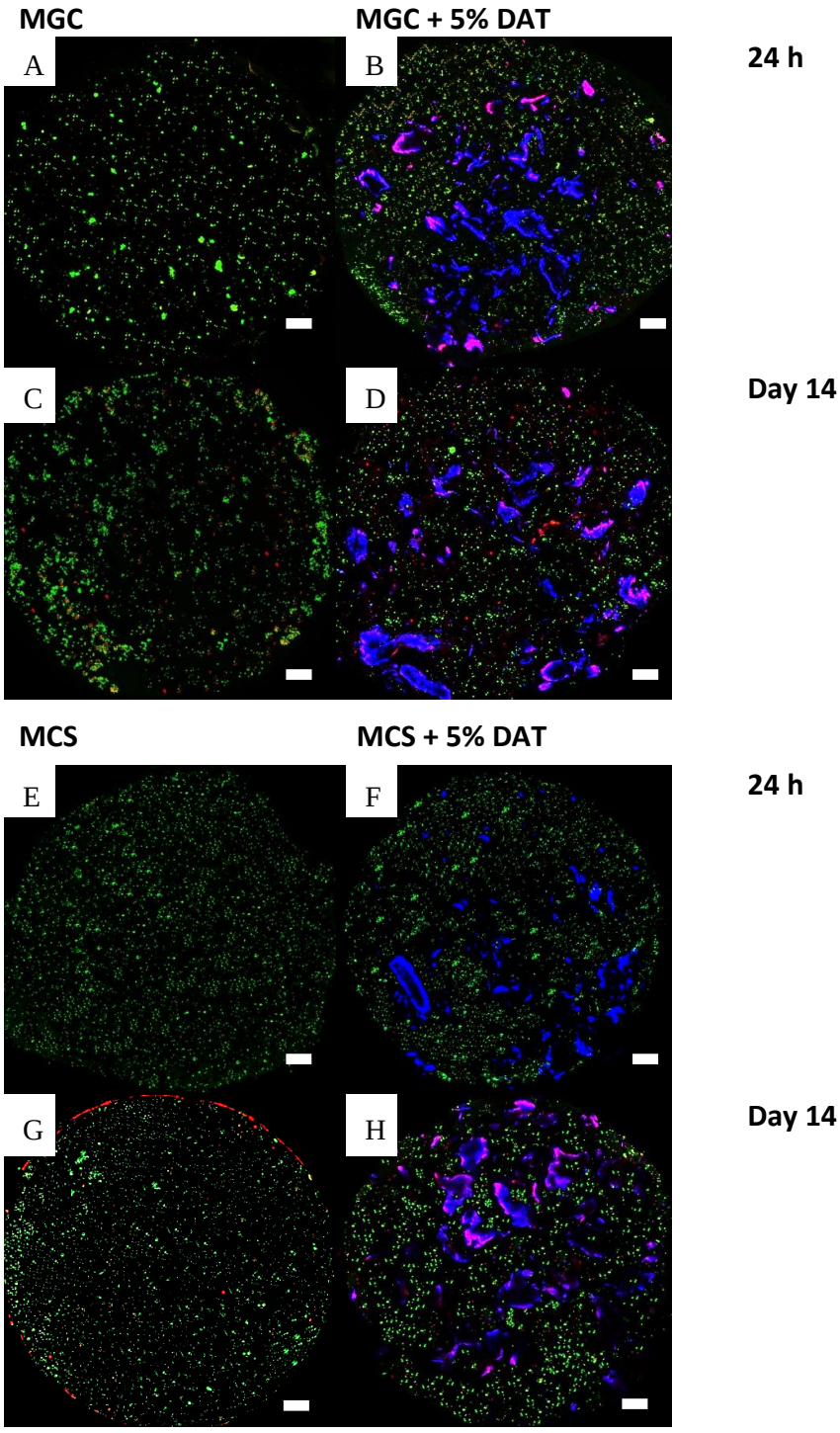

Figure 5.1: Laser scanning confocal microscope images of ASC-encapsulated gels. Viable cells are stained green, dead cells are stained red, and the DAT is blue. Representative cell

viability images of MGC, MGC + 5% (w/v) DAT, MCS, and MCS + 5% (w/v) DAT at 24 h prior and 14 days post adipogenic differentiation induction. Scale bar = 200 μm.

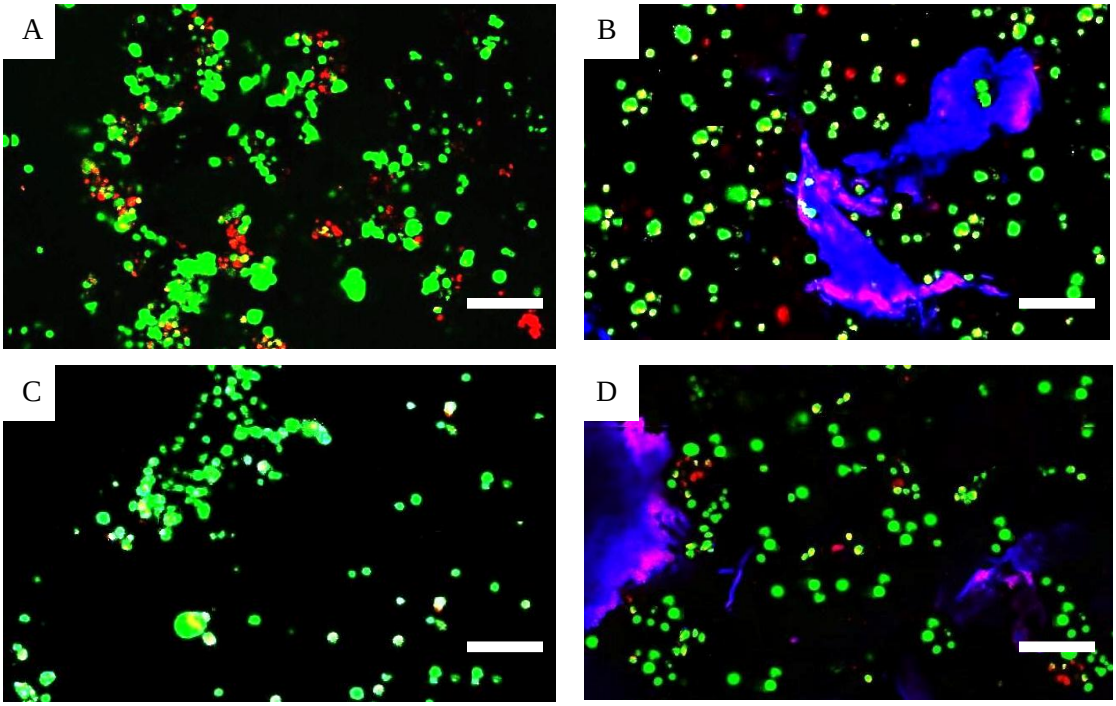

Figure 5.2: Enlargement cell viability staining images taken from Fig 5.1 at 14 days after adipogenic differentiation induction; a) MGC, b) MGC+5% (w/v) DAT, c) MCS and d) MCS+5% (w/v) DAT. Viable cells are stained green, dead cells are stained red, and the DAT is blue. The pink represents the ethidium homodimer (used for staining dead cells) that binds to DAT on a small scale. Scale bar = 100 μm.

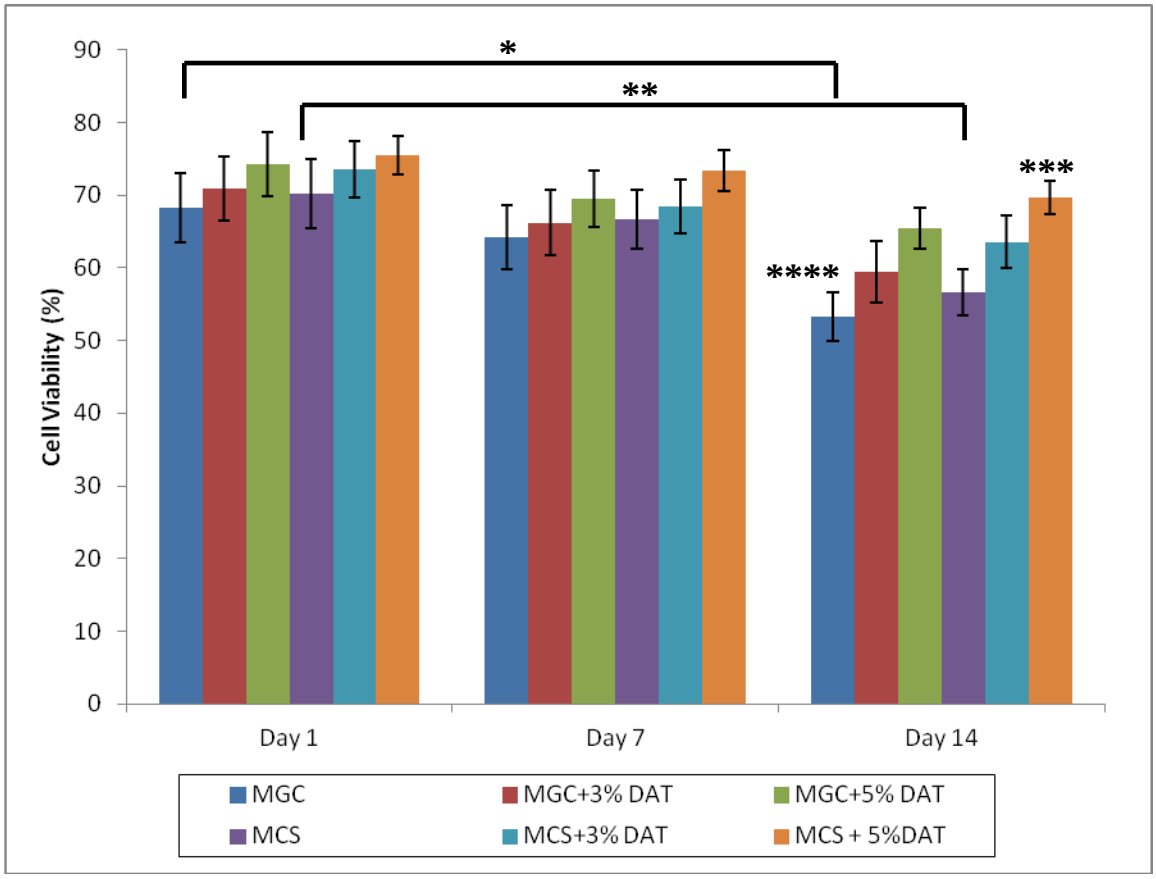

Figure 5.3: ASC viability after encapsulation in MGC and MCS-DAT composite scaffolds and adipogenic differentiation induction for up to 14 days (n=3, N=3). Statistical significance was determined after converting percentages to arcsin values by one-way ANOVA with a Tukey's post-hoc comparison of means ($p<0.05$) between: (i) time points within each scaffold group; *MGC groups are statistically different at 14 days from 24 h; **MCS groups are statistically different at 14 days from 24 h. (ii) Scaffold groups at each time point; ***MCS+5% DAT at 14 days statistically different than all scaffold groups at 14 days; ****MGC at 14 days statistically different than MGC+5% DAT and MCS+3% DAT at 14 days. Data is presented as the mean ± the standard deviation.

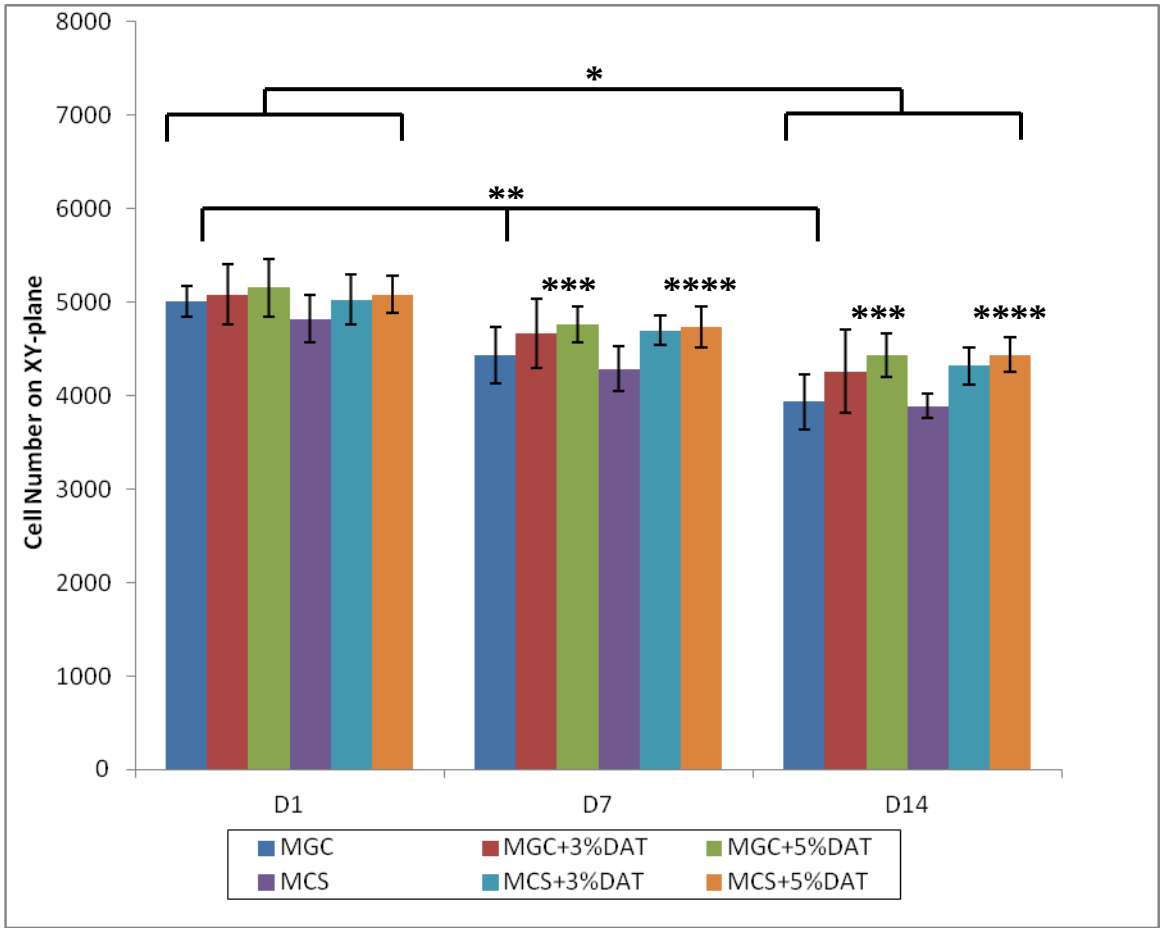

Figure 5.4: Average number of cells taken over 3 xy-planes from the cross-section of the MGC- and MCS-based scaffolds after cell encapsulation and adipogenic differentiation induction for up to 14 days (n=3, N=3). Differences between groups were determined by one-way ANOVA with a Tukey's post-hoc comparison of means ($p<0.05$) between: (i) time points within each scaffold group; *all groups are statistically different at 14 days from 24 h; **MGC groups are statistically different at all time points. (ii) Scaffold groups at each time point; ***MGC+5% DAT at 7 and 14 days are statistically different than MGC and MCS at 7 days and 14 days respectively; ****MCS+5% DAT at 7 and 14 days are statistically different than MGC and MCS at 7 and 14 days respectively. Data is presented as the mean ± the standard deviation.

5.2.4 Enzymatic Activity

Adipogenesis was quantitatively assessed in differentiating ASCs that were encapsulted in MGC- and MCS-based scaffolds, DAT, and 2-D TCPS at 72 h, 7 days and 14 days after adipogenic induction by determining the mean GPDH activities using a spectrophotometric assay (Fig. 5.5). Undifferentiated ASCs cultured in proliferation medium on 2-D TCPS were used as a negative control. Adipogenesis was detected to a certain extent in all of the induced groups over the 14 day culturing period, as measured by increased GPDH activities. At 72 h and 7 days following adipogenic differentiation induction, the mean GPDH activities of the ASCs within the MGC-DAT scaffolds, MCS, MCS-DAT scaffolds, and DAT alone were significantly greater than the mean GPDH activities of the ASCs seeded on the MGC alone (11.5 ± 3.6 mU/mg protein and 17.0 ± 2.8 mU/mg protein respectively). However, at the 72 h time point, the mean GPDH activities for all of the other scaffold groups were not significantly different from each other. After one week of culturing, the mean GPDH activities for MGC+5% (w/v) DAT (29.1 ± 5.3 mU/mg protein), MCS+3% (w/v) DAT (28.6 ± 6.9 mU/mg protein), and MCS+5% (w/v) DAT (38.8 ± 5.0 mU/mg protein) were higher than the MGC and MCS alone scaffolds. Interestingly, at the day 14 time point, the mean GPDH activity of the MCS+5% (w/v) DAT group was significantly higher than all of the other scaffold groups (45.3 ± 3.7 mU/mg protein), suggesting that this scaffold was the most conducive to adipogenesis. In contrast, the mean GPDH activity levels of the ASCs cultured in MGC were significantly lower than all other scaffold groups.

From Figure 5.5, the inclusion of DAT within the hydrogels led to higher GPDH activities, indicating that the DAT was promoting adipogenesis. This is supported by the work of Flynn, where ASC-seeded DAT induced higher GPDH activity levels than observed in ASCs cultured on TCPS and or in the form of 3-D cell aggregates over 7 days [121]. In the current study, throughout the culture period, the GPDH activity levels for the ASC-seeded DAT alone remained comparable to the DAT-containing MGC hydrogels, as well as the MCS alone and MCS+3% DAT, although the MCS alone had a slightly lower mean GPDH activity level. The combination of MCS and 5% DAT led to the highest GPDH activity levels out of the scaffold groups, which were consistent regardless of the cell donor source, suggesting that the chondroitin sulphate-based scaffolds were more conducive to adipogenic differentiation than the glycol chitosan-based biomaterials. These results compare favorably to another study where photo-crosslinked methacrylated alginate hydrogels of varying stiffness (3.3, 7.9, and 12.4 kPa) were used to encapsulate 3T3-L1 preadipocytes [141]. Following 8 days of differentiation, the mean GPDH activities were within the range of 0.1 – 0.3 mU/mg protein, with the stiffest hydrogel having the lowest GPDH activity. These GPDH activity levels could be influenced by the high levels of cell death (>50%) noted at the time of assay [141].

In another study, human ASCs from middle-aged, non-obese women were seeded onto hyaluronic acid scaffolds and cultured for up to 30 days in adipogenic differentiation medium [142]. At day 12, the average GPDH activity level was recorded as 60 mU/mg

protein. This level is comparable to the activity levels obtained from the seeded ASCs in MCS-5% (w/v) DAT from this study (45.3 ± 3.7 mU/mg protein), which were extracted from obese and overweight donors at varying ages [142]. Generally factors that impeded adipogenic differentiation include increasing donor age and a high donor-BMI value, often associated with desensitization to the effects of insulin in the differentiation medium [121].

Collagen Type 1 gels were investigated in a study by Si et al. where adipogenic differentiation was induced immediately after the scaffolds were seeded with 3T3-L1 murine cells [143]. After a culture period of 12 days, GPDH activity levels were reported to be 30 mU/mg protein [143]. While this value compares favourably to the results obtained from the MCS-5% (w/v) DAT scaffold groups, the human ASCs used on MCS scaffolds were isolated from non-ideal sources, which restricted its differentiation potential compared to 3T3-L1 cells [121].

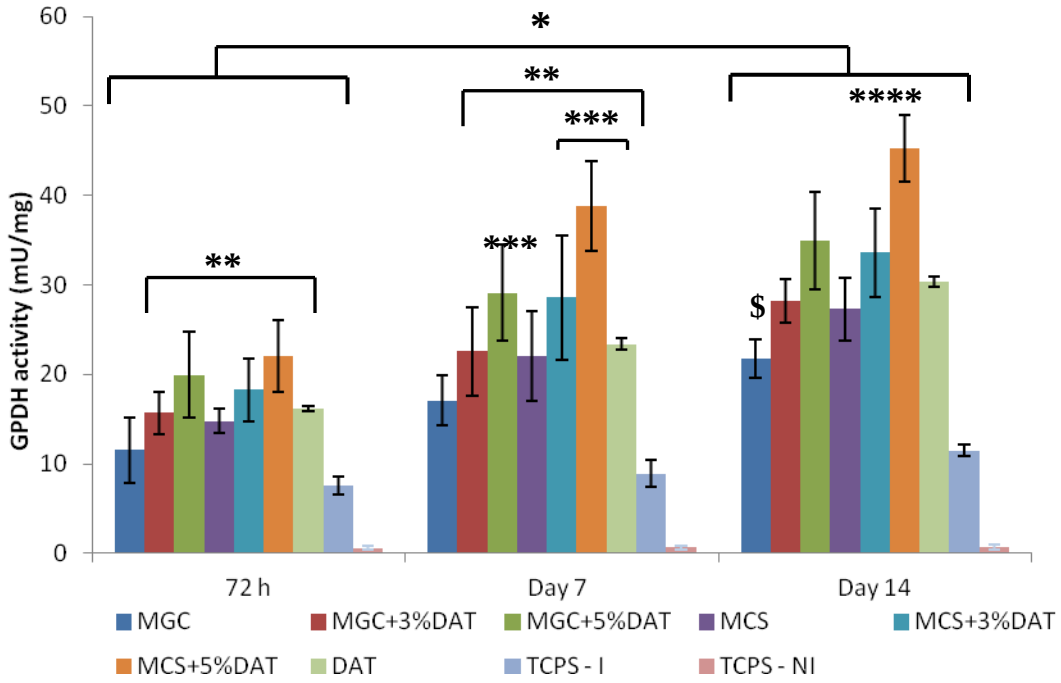

Figure 5.5: GPDH activity of encapsulated ASCs after adipogenic differentiation induction for 72 h, 7 days and 14 days (n=3, N=3). The results were averaged over three sets of results from ASCs obtained from 3 donors (donor body mass index (BMI): 30 (obese) aged 31, 26.4 (overweight) aged 41, 32.8 (obese) aged 46). Statistical significance was determined by one-way ANOVA with a Tukey's post-hoc comparison of means ($p<0.05$) between: (i) time points within each scaffold group; *all groups were statistically different at 14 days from 72 h, except for the TCPS non-induced control. (ii) Scaffold groups at each time point; **statistically different than MGC for all time points, * statistically different than MGC and MCS at 7 days, **** statistically different than all other scaffolds at 14 days; $ statistically different than MGC+5% DAT and MCS+3% DAT at 14 days. Additionally, TCPS non-induced negative controls are statistically different than all other groups at all time points. TCPS induced are statistically different than all groups at all time points except MGC at 72 h (statistically different at 7 and 14 days only).**

5.2.5 Gene Expression

End-point RT-PCR was used to qualitatively evaluate the expression of three key adipogenic markers: PPARγ, C/EBPα, and LPL, with GAPDH as the housekeeping gene. As discussed in Chapter 2, PPARγ and C/EBPα are key transcriptional regulators for adipogenic differentiation, and the expression of both genes results in cellular growth arrest and the up-regulation of genes responsible for the adipogenic phenotype [57, 64]. LPL is commonly expressed in adipocytes and it is heavily involved in adipogenesis by hydrolyzing triacylglycerol prior to cellular intake of free fatty acids for lipid storage during lipogenesis [33, 36].

For this study, induced ASCs were cultured for up to 14 days on TCPS and the following scaffolds: DAT, MGC, MGC+5% (w/v) DAT, MCS, MCS + 5% (w/v) DAT Representative results from one cell donor (aged = 46, BMI = 26) are shown in Fig 5.6, with the complete data sets from all three donor study repeats (n=2, N=3) included in the Appendix. All groups expressed levels of adipogenic gene expression over the course of the culture period. At the 7 day time point, the samples containing DAT showed relatively higher adipogenic gene expression than the TCPS, MGC alone and MCS alone samples, particularly in terms of the expression levels of PPARγ and C/EBPα, which are master regulators and early markers of adipogenesis [57]. The TCPS controls, in contrast, showed the lowest levels of expression. Similar trends were seen at the 14 day time point, supporting the quantitative GPDH enzyme activity results that the DAT promoted the adipogenic differentiation of the ASCs. In general, at 14 days induction, all of the

samples expressed higher levels of PPARγ, C/EBPα, and LPL, consistent with the progression of adipogenic differentiation. However, the MCS+5% (w/v) DAT samples appeared to have the highest levels of adipogenic gene expression, consistent with the GPDH data. Once again, these results suggest that in the presence of the DAT, the MCS was more supportive of adipogenesis than the MGC.

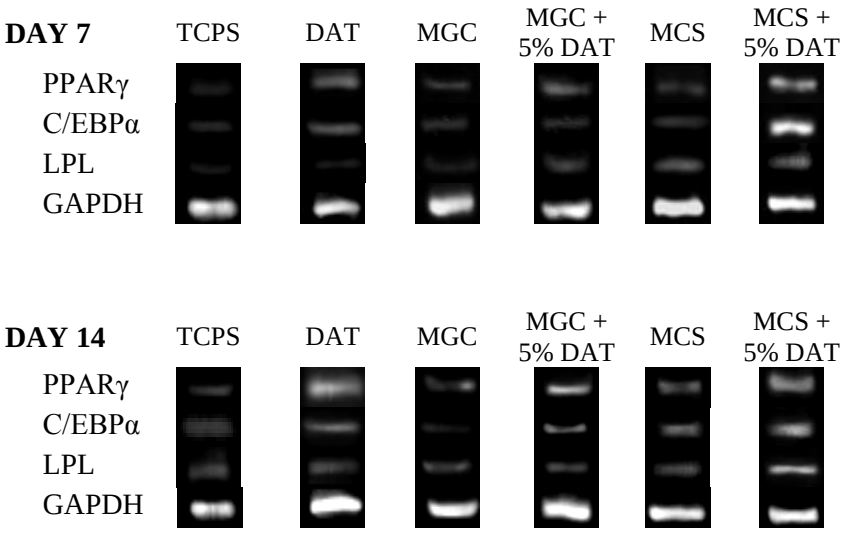

Figure 5.6: Representative end point RT-PCR gel bands showing the expression of the adipogenic markers PPARγ, C/EPBα and LPL in ASC-seeded TCPS, DAT, MGC, MGC + 5% (w/v) DAT, MCS, and MCS + 5% (w/v) DAT cultured in adipogenic medium for 7 or 14 days. GAPDH was used as the housekeeping gene. Data shown is obtained from ASC donor with a BMI of 26.0, aged 46.

5.2.6 Oil Red O staining for Intracellular Lipid

Intracellular lipid staining was conducted on the ASC-seeded MGC, MGC+5% (w/v) DAT, MCS, and MCS+5% (w/v) DAT hydrogels after the cells were cultured in adipogenic differentiation medium for up to 2 weeks [Fig 5.7]. Under confocal microscopy, the lipid droplets fluoresced red through Oil Red O staining, while the DAT appeared blue, as it was pre-stained with the amine-reactive Alexa Fluor® 350 carboxylic acid, succinimidyl ester dye, as described in Chapter 3.

During adipogenic differentiation, differentiating ASCs store a large amount of triacylglycerol in the form of a unilocular lipid vacuole that occupies 90% of the cell volume [31-33]. As such, the presence of large rounded intracellular lipid droplets is indicative of cells that have undergone adipogenesis, as can be seen in all of the samples shown in Figure 5.6 [32, 33]. The scaffolds with the addition of the DAT appeared to contain larger lipid droplets, characteristic of a more mature adipocyte phenotype, than the MGC or MCS scaffolds alone, which implies that the DAT supported ASC lipogenesis in the composite hydrogels. In addition, a larger number of intracellular lipid droplets are present per field in the DAT-containing hydrogels, associated with a higher number of differentiating cells, especially after 14 days of culturing compared to the 7 days time point, which supports the idea that DAT is promoting adipogenesis and a more uniform, higher-level cell response within the encapsulated cell populations. While the intracellular lipid staining data is qualitative in nature, the cellular phenotype and consistency observed in the composite scaffolds containing the DAT+hydrogels was very

promising and consistent with a progression in adipogenesis. The ASCs in these samples were displaying a morphology characteristic of mature adipocytes, supporting the gene and protein expression data.

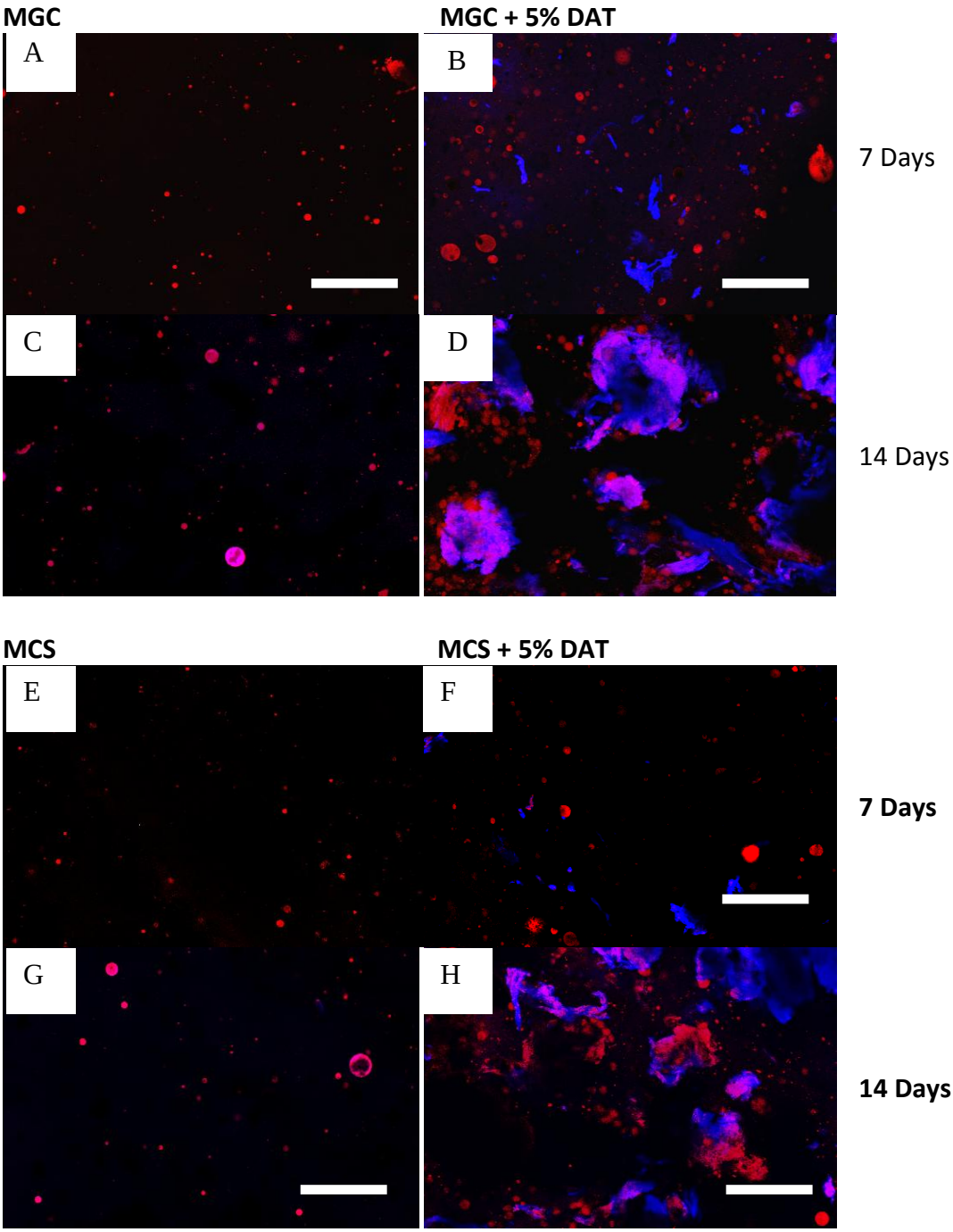

Figure 5.7: Oil Red O staining of hydrogels after adipogenic induction; a) MCS and b) MCS+5% (w/v) DAT at 7 days, c) MCS and d) MCS+5% (w/v) DAT at 14 days, e) MGC and f) MGC+5% DAT at 7 days, g) MGC and h) MGC+5% DAT at 14 days. Lipid droplets are stained red and the DAT is blue. Scale bars = 100 μm.

5.3 Conclusions

Human ASCs are a cell source of interest for adipose tissue engineering applications due to their ability to undergo proliferation and adipogenesis, which holds promise for regenerating functional and viable adipose tissue. ASCs from human donors were seeded on two different groups of composite hydrogels derived from methacrylated glycol chitosan (MGC) with decellularized adipose tissue (DAT), and methacrylated chondroitin sulphate (MCS) with DAT, that were developed in the previous chapter. A comparison between these two scaffold groups was conducted based on the cell response over 2 weeks in culture in adipogenic differentiation medium. This comparison was done to determine the effects of the polymer composition and the DAT concentration on cell viability and adipogenic differentiation. Overall, the presence of the DAT within the hydrogels promoted ASC viability and induced adipogenic gene expression. These effects were amplified as the DAT concentration was increased in the scaffolds. Interestingly, the combination of MCS with 5% (w/v) DAT consistently promoted the best cell response of all of the scaffold groups that were tested, supporting the highest level of cell viability, cell attachment (which was determined via cell count), and adipogenic gene and protein expression. Adipogenesis may have been promoted by the cells being encapsulated in the hydrogels, improving the cell seeding density on the DAT and preventing cell washout during routine culturing and medium changes. A high level of cell-to-cell contact is recognized as being an important factor in promoting adipogenesis. In addition, based on the results, the chondroitin sulphate may have

mediated ASC adipogenesis within the composites by influencing the mechanical micro-environment or the cell shape, or through direct interactions that altered the lineage-commitment and differentiation.

Chapter 6

Conclusions and Future Work

6.1 Summary and Conclusions

Loss of soft tissue can be caused by trauma, post-surgical defects, tumours, congenital defects, and from aging [6]. Clinically, the degree of soft tissue damage dictates the treatment prescribed – for severe soft tissue loss, invasive surgical transfer of autologous vascularised tissue flaps is the current standard, whereas for smaller defects, synthetic or natural-based filler materials can be injected into the defect site for temporary augmentation [4, 6, 7, 89]. Unfortunately, these treatments have limited success and are associated with donor site morbidity and implant volume loss over time, respectively [4, 7]. As such, adipose tissue engineering presents a unique and permanent solution for treating soft tissue defects through the construction of viable, functioning tissues that could be implanted into the host.

Presently, there are two common tissue engineering strategies that are employed for soft tissue regeneration. The first approach involves seeding and culturing the cell source of interest on a defined three-dimensional, structural scaffold, followed by surgical implantation of the seeded construct. The second strategy focuses on delivering the cells within an injectable carrier that will allow a scaffold to form *in situ* [3, 4, 6]. For correcting soft tissue defects, the second strategy is appealing since an injectable scaffold

could be delivered in a minimally invasive method and could evenly fill irregularly-shaped defect volumes, which are commonly associated with soft tissue loss [1, 4, 6]. Other factors to consider for adipose tissue engineering include the cell source and the scaffolding material. While using mature adipocytes is a logical choice for the construction of adipose tissue, these terminally-differentiated cells cannot undergo mitotic division, thereby limiting their regenerative abilities [1, 6]. Human multipotent adipose-derived stem cells (ASCs), on the other hand, have the ability to proliferate and differentiate along the adipogenic lineage, making ASCs a very attractive regenerative cell source for this application [1, 4, 9, 26].

A variety of synthetic and natural scaffolds for adipose tissue engineering have been investigated. Recent literature points to the use of decellularized extracellular matrix, in particular decellularized adipose tissue (DAT), as a scaffold as its natural protein composition can promote cell viability, proliferation and differentiation [80]. Therefore, the objective of this work was to develop a photopolymerizable, injectable scaffold incorporating DAT and human ASCs with the goal of promoting cell viability and adipogenic differentiation to engineer adipose tissue.

Photopolymerizable hydrogels were chosen to serve as DAT carriers since they can be photo-crosslinked rapidly and *in situ*, allowing for more spatial control over the scaffold. By definition, hydrogels are water insoluble networks formed by the crosslinking of water soluble polymer chains. These gels have the ability to swell in aqueous media, absorbing and retaining a high, tissue-like water content, while

maintaining a specific geometry [10, 101, 102]. As their microstructure can be engineered to closely resemble the ECM, synthetic and natural based hydrogels have been used extensively for tissue engineering applications [12, 101, 105, 106]. In this project, methacrylated chondroitin sulphate (MCS) and methacrylated glycol chitosan (MGC) were chosen to form the hydrogel portion of the DAT-polymer composite scaffolds. Chondroitin sulphate is a material naturally found within the extracellular matrix and as such, it is a compound that the seeded cells recognize [114-116]. Although studies are limited regarding its effect on adipogenesis, chondroitin sulphate has been used extensively in conjunction with mesenchymal stem cells (MSCs), where high cell viability and cell adhesion were recorded [127]. Likewise, chitosan can promote cell attachment, viability, and it naturally exerts wound healing and antimicrobial properties. Previous *in vitro* and *in vivo* studies involved blending chitosan and chitosan derivatives with gelatin and collagen injectable hydrogels for adipose tissue engineering applications. Overall, these chitosan-based hydrogels showed promise in terms of promoting adipogenesis after being seeded with ASCs [111, 125, 126].

This thesis focused on the comparison of MCS-DAT and MGC-DAT composite scaffolds with the goal of regenerating adipose tissue. The first half of this study involved scaffold fabrication and characterization. Chondroitin sulphate and glycol chitosan were methacrylated, to enable photo-polymerization. ^{1}H NMR spectroscopy was used to determine if the methacrylation reaction was successful. Construction for MCS and MGC scaffolds were optimized in order to achieve a similar elastic modulus within both

hydrogels. Since gel stiffness can impact stem cell lineage commitment, similar mechanical properties in MGC and MCS are important for the comparison to be made on an equal basis [98]. DAT was cryo-milled and incorporated within the MGC and MCS pre-polymer solutions at concentrations of 0, 3 or 5% (w/v). These composite hydrogels were subsequently characterized through sol content determination, equilibrium water content measurement, and mechanical testing. Overall, the DAT functioned as a volume filler, contributing to the crosslink density and mechanical stiffness of the composites, as was seen in the decrease in water content and sol content, combined with the increase in gel stiffness of the scaffolds that contained a higher DAT concentration.

The second portion of this project involved encapsulating ASCs within the MGC- and MCS-DAT composite hydrogels to determine the effects of the polymer formulation and DAT concentration on the cell response in terms of viability and adipogenesis. The cell seeded scaffolds were cultured in adipogenic medium for up to 2 weeks before the cell response was investigated by determining cell viability, cell count, and adipogenic differentiation levels through quantitative methods (mean glycerol-3-phosphate dehydrogenase (GPDH) activity) and qualitative techniques (gene expression and intracellular lipid staining). ASCs were found to have a more favourable cell response in terms of viability and differentiation in the hydrogels that contained higher DAT content, suggesting that the DAT promoted cell viability and adipogenesis. ASCs cultured in the MCS with 5% (w/v) DAT composites demonstrated the highest levels of cell viability

and adipogenic differentiation, indicating that the MCS was a better delivery vehicle for adipose tissue engineering with human ASCs as compared to MGC.

The goal of this project was to construct an injectable, photopolymerizable DAT-containing scaffold that could effectively and quickly gel *in situ* for adipose tissue engineering. DAT was mechanically rendered into powder form through general milling, allowing the tissue to be readily incorporated within the hydrogels. Overall, an injectable, DAT-containing scaffold has great potential for adipose tissue engineering as it compares favourably against synthetic and natural scaffolds including alginate, hyaluranon and collagen by consistently promoting cell viability and adipogenic differentiation levels. Additionally, it is notable that the DAT-based scaffolds provided a conducive micro-environment for differentiation of the ASCs regardless of the cell donor source, as working with primary cell populations is often noted as a reason for great variability in the differentiation response.

6.2 Contributions

The most significant contributions that this thesis provided to the field include the following:

- The design and construction of a photopolymerizable, injectable, DAT-based scaffold by incorporating biocompatible hydrogels derived from chondroitin sulphate and glycol chitosan of similar mechanical properties with powdered, cryo-milled DAT.

- Scaffold characterization to gain a better understanding of polymer-DAT interactions.
- A comparison between methacrylated chondroitin sulphate and glycol chitosan to determine the influence of the polymer on cell viability and adipogenic differentiation.
- A comparison between different DAT concentrations (0, 3 and 5% (w/v)) to determine if the amount of incorporated DAT affected the cell response.
- Successfully demonstrated that incorporating the DAT within the composite scaffolds promoted viability and adipogenic differentiation. In addition, the MCS with DAT scaffolds promoted higher cell viability and adipogenesis relative to the MGC with DAT scaffolds.

6.3 Future Work

While this study provides a solid basis towards the development of an injectable, polymer-DAT bioscaffold for the repair of soft tissue defects, several more in-depth investigations are required to achieve a more optimized injectable DAT-based scaffold that could transition into clinical applications. The following list of recommendations is divided into *in vitro* and *in vivo* studies that could be performed in future work.

In vitro studies:

- The development and optimization of the photopolymerization protocol to develop thicker hydrogels for the purpose of filling larger volume defect sites. The current protocol used has been optimized for gels of a set size (diameter = 7 mm, height = 3 mm). Photo-polymerization can occur unevenly in gels if UV exposure occurs at the top of the surface and proceeds downwards, leaving the top portion of the scaffold more tightly crosslinked than the bottom [115]. This effect can be seen more prominently in larger scaffolds and as such, a new protocol needs to be developed that will adjust for scaffold volume, while allowing for a high cell viability retention during photo-encapsulation.
- The development of alternative hydrogel crosslinking methods that could result in the *in situ* formation of the scaffold, such as thermal gelling. A comparison of these new methods for photopolymerization should also be made to determine which crosslinking method is most appropriate.
- An in-depth characterization of the protein composition found within DAT to gain a better understanding of the effects of this biomaterial on the seeded cells.
- An in-depth chemical analysis to see how DAT has contributed to the crosslink density when forming the DAT-polymer hydrogels. This will help to gain a better understanding of the DAT-polymer interactions in the photo-polymerization reactions.

- Potentially investigate other natural and synthetic based polymers for the hydrogel construction (ex. collagen) and conduct a comparison with the DAT-polymer composite scaffolds used in this study. This would be done to help develop an understanding of the role of the cell-ECM interactions in mediating the ASC response, with the goal of optimizing the scaffold design to allow for enhanced cell viability and adipogenesis.
- Longer *in vitro* culturing periods to gain a more thorough understanding of ASC longevity within the hydrogels.

In vivo studies:

- *In vivo* implantation of the ASC seeded, MGC- and MCS-DAT composite scaffolds to characterize the ASC response in the subcutaneous environment. *In vivo* assessments should include determining the levels of adipogenic gene expression, as well as angiogenesis.
- The use of other sources of decellularized tissues as a comparison against DAT to determine if the matrix source influences the seeded ASCs and host responses.

References

[1] Gomillion CT, Burg KJL. Stem cells and adipose tissue engineering. Biomaterials 2006;27: 6052-63.

[2] Vallée M, Côté JF, Fradette J. Adipose-tissue engineering: taking advantage of the properties of human adipose-derived stem/stromal cells. Pathologie-biologie 2009;57: 309-17.

[3] Patrick CW. Adipose tissue engineering: the future of breast and soft tissue reconstruction following tumor resection. Seminars in Surgical Oncology 2000;19:302-311

[4] Stosich MS, Mao JJ. Adipose tissue engineering from human adult stem cells: clinical implications in plastic and reconstructive surgery. Plastic and Reconstructive Surgery 2007;119:71-83

[5] American Society of Plastic Surgeons (Web site). Available at: http//www.plasticsurgery.org. Accessed July 31, 2011.

[6] Flynn L, Woodhouse K. Adipose tissue engineering with cells in engineered matrices. Oganogenesis 2008;4:228-35

[7] Murray C, Zloty D, Warshawski L. The evolution of soft tissue fillers in clinical practice. Dermatologic clinics 2005;23(2):343-63

[8] Hodde J. Extracellular matrix as a bioactive material for soft tissue reconstruction. ANZ Journal of Surgery 2006;76(12):1096-100

[9] Gimble J. Guilak F. Adipose-derived adult stem cells: isolation, characterization, and differentiation potential. Cytotherapy 2003;5(5):362-9.

[10] Drury JL, Mooney DJ. Hydrogels for tissue engineering: scaffold design variables and applications. Biomaterials (2003);24(24):4337-4351.

[11] Tan H, Marra KG. Injectable, biodegradable hydrogels for tissue engineering applications. Materials 2010;3(3):1746-1767.

[12] Brandl FP, Seitz AK, Tessmar JKV, Blunk T, Göpferich AM. Enzymatically degradable poly(ethylene glycol) based hydrogels for adipose tissue engineering. Biomaterials 2010;31(14):3957-66.

[13] Gentleman E, Nauman EA, Livesay GA, Dee KC. Allowing development of adipocytic soft tissue in vitro. Tissue Engineering 2006;12(6):1639-49.

[14] Bryant SJ, Davis-Arehart KA, Luo N, Shoemaker RK, Arthur JA, Anseth KS. Synthesis and characterization of photopolymerized multifunctional hydrogels : water-soluble poly (vinyl alcohol) and chondroitin sulfate macromers for chondrocyte encapsulation. Macromolecules 2004;37:6726-6733.

[15] Lee CT, Kung PH, Lee YD. Preparation of poly(vinyl alcohol)-chondroitin sulfate hydrogel as matrices in tissue engineering. Carbohydrate Polymers 2005;61(3):348-354.

[16] Ishihara M, Ono K, Sato M, Nakanishi K, Saito Y, Yura H. Acceleration of wound contraction and healing with a photocrosslinkable chitosan hydrogel. Sensors and Actuators A: Physical 2002; 95(3), 120-134.

[17] Paus LR, Klein J, Permana P, Owecki M, Chaldakov GN, Bohm M, Ryan TJ Sowinski J. What are subcutaneous adipocytes really good for? Experimental Dermatology 2007;16:45-70.

[18] Butterwith SC. Molecular events in adipocyte development. Pharmacology & Therapeutics 1994;61:399-411.

[19] Bouchard C. Genetic detrerminants of regional fat distribution. Human Reproduction & Embryology 1997;12:1-5

[20] Wajchenberg BL. Subcutaneous and Visceral Adipose Tissue: Their Relation to the Metabolic Syndrome. Endocrine Reviews 2000;21(6):697-738.

[21] Fantuzzi G. Adipose tissue, adipokines, and inflammation. The Journal of Allergy and Clinical Immunology 2005;115:911-9

[22] Langin D. Adipose tissue lipolysis as a metabolic pathway to define pharmacological strategies against obesity and the metabolic syndrome. Pharmacological Research 2006;53:482-91

[23] Langin D. Recruitment of brown fat and conversion of white into brown adipocytes: strategies to fight the metabolic complications of obesity? Biochimica et Biophysica Acta 2010;1801:372-6

[24] Cannon B, Nedergaard J. Neither fat nor flesh. Nature 2008;454:947-8

[25] Cannon B, Nedergaard J. Brown adipose tissue: function and physiological significance. Physiological Reviews 2004;84:277-359

[26] Choi JH, Gimble HM, Lee K, Marra KG, Rubin JP, Yoo JJ, Vunjak-novakovic G, Kaplan DL. Adipose tissue engineering for soft tissue regeneration. Tissue Engineering: Part B Reviews 2010;16:413-26.

[27] Gesta S, Tseng YH, Kahn RC. Developmental origin of fat: tracking obesity to its source. Cell 2007;131:242-56.

[28] Miller KK, Daly PA, Sentochnik D, Doweiko J, Samore M, Basgoz NO, Grinspoon SK. Pseudo-Cushing's syndrome in human immunodeficiency virus-infected patients. Clinical Infectious Diseases 1998;27:68-72.

[29] Li Y, Bujo H, Takahashi K, Shibasaki M, Zhu Y, Yoshida Y, Otsuka Y, Hashimoto N, Saito Y. Visceral fat : Higher responsiveness of fat mass and gene expression to calorie restriction than subcutaneous fat. Experimental Biology and Medicine 2003;228:1118-23.

[30] Cinti S. Transdifferentiation properties of adipocytes in the adipose organ. American Journal of Physiology, Endocrinology and Metabolism 2009;297:977-86.

[31] Cinti S. The adipose organ. Prostaglandins, Leukotrienes and Essential Fatty Acids 2005;73:9-15.

[32] Prattes S, Horl G, Hammer A, Blaschitz A, Graier WF, Sattler W, Zechner R, Steyrer E. Intracellular distribution and mobilization of unesterified cholesterol in adipocytes: triglyceride droplets are surrounded by cholesterol-rich ER-like surface layer structures. Journal of Cell Science 2000; 113:2977-89.

[33] Beylot M. Metabolism of white adipose tissue, in adipose tissue and adipokines in health and disease. Humana Press, Totowa 2007;21-33.

[34] Sorisky A. From preadipocyte to adipocyte: differentiation-directed signals of insulin from the cell surface to the nucleus. Critical reviews in clinical laboratory sciences: 1999;36:1-34.

[35] Lelliott CJ, Orešič M, Vidal-Puig A. Obesity and diabetes: lipotoxicity, in adipose tissue in health and disease. John Wiley & Sons, Weinheim, Germany 2010; 347-68.

[36] Large V, Peroni O, Letexier D, Ray H, Beylot M. Metabolism of lipids in human white adipocyte. Diabetes Metabolism 2004;30:294-309.

[37] Cornelius P, Macdougald OA, Lane MD. Regulation of adipocyte development. The Annual Review of Nutrition 1994;14:99-129.

[38] Goldrick RB, McLoughlin GM. Lipolysis and lipogenesis from glucose in human fat cells of different sizes. The Journal of Clinical Investigation 1970;49:1213-23.

[39] Zmuda-Trzebiatowska E, Oknianska A, Manganiello V, Degerman E. Role of PDE3B in insulin-induced glucose uptake, GLUT-4 translocation and lipogenesis in primary rat adipocytes. Cellular Signaling 2006; 18:382-90.

[40] Shepherd E, Noble EG, Klug GA, Gollnick D, Raymond E. Lipolysis and CAMP accumulation in response to physical training in adipocytes. Journal of Applied Physiology 1981;50:143-8.

[41] Zechner R, Kienesberger PC, Haemmerle G, Zimmermann R, Lass A. Adipose triglyceride lipase and the lipolytic catabolism of cellular fat stores. Journal of Lipid Research 2009;50:3-21.

[42] Coppack SW, Persson M, Judd RL, Miles JM. Glycerol and nonesterified fatty acid metabolism in human muscle and adipose tissue in vivo. American Journal of Physiology, Endocrinology and Metabolism 1999;276:E233-40.

[43] Weisberg SP, Mccann D, Desai M, Rosenbaum M, Leibel RL, Ferrante AW. Obesity is associated with macrophage accumulation. Journal of Clinical Investigation 2003;112: 1796-808.

[44] Galinier A, Segafredo C, Nibbelink M, André M, Casteilla L, Pénicaud L. Adipose tissues as an ancestral immune organ: site-specific change in obesity. FEBS letters 2005;579: 3487-92.

[45] Xu H, Barnes GT, Yang Q, Tan G, Yang D, Chou CJ, Sole J, Nichols A, Ross JS, Tartaglia LA, Chen H. Chronic inflammation in fat plays a crucial role in the development of obesity-related insulin resistance. Journal of Clinical Investigation 2003;112:1821-1830.

[46] Schäffler A, Büchler C. Concise review: adipose tissue-derived stromal cells – basic and clinical implications for novel cell-based therapies. Stem Cells 2007;25:818-27.

[47] Zuk P, Zhu M, Mizuno H, Huang J, Futrell JW, Katz J, Benhaim P, Lorenz HP, Hedrick MH. Multilineage cells from human adipose tissue: implications for cell-based therapies. Tissue Engineering 2001; 7:211-28.

[48] Bunnell B, Flaat M, Gagliardi C, Patel B, Ripoll C. Adipose-derived stem cells: isolation, expansion and differentiation. Methods 2008;45:115-20.

[49] Rosen ED, Hsu CH, Wang X. C/EBPa induces adipogenesis through PPARg: a unified pathway. Genes and Development 2002;16:22-26.

[50] Gimble JM, Katz AJ, Bunnell B. Adipose-derived stem cells for regenerative medicine. Circulation Research 2007;100:1249-60.

[51] Rosenbaum AJ, Grande DA, Dines JS. The use of mesenchymal stem cells in tissue engineering - A global assessment. Organogenesis 2008;4:23-7.

[52] Locke M, Windsor J, Dunbar PR. Human adipose-derived stem cells: isolation, characterization and applications in surgery. ANZ Journal of Surgery 2009;79: 235-44.

[53] Doyonnas R, LaBarge M, Sacco A, Charlton C, Blau HM. Hematopoietic contribution to skeletal muscle regeneration by myelomonocytic precursors. PNAS 2004;101: 13507-12.

[54] Sengenès C, Lolmède K, Zakaroff-Girard A, Busse R, Bouloumié A. Preadipocytes in the Human subcutaneous adipose tissue display distinct features from the adult mesenchymal and hematopoietic stem cells. Journal of Cellular Physiology 2005;205,114-22.

[55] Baglioni S, Francalanci M, Squecco R, Lombardi A, Cantini G, Angeli R, Gelmini S, Guasti D, Benvenuti S, Annunziato F, Bani D, Liotta F, Francini F, Perigli G, Serio M, Luconi M. Characterization of human adult stem-cell populations isolated from visceral and subcutaneous adipose tissue. Journal of the Federation of American Society for Experimental Biology 2009;23:3494-505.

[56] McIntosh K, Zvonic S, Garrett S, Mitchell JB, Floyd EZ, Hammill L. The immunogenicity of human adipose-derived cells: temporal changes in vitro. Stem Cells 2006;24:1246-53.

[57] Rosen ED, Spiegelman BM. Molecular regulation of adipogenesis. Annual Review of Cell and Developmental Biology 2000;16:145-71.

[58] Gregoire F. Adipocyte differentiation: from fibroblast to endocrine cell. Experimental Biology and Medicine 2001;226:997-1002.

[59] Baksh D, Song L, Tuan RS. Adult mesenchymal stem cells: characterization, differentiation, and application in cell and gene therapy. Journal of Cellular and Molecular Medicine 2004;8:301-16.

[60] Schwarz C, Leicht U, Rothe C, Drosse I, Luibl V, Röcken M, Schieker M. Effects of different media on proliferation and differentiation capacity of canine, equine and porcine adipose derived stem cells. Research in Veterinary Science 2011; doi:10.1016/j.rvsc.2011.08.010.

[61] Kras KM, Hausman DB, Hausman GJ, Martin RJ. Adipocyte development is dependent upon stem cell recruitment and proliferation of preadipocytes. Obesity Research 1999;7(5):491

[62] Chen HT, Lee MJ, Chen CH, Chuang SC, Chang LF. Proliferation and differentiation potential of human adipose-derived mesenchymal stem cells isolated from elderly patients with osteoporotic fractures. Journal of Cellular and Molecular Medicine 2011; doi: 10.1111/j.1582-4934.2011.01335.x.

[63] Van Harmelen V, Röhrig K, Hauner H. Comparison of proliferation and differentiation capacity of human adipocyte precursor cells from the omental and subcutaneous adipose tissue depot of obese subjects. Metabolism 2004 May;53(5):632-7.

[64] Mandrup S, Lane MD. Regulating adipogenesis. The Journal of Biological Chemistry 1997;272(9):5367-70.

[65] Tanaka T, Yoshida N, Kishimoto T, Akira S. Defective adipocyte differentiation in mice lacking the C/EBPβ and or C/EBPδ gene. The EMBO Journal 1997;16(24):7432-43.

[66] Gregoire FM, Smas CM, Sul HS. Understanding adipocyte differentiation. Physiological Reviews 1998;78(3):783-809.

[67] Holly J, Sabin M, Perks C, Shield J. Adipogenesis and IGF-1. Metabolic Syndrome and Related Disorders 2006;4:43-50.

[68] Kim WK, Jung H, Kim DH, Kim EY, Chung JW, Cho YS, Park SG. Regulation of adipogenic differentiation by LAR tyrosine phosphatase in human mesenchymal stem cells and 3T3-L1 preadipocytes. Journal of Cell Science 2009;122:4160-7

[69] Chapman AB, Knight DM, Ringold GM. Glucocorticoid regulation of adipocyte differentiation: hormonal triggering of the developmental program and induction of a differentiation-dependent gene. The Journal of Cell Biology;1985(4):1227-35.

[70] Obregon MJ. Metabolic effects of thyroid hormones-beyond traditional prospects. Thyroid 2008;18(2):185-95.

[71] Wang Y, Zhao L, Smas C, Sul HS. Pref-1 interacts with fibronectin to inhibit adipocyte differentiation. Molecular and Cellular Biology 2010;30(14):3480-92.

[72] Friedman JM, Halaas JL. Leptin and the regulation of body weight in mammals. Nature 1998;395:763-70.

[73] Stefan N, Stumvoll M, Vozarova B, Weyer C, Funahashi T, Matsuzawa Y. Plasma adiponectin and endogenous glucose production in humans. Diabetes Care 2003;26(12):3315-9.

[74] Kershaw EE, Flier JS. Adipose tissue as an endocrine organ. The Journal of Clinical Endocrinology and Metabolism 2004;89(6):2548-56.

[75] Massiéra F, Bloch-Faure M, Ceiler D, Murakami K, Fukamizu A, Gasc JM. Adipose angiotensinogen is involved in adipose tissue growth and blood pressure regulation. Federation of American Societies for Experimental Biology 2001;15(14):2727-9.

[76] Engeli S, Schling P, Gorzelniak K, Boschmann M, Janke J, Ailhaud G. The adipose-tissue renin-angiotensin-aldosterone system: role in the metabolic syndrome? The International Journal of Biochemistry & Cell Biology 2003;35(6):807-25.

[77] Flaster H, Bernhagen J, Calandra T, Bucala R. The macrophage migration inhibitory factor-glucocorticoid dyad: regulation of inflammation and immunity. Molecular Endocrinology 2007;21(6):1267-80.

[78] Lyon CJ, Hsueh WA. Effect of plasminogen activator inhibitor-1 in diabetes mellitus and cardiovascular disease. The American Journal of Medicine 2003;115(8):62-68.

[79] Liang X, Kanjanabuch T, Mao SL, Hao CM, Tang YW, Declerck PJ. Plasminogen activator inhibitor-1 modulates adipocyte differentiation. American journal of physiology. Endocrinology and Metabolism 2006;290:E103-E113.

[80] Badylak SF. The extracellular matrix as a scaffold for tissue reconstruction. Seminars in Cell and Developmental Biology 2002;13(02):377-383

[81] Divoux A, Clément K. Architecture and the extracellular matrix: the still unappreciated components of the adipose tissue. Obesity Reviews 2011;12(5):e494-503.

[82] Mariman ECM, Wang P. Adipocyte extracellular matrix composition, dynamics and role in obesity. Cellular and Molecular Life Sciences 2010;67(8):1277-92.

[83] Alberts B, Johnson A, Lewis J, Raff M, Roberts K, Walter P. Molecular Biology of the Cell. Garland Science: New York;2002.

[84] Gelse K. Collagens—structure, function, and biosynthesis. Advanced Drug Delivery Reviews 2003;55:1531-46.

[85] Fraser RD, MacRae TP, Suzuki E. Chain Conformation in the Collagen Molecule. Journal of Molecular Biology 1979;129(3):463-81.

[86] Ottani V, Raspanti M, Ruggeri A. Collagen structure and functional implications. Micron 2001;32(3):251-60.

[87] Martin GR, Timpl R. Laminin and other basement membrane components. Annual Review of Cell Biology 1987;3:57-85.

[88] Venstrom KA, Reichardt LF. Extracellular matrix 2: Role of extracellular matrix molecules and their receptors in the nervous system. Federation of American Societies for Experimental Biology 1993;7(11):996-1003.

[89] Livaoğlu M, Yavuz E. Soft tissue augmentation with autologous fat graft: the dissected pouch technique. Journal of Cutaneous and Aesthetic Surgery 2009;2:21-5.

[90] Narins RS, Brandt F, Leyden J, Lorenc ZP, Rubin M, Smith S. A randomized, double-blind, multicenter comparison of the efficacy and tolerability of Restylane versus Zyplast for the correction of nasolabial folds. Dermatologic Surgery 2003;29(6):588-95.

[91] Lupo P. Hyaluronic acid fillers in facial rejuvenation. Seminars in Cutaneous Medicine and Surgery 2006;25(3):122-6.

[92] Buck DW, Alam M, Kim JYS. Injectable fillers for facial rejuvenation: a review. Journal of Plastic, Reconstructive & Aesthetic Surgery 2009;62:11-8.

[93] Valantin MA, Aubron-Olivier C, Ghosn J, Laglenne E, Pauchard M, Schoen H, Bousquet R, Katz P, Costagliola D, Katlama C. Polylactic acid implants (New-Fill)

to correct facial lipoatrophy in HIV-infected patients: results of the open-label study VEGA. AIDS 2003;17(17):2471-7.

[94] Hamilton T. Skin augmentation and correction: the new generation of dermal fillers—A dermatologist's experience. Clinics in Dermatology 2009;27(3):S13-S22.

[95] Convery FR, Gunn DR, Hughes JD, Martin WE. The relative safety of polymethylmethacrylate. A controlled clinical study of randomly selected patients treated with charnley and ring total hip replacements. Journal of Bone and Joint Surgery 1975;57:57- 64.

[96] Mok D. Schwarz J. The use of polymethyl-methacrylate (Artecoll) as an adjunct to facial reconstruction. The Canadian Journal of Plastic Surgery 2004;12:39-42.

[97] Jacovella PF. Use of calcium hydroxylapatite (Radiesse) for facial augmentation. Clinical Interventions in Aging 2008;3:161-74.

[98] Guilak F, Cohen DM, Estes BT, Gimble JM, Liedtke W, Chen CS. Control of stem cell fate by physical interactions with the extracellular matrix. Cell Stem 2009;5:17-26.

[99] Green H, Meuth M. An established pre-adipose cell line and its differentiation in culture. Cell 1974;3(2):127-33.

[100] Li Q, Williams CG, Sun DDN, Wang J, Leong K, Elisseeff JH. Photocrosslinkable polysaccharides based on chondroitin sulfate. Journal of Biomedical Materials Research. Part A;2004(68):28-33.

[101] Tan H, Rubin JP, Marra KG. Injectable in situ forming biodegradable chitosan-hyaluronic acid based hydrogels for adipose tissue regeneration. Organogenesis 2006;6(3):173-80.

[102] Nicodemus GD, Bryant SJ. Cell encapsulation in biodegradable hydrogels for tissue engineering applications. Tissue Engineering. Part B, Reviews 2008;14(2):149-65.

[103] Hou QP, De Bank PA, Shakesheff KM. Injectable scaffolds for tissue regeneration. Journal of Materials Chemistry. 2004:(14):1915-23.

[104] Tememoff JJ, Mikos AG. Injectable biodegradable materials for orthopedic tissue engineering. Biomaterials 2000;(21):2405–12.

[105] Brandl F, Sommer F, Goepferich A. Rational design of hydrogels for tissue engineering: Impact of physical factors on cell behavior. Biomaterials 2007;28:134–146.

[106] Rehfeldt R, Engler AJ, Eckhardt A, Ahmed F, Discher DE. Cell responses to the mechanochemical microenvironment--implications for regenerative medicine and drug delivery. Advanced Drug Delivery Reviews. 2007;(59):1329–39.

[107] Mano JF, Silva G, Azevedo HS, Malafaya PB, Sousa R, Silva SS. Natural origin biodegradable systems in tissue engineering and regenerative medicine: present status and some moving trends. Journal of the Royal Society Interface 2007;4(17):999-1030.

[108] Weiser B, Prantl L, Schubert TE, Zellner J, Fischbach-Teschl C, Spruss T, Seitz AK, Tessmar J, Goepferich A, Blunk T. In vivo development and long-term survival of engineered adipose tissue depend on in vitro pre- cultivation strategy. Tissue Engineering Part A 2008;14(2):275-84.

[109] Fischbach C, Seufert J, Staiger H, Hacker M, Neubauer M, Göpferich A. Three-dimensional in vitro model of adipogenesis: comparison of culture conditions. Tissue Engineering 2004;10(2):215-29.

[100] Mauney JR, Nguyen T, Gillen K, Kirker-Head C, Gimble JM, Kaplan DL. Engineering adipose-like tissue in vitro and in vivo utilizing human bone marrow and adipose-derived mesenchymal stem cells with silk fibroin 3D scaffolds. Biomaterials 2007;28(35):5280-90.

[111] Kang SW, Seo SW, Choi CY, Kim BS. Porous poly(lactic-co-glycolic acid) microsphere as cell culture substrate and cell transplantation vehicle for adipose tissue engineering. Tissue Engineering. Part C, Methods 2008;14:25-34.

[112] Patrick CW, Zheng B, Johnston C, Reece GP. Long-term implantation of preadipocyte-seeded PLGA scaffolds. Tissue Engineering 2002;8(2):283-93.

[113] Mano JF, Silva G, Azevedo HS, Malafaya PB, Sousa R, Silva SS, et al. Natural origin biodegradable systems in tissue engineering and regenerative medicine present status and some moving trends. Journal of the Royal Society, Interface 2007;4(17):999-1030.

[114] Knight DK, Shapka SN, Amsden BG. Structure, depolymerization, and cytocompatibility evaluation of glycol chitosan. Journal of Biomedical Materials Research Part A 2007;83(3):787-98.

[115] Amsden BG, Sukarto A, Knight DK, Shapka SN. Methacrylated glycol chitosan as a photopolymerizable biomaterial. Biomacromolecules 2007;8(12):3758-66.

[116] Arca HC, Şenel S. Chitosan based systems for tissue engineering part II : Soft tissues. FABAD Journal of Pharmaceutical Sciences 2008;33(2):211-216.

[117] Wu X, Black L, Santacana-laffitte G, Patrick CW. Preparation and assessment of glutaraldehyde-crosslinked collagen – chitosan hydrogels for adipose tissue engineering. Journal of Biomedical Materials Research Part A 2006;81(1):59-65.

[118] Varum KM, Ottøy MH, Smidsrød O. Water-solubility of partially N-acetylated chitosans as a function of pH—Effect of chemical-composition and depolymerisation. Carbohydrate Polymers 1994;25:65–70.

[119] Zhang L, Gao Y, Kong L, Gog Y, Zhao N, Zhang X. Compatibility of chitosan-gelatin films with adipose tissue derived stromal Cells. Tsinghua Science and Technology 2006;14(4):11-4.

[120] Gilbert TW, Sellaro TL, Badylak SF. Decellularization of tissues and organs. Biomaterials 2006;27:3675-83.

[121] Flynn LE. The use of decellularized adipose tissue to provide an inductive microenvironment for the adipogenic differentiation of human adipose-derived stem cells. Biomaterial 2010;31(17):4715-24.

[122] Choi JS, Yang HJ, Kim BS, Kim JD, Kim JY, Yoo B. Human extracellular matrix (ECM) powders for injectable cell delivery and adipose tissue engineering. Journal of Controlled Release 2009;139:2-7.

[123] Coman CG, Macsim MA, Oprea AM, Hurjui L, Petreus T, Neamtu A. Study on cellulose/chondroitin sulfate hydrogel used in drug release systems. IFMBE Proceedings 2011;36(5):348-351.

[124] Wang AN, Varghese S, Sharma B, Strehin I, Fermanian S, Gorham J. Multifunctional chondroitin sulphate for cartilage tissue-biomaterial integration. Nature Materials 2007;6(5)385-92.

[125] Tsai MF, Tsai H, Peng Y, Wang L. Chen J, Lu SC. Characterization of hydrogels prepared from copolymerization of the different degrees of methacrylate- grafted chondroitin sulfate macromers and acrylic acid. Journal of Biomedical Materials Research Part A 2007;84(3):727-39.

[126] Van Vlierberghe S, Dubruel P, Schacht E. Biopolymer-based hydrogels as scaffolds for tissue engineering applications: a review. Biomacromolecules 2011;12(5):1387-408

[127] Park JS, Yang HJ, Woo DG, Yang HN, Na K, Park KH. Chondrogenic differentiation of mesenchymal stem cells embedded in a scaffold by long-term release of TGF-beta 3 complexed with chondroitin sulphate. Journal of Biomedical Materials Research. Part A: 2010;92(2):806-16.

[128] Hayes WC, Keer LM, Herrmann G, Mockros LF. A mathematical analysis tests of articular cartilage. Journal of Biomechanics 1972;5(5):541-551.

[129] Hayes AW. Principles and Methods of Toxicology. Raven Press: 1994;3:1231–58

[130] Wang LF, Shen SS, Lu SC. Synthesis and characterization of chondroitin sulfate – methacrylate hydrogels. Carbohydrate Polymers 2003;52:389-396

[131] Ma PM, Elisseeff JH. Scaffolding in tissue engineering. CRC Press:Florida;2005.

[132] Ahearne M, Yang Y, Liu KK. Mechanical characterization of hydrogels for tissue engineering applications. In: Ashammakhi N, ed, Topics in Tissue Engineering 4 2008;12:1-16.

[133] Golemis E, Adams PD. Protein-protein interactions: a molecular cloning manual. CSHL Press:New York;2005.

[134] Obrink B. Wasteson A. Nature of the interaction of chondroitin 4-sulphate and chondroitin sulphate-proteoglycan with collagen. The Biochemical Journal 1971: 121(2):227-33.

[135] Jin M, Grodzinsky AJ. Effect of Electrostatic Interactions between glycosaminoglycans on the shear stiffness of cartilage: A molecular model and experiments. Macromolecules 2001;34(23):8330-9.

[136] Richter S, Boyko V, Schröter K, Gelation studies: Comparison of the critical exponents obtained by dynamic light scattering and rheology. Macromolecular Rapid Communication 2004;25:542.

[137] Fathima NN, Suresh R, Rao JR, Nair BU. Effect of UV irradiation on the physicochemical properties of collagen stabilized using aldehydes. Polymer 2007;104:3642-3648.

[138] Lazovic G, Colic M, Grubor M, Jovanovic M. The application of collagen sheet in open wound healing. Annals of Burns and Fire Disasters 2005;18(3):151–156.

[139] Poulain-Godefroy O, Lecoeur C, Pattou F, Frühbeck G, Froguel P. Inflammation is associated with a decrease of lipogenic factors in omental fat in women. Journal of Physiology - Regulatory, Integrative and Comparative Physiology 2008;295:R1-R7.

[140] Choi JK, Kim BS, Kim JY, Kim JD, Choi YC, Yang HJ. Decellularized extracellular matrix derived from human adipose tissue as a potential scaffold for allograft tissue engineering. Journal of Biomedical Materials Research. Part A 2011;97(3):292-9.

[141] Chandler EM, Berglund CM, Lee JS, Polacheck WJ, Gleghorn JP, Kirby BJ. Stiffness of photocrosslinked RGD-alginate gels regulates adipose progenitor cell behavior. Biotechnology and Bioengineering 2011;108(7):1683-92.

[142] Halbleib M, Skurk T, de Luca C, von Heimburg D, Hauner H. Tissue engineering of white adipose tissue using hyaluronic acid-based scaffolds. I: in vitro differentiation of human adipocyte precursor cells on scaffolds. Biomaterials 2003;24(18):3125-32.

[143] Si Y, Yoon J, Lee K. Flux profile and modularity analysis of time-dependent metabolic changes of de novo adipocyte formation. American journal of physiology, endocrinology and metabolism 2007;292(6):E1637-46.

Appendix: End Point RT-PCR Data

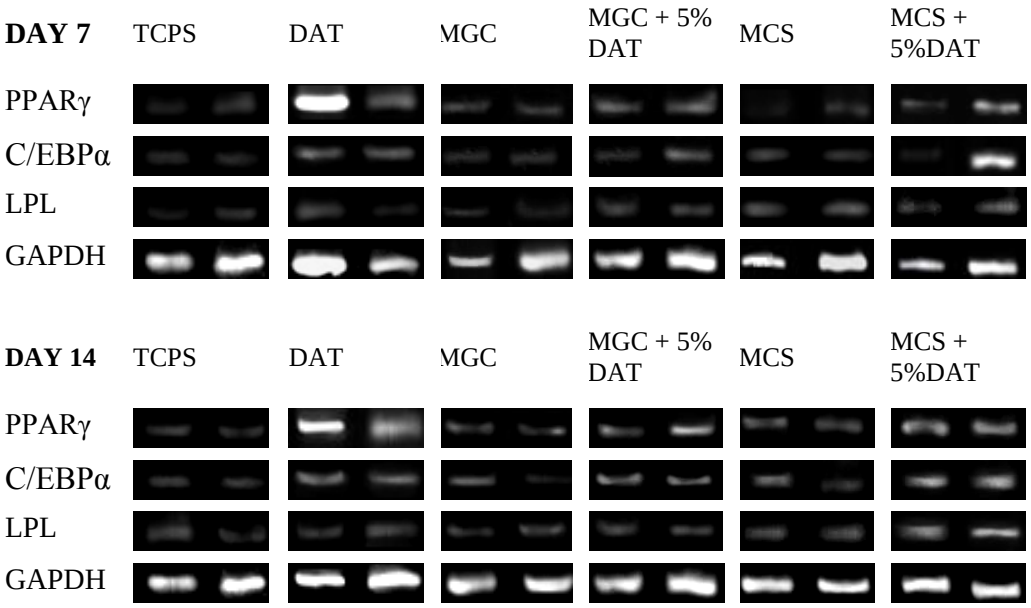

Figure A.1 Representative end point RT-PCR gel bands showing the expression of the adipogenic markers PPARγ, C/EPBα and LPL in ASC-seeded TCPS, DAT, MGC, MGC + 5% (w/v) DAT, MCS, and MCS + 5% (w/v) DAT cultured in adipogenic medium for 7 or 14 days. GAPDH was used as the housekeeping gene. Data shown is obtained from ASC donor with a BMI of 26.0, aged 46.

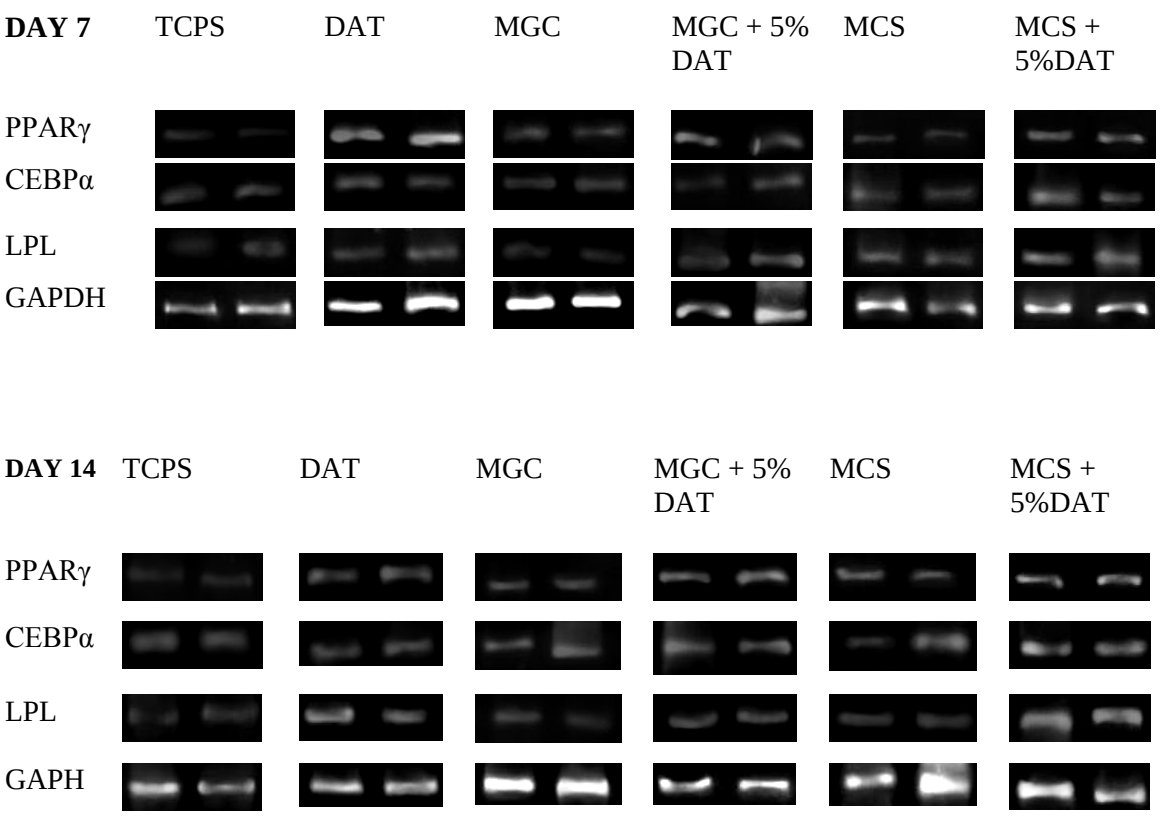

Figure A2: End point RT-PCR study examining the adipogenic markers (PPARγ, CEBPα, LPL) expression with housekeeping gene GAPDH of ASC after being seeded on MGC and MCS-DAT scaffold (0 and 5 w/v% DAT), DAT scaffold, and cultured in adipogenic differentiation medium for 7 and 14 days. Data shown is obtained from ASC donor with a BMI of 27.6, aged 36.

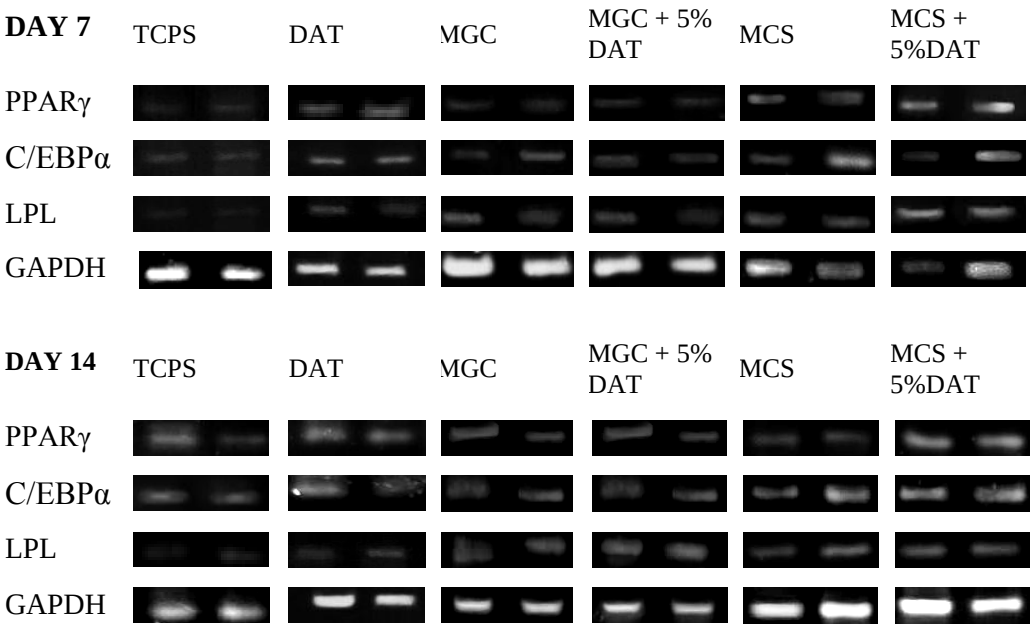

Figure A3: End point RT-PCR study examining the adipogenic markers (PPARγ, CEBP*α*, LPL) expression with housekeeping gene GAPDH of ASC after being seeded on MGC and MCS-DAT scaffold (0 and 5 w/v% DAT), DAT scaffold, and cultured in adipogenic differentiation medium for 7 and 14 days. Data shown is obtained from ASC donor with a BMI of 26.8, aged 41.